Republic of Iraq
Ministry of Higher Education and Scientific Research
Al-NahrainUniversity
College of Science
Department of Chemistry

Synthesis of inorganic complexes derived from 4-amino-5-(pyridyl)-4H 1,2,4 triazole-3-thiol and study their photochemical stability with polystyrene

A Thesis
Submitted to the College of Science Al-Nahrain University as a Partial Fulfillment of the Requirements for the Degree of M. Sc. in Chemistry

By:

Raghad Ali AbdulRasool Haddad

(B. Sc. 2011)

Supervised by:

Assist. Prof. Dr. Emad A. Yousif

2014

بِسْمِ اللّه الرَحْمِنْ الرَحِيَمِ

إِنَّا فَتَحْنَا لَكَ فَتْحًا
مُّبِينًا لِيَغْفِرَ لَكَ
اللّه مَا تَقَدَّمَ مِن ذَنبكَ وَمَا
تَأَخَّرَ وَيُتِمَّ نِعْمَتَهُ عَلَيْكَ
وَيَهْدِيَكَ صِرَاطًا مُّسْتَقِيمًا
وَيَنصُرَكُ اللّه نَصْرًا عَزِيزًا

صَدَقَ اللّهُ العَظيِم

سورة الفتح

الاية (1 – 3)

To
My Lovely Parents
And
My Brothers

Raghad

“Experiment is the only means of knowledge
at our disposal,
everything else is poetry, imagination”

-Max Planck

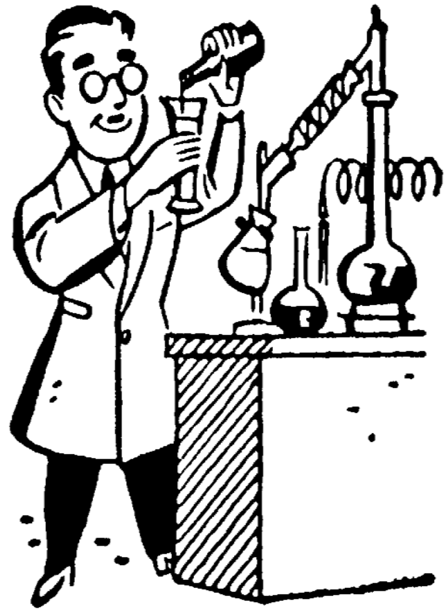

Acknowledgements

It is a pleasure to express my sincere thanks and appreciation to my supervisor, Assistant Prof. ***Dr. Emad A. Yousif*** *for suggesting the subject of this thesis and supervision in my work. His enthusiasm, encouragement, and faith in me throughout have been extremely helpful. Without him this work would not be completed.*

I am very grateful to ***Dr. Ahmed A. Ahmed*** *for his supporting and helping me in my study and work.*

I would like to thank my ***father****, my* ***mother****, my two* ***brothers*** *and all of my* ***friends*** *for their supporting me during the course of the study and work.*

Thanks to the staff of the chemistry department, college of science, AL-Nahrain University.

Also, I am very grateful to all the people who helped me during my work.

Raghad

Supervisor Certification

I certify that this thesis was prepared under my supervision at the Department of Chemistry, College of Science, Al-Nahrain University as a partial requirements for the Degree of Master of Science in Chemistry.

Assistant Professor

Dr. Emad A. Yousif

In view of the available recommendation, I forward this thesis for debate by the Examining Committee.

Assistant Professor

Dr. Nasreen R. Jber

Head of Department Chemistry
College of science
Al Nahrain university

Examining Committee Certfication

We, the examining committee, certify that we read this thesis and have examined the student (**Raghad Ali AbdulRasool)** in its contents and that in our opinion; it is adequate as a thesis for the Degree of Master of Science in Chemistry.

Chairman
Signature:
Name: Assist. Prof. Dr. Basim Ibrahim Mahdi
Date: /   /2014

Member	Member
Signature:	Signature:
Name: Assist. Prof.	Name: Assist. Prof.
Dr. Hadi M. A. Abood	Dr. Ahmed A. Ahmed
Date: / /2014	Date: / /2014

Supervisor
Signature:
Name: Assist. Prof.
Dr. Emad A. Yousif
Date: /   /2014

Approved for the College Committee of Graduate Studies

Signature:
Name: **Assist. Prof. Dr. Hadi M. A. Abood**
Dean of the College of Science.
Date: /   /2014

Abstract

Five transition metal complexes of Ni(II), Cu(II), Zn(II), Cd(II) and Sn(II) with {4-amino-5-(pyridyl)-4H-1,2,4-triazole-3-thiol}, as a ligand (L) has been prepared in alcoholic medium.

These complexes are:

1. Bis(4-amino-5-(pyridyl)-4H-1,2,4-triazole-3-thiol) Nickel(II), $Ni(L)_2$.
2. Bis(4-amino-5-(pyridyl)-4H-1,2,4-triazole-3-thiol) Cupper(II), $Cu(L)_2$.
3. Bis(4-amino-5-(pyridyl)-4H-1,2,4-triazole-3-thiol) Zinc(II), $Zn(L)_2$.
4. Bis(4-amino-5-(pyridyl)-4H-1,2,4-triazole-3-thiol) Cadmium(II), $Cd(L)_2$.
5. Bis(4-amino-5-(pyridyl)-4H-1,2,4-triazole-3-thiol) Tin(II), $Sn(L)_2$.

The ligand (L) and its metal complexes were characterized quantitatively and qualitatively by using: FTIR, UV-visible spectroscopy, ^{1}H and ^{13}C NMR, magnetic susceptibility and conductivity measurements. This ligand act as bidentate that coordinated to the metal ions through sulphur and nitrogen of amine group. According to the spectral data of the complexes a tetrahedral geometry was suggested for these complexes except Cu(II) complexes which exhibit a square structure.

In this work the prepared complexes of 4- amino-5-(pyridyl)-4H 1,2,4 triazole -3- thiol were used to enhance the photostabilization of Polystyrene (PS).

Polystyrene has been mixed with these complexes in chloroform solvent which containing concentration of complex 0.5 % by weight, which produced by the casting method from chloroform solvent. The photostabilization of polystyrene

films were studied at room temperature under irradiation of light λ=365 nm wave length with intensity $6.02*10^{-9}$ Ein Dm^{-3} S^{-1} .

The photostabilization activity of these compounds was determined by monitoring the carbonyl (I_{CO}) and hydroxyl (I_{OH}) indexes, weight loss method with irradiation time. It was found that the (I_{CO}) and (I_{OH}) indexes values increased with irradiation time and this increase depend on the type of additives. The surface morphology for these films was studied during irradiation time. The changes in viscosity average molecular weight of PS with irradiation time were also tracked (using chloroform as a solvent). The quantum yield of the chain scission (Φ_{cs}) of these complexes in PS films was also evaluated.

The following trend is obtained for the photostabilization effect on PS films in presence of additives as shown below:

$$\xrightarrow[\textbf{Increasing the photostability}]{\mathbf{Sn(L)_2\ ,\ Cd(L)_2\ ,\ Ni(L)_2\ ,\ Zn(L)_2\ ,\ Cu(L)_2}}$$

According to the experimental results obtained, mechanisms were suggested, depending on the structure of the complexes.

Symbols & Observations

Symbol	**Full meaning**
PS	Polystyrene
UV.	Ultraviolet-visible
P	Polymer
HALS	Hindered Amine Light Stabilizer
$P^{\cdot}$	Polymer radical
POOH	Hydroperoxide
$POO^{\cdot}$	Peroxy radical
$PO^{\cdot}$	Polymer alkyl radical
$[O_2^{*}]^1$	Singlate Oxygen excited state
FTIR	Fourier Transform Infrared
CT	Charge transfer
NMR	Nuclear Magnetic Resonance
(I_{OH})	Hydroxyl index
(I_{CO})	Carbonyl index
Mv	Average Molecular Weight
ϕ_{cs}	Quantum yield
S	Main chain scission
α	Degree of deterioration
Kd	Dissociation constant
Dp	Degree of polymerization
Pt	Reciprocal of degree of polymerization

Chapter two

Chapter three

Chapter One

1

INTRODUCTION

1.1 Chemistry of 1,2,4 – Triazole Ring

Heterocyclic chemistry has now become a separate field of chemistry with long history, present society and future prospects. Life, like ours, is totally dependent on the heterocyclic compounds, it takes birth with purine / pyrimidine bases, nourishes on carbohydrates and in case of disease, is cured from medicines, many of which are heterocyclic in nature. A variety of atoms, such as N, O, S, Se, P, Si, B and As can be incorporated into the ring structures.

Today, the heterocyclic chemistry delivers reagents and synthetic methods of its own traditional activity in synthesis of drugs, pesticides and detergents as well as into the related fields such as biochemistry, polymers and material sciences(1-3).

1.1.1. Triazoles

Triazoles are five memberd heterocyclic compounds containing three nitrogen and two carbon atoms. This may be of two types, the 1,2,3-triazoles **(1)** and the 1,2,4-triazoles **(2)**.

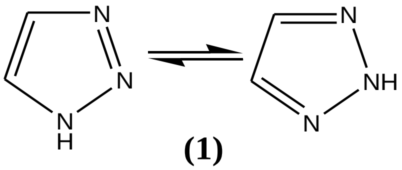

(1)

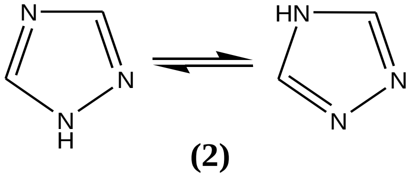

(2)

The name triazole was first given to the carbon nitrogen ring system $C_2N_3H_3$ by Bladin who described its derivatives in early 1885, although the structures reported slightly incorrect(4-6).

In this work substituted 1,2,4 triazole ligand has been prepared . 1, 2, 4-Triazoles exhibit two tautomeric forms namely [4*H*]-1,2, 4- triazoles **(3)** and [1*H*]-1,2,4-triazoles **(4)**.

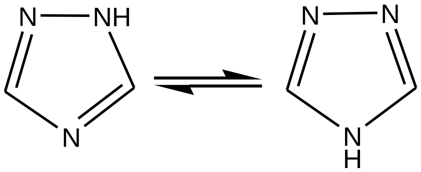

(3) **(4)**

Among the substituted 1,2,4-triazoles, 3-mercapto-1,2,4-triazoles exist in two tautomeric forms, because the labile hydrogen may be attached either to the nitrogen or the sulfur atom. It exhibits thione-thiol tautomeric forms shown below. This compound exists predominantly in thione **(5)** form(7).

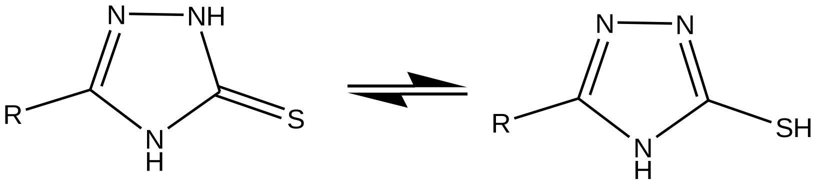

The 1, 2, 4- triazole is a ubiquitous feature of many pharmaceutical and agrochemical products. The substituted 1, 2, 4 triazole nucleus is particularly common, and can be found in marketed drags such as fluconozole and terconazole. Triazole nucleus is associated with various pharmacological activities like antimicrobial, antibacterial, antiviral, antifungal effects(8) .

1.1.2 Triazole complexes:

The tendency of metal ion to form a stable complex with ligands depend on many rules such as the hard and soft acids and bases (HSAB) theory for Pearson (9).Which imply that metal ion tend to coordinate with certain functional groups of the ligand to form a stable complex.

Increasing the positive charge on the central transition metal ions strengthens the metal-ligand bonds. The metal ion prefers to bind with atoms of high electron density such as N^{-3}, O^{-2}, P^{-3}, S^{-2} and C^{-4} (10).

A second observation is that certain ligands form their most stable complexes with metal ions such as Ag^+, Hg^{+2}, and Pt^{+2}, but other ligands seem to prefer ions such as Al^{+3}, Ti^{+4}, and Co^{+3}. Ligands and metal ions were classified as belonging to type (a) or (b) according to their preferential bonding.

Class (a) metal ions include those of alkali metals, alkaline earth metals, and lighter transition metals in higher oxidation states(11)such as Ti^{+4}, Cr^{+3}, Fe^{+3}, Co^{+3} and the hydrogen ion, H^+.

Class (b) metal ions include those of the heavier transition metals, and those in lower oxidation states(12)such as Cu^+, Ag^+, Hg^{+2}, Pd^{+2}, and Pt^{+2}.

The substituted triazole with sulphur atom and amine group are considered to be good coordinating ligands because they involved both hard nitrogen and soft sulfur atom as thio amide group, this ligand have doner group that coordinate with wide range of metal ions(13-14).

Since metal ions of class (a) have a performance for coordination with hard Nitrogen and class (b) metal ions have a performance for coordination with soft sulphur, it would be interesting to investigate this aspect using both type of metal ions as these ligands contain both hard nitrogen and soft sulphur as donor atoms.

3-substiuted -4- amino-5-mercepto-1,2,4-triazole are sulphur and nitrogen doner ligands and are potentially multidentate. The potential coordination sites are: (i) Sulphur of thiol group, (ii) nitrogen of primary amino group and (iii) two nitrogen atom at position 1 & 2 in triazol ring systems(15) . Thus this ligand is polydentate, it has been shown and experimentally verified that bidentate or polydentate ligands in general form more stable complexes than monodentate ligands(14).

The 4-amino-3-(aryl or alkyl)-1,2,4-triazole- 5-thione molecule contains an S=C-N-N unit that allows for bidentate coordination to a metal ion through the amine and thione substituents to form a stable five-membered ring(16).

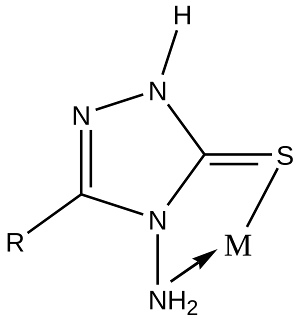

Many quantitave studies have confirmed that Complexes of polydentate ligand are tend to be more stable than complexes derived from monodentate ligands. Furthermore, five or six membered chelates are by far the most common and are in general the most stable(17).

Amine and thione-substituted triazoles have been studied as anti-inflammatory and anti-microbial agents(18)and other applications. A new thio-Triazole ligand and its complexes with selected metals was prepared and characterized by Majeed and Alabdeen(19).

Photostability of the polymers is one of their most important properties. To solve the problem of polymers degradation, a number of different stabilizers have successfully been applied. In this work the preparation of Zn(II), Cd(II), Sn(II), Ni(II) & Cu (II) with 4- amino-5-(pyridiyle)-4H 1,2,4 triazol -3- thiol were used for photostabilization of Polystyrene .

Aliwi et al. were used Nichel and Copper tetradentate Schiff base complexes as photostabilization of Polystyrene(20).

1.2. Definitions and Historical Aspects of Photodegradation of Polymers

Polymers are a broad class of materials which are made from repeating units of smaller molecule called monomers.

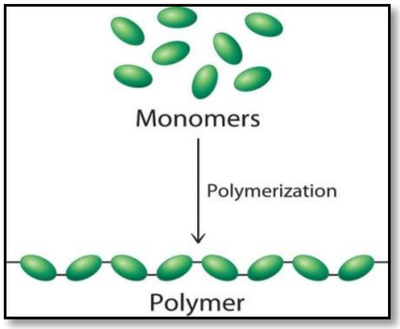

Figure (1.1) Simple Structure of Monomer and Polymer

Polymers can be natural in origin such as the lignin of tree branches. Other polymers are synthetic such as polyester, Polyvinyl chloride and polystyrene.

One of the disadvantages of using polymers is that they degrade when they are used in high temperature conditions or in outdoor applications. When polymers are used in outdoor applications, the environment negatively influences the servicelife. This process is called weathering(21-22).

A wide variety of synthetic and naturally polymers absorb solar ultraviolet radiation and undergo photolytic, photooxidative, and thermooxidative reactions that result in the degradation of the material(23-25) .

In recent years, the use of polymeric materials has rapidly increased but it is well established that rapid photodegradation of these materials is possible when they are exposed to natural weathering(26-29).

Exposure to ultraviolet, UV- radiation may cause the significant degradation of many materials. Damage by UV radiation is commonly the main reason for the discoloration of dyes and pigments, weathering, yellowing of plastics, loss of gloss and mechanical properties (cracking), and other problems associated with UV light. The manufacturers of paints, plastics, contact lenses, and cosmetics have a great interest in offering products that remain unaltered for long periods under conditions of light exposure(30-33).

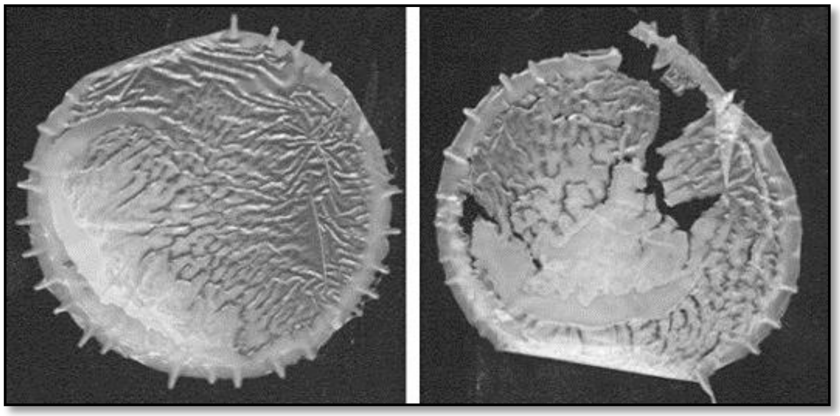

Figure (1.2) Polymer Film Before and After Exposure to UV Light

The use of plastics in building applications is popular in the developing world because of the low cost and the ease of use of plastic components compared to the conventional metal, glass, mortar, wood and other materials. Plastics are used in other products such as outdoor furniture, fishing gear, and marine craft, which are also routinely used outdoors(34-35).

Solar radiation reaching the surface of the earth is characterized by wave lengths from approximately 295 up to 2500 nm. The solar radiation classified as UV-B (280 – 315 nm) has an energy of 426 – 380 KJ mol^{-1}. Fortunately, the higher energetic part of UV-B; 280 – 295 nm, is filtered by the stratosphere and does not reach the earth’s surface ,UV-A (315 – 400 nm), has energy between 389 and 300

KJ mol^{-1} and is less harmful for organic materials than UV-B., Visible (400 – 760 nm), and infrared (760 – 2500nm.) (36).

Photooxidation of organic materials is a major cause of irreversible deterioration for a large number of substances. It is responsible not only for the loss of physical properties of plastics, rubber, but also for foodstuffs (37).

1.2.1. The Factors Causing Photodegradation:

Generally, many factors are responsible in causing photodegradation of polymeric materials, they are divided into two categories(38):

I) Internal impurities, which contain chromophoric groups; which are introduced into macromolecules during polymerization processing and storage; they include:

- a- Hydroperoxide.
- b- Carbonyl.
- c- Unsaturated bonds (C=C).
- d- Catalyst residue.
- e- Charge–transfer (CT) complexes with oxygen.

II) External impurities, which may contain chromophoric groups, are:

- a- Traces of solvents, catalyst, …. etc.
- b- Compounds from polluted urban atmosphere and smog, e.g. polynuclear hydrocarbons such as naphthalene and anthracene in polypropylene and polybutadiene.
- c- Additives (Pigments, dyes, thermal stabilizers, photostabilizers, …. etc.).
- d- Traces of metals and metal oxides from processing equipment and containers, such as Fe, Ni or Cr.

1.2.2. Types of polymers degradation

The degradation of polymers usually starts at the outer surface and penetrates gradually into the bulk of the material(39).

Polymer degradation can be caused by heat (thermal degradation), light (photodegradation), ionizing radiation (radio degradation), mechanical action, or by fungi, bacteria, yeasts, algae, and their enzymes (biodegradation). The deleterious effects of weathering on polymers generally has been ascribed to a complex set of processes in which the combined action of UV. light and oxygen predominant. A pure thermal effect impossible because oxygen is always present and so the process is thermaloxidative degradation(40).

There are many different modes of polymer degradation. These are very similar since they all involve chemical reactions that result in bond scission. These modes are:(38)

(i) Chemical degradation

Chemical degradation refers to processes, which are induced under the influence of chemical reagent (e.g. acids, bases, solvents reactive gases, etc)(41) .

(ii) Biodegradation

Biologically initiated degradation also is strongly related to chemical degradation as far as microbial attack is concerned. Microorganisms produce variety of enzymes which are capable of reaction with natural and synthetic polymers(42).

(iii) Radiolytic degradation

When polymeric materials are subjected to high energy radiation (e.g. gamma radiation) changes are observed on their molecular structure, mainly chain scission, which leads to reduction in molar mass(43).

(iv) Thermal degradation

Thermal degradation refers to the case where the polymer, at elevated temperatures, starts to undergo chemical changes without the simultaneous involvement of another compound(44).

(v) Mechanical degradation

This generally, refers to macroscopic effects under the influence of shear forces. These forces result in the formation of macro radicals as follows:

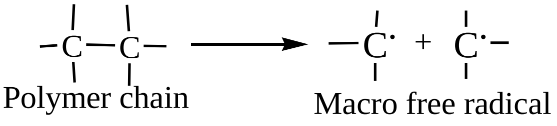

$$-C-C- \longrightarrow -C^{\bullet} + C^{\bullet}-$$

(1.1)

Such radicals can recombine in the absence of oxygen. In the presence of oxygen peroxy radicals may be formed, which leads to degradation of polymer chains (45).

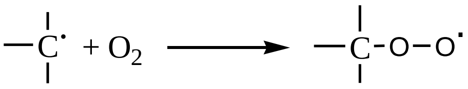

$$-C^{\bullet} + O_2 \longrightarrow -C-O-O^{\bullet}$$

(1.2)

(vi) Photodegradation:

Photodegradation is degradation of a photodegradable molecule caused by the absorption of photons, particularly those wavelengths found in sunlight, such as infrared radiation, visible light, and ultraviolet light. Photodegradation includes photodissociation, the breakup of molecules into smaller pieces by photons. It also includes the change of a molecule's shape to make it irreversibly altered. A common photodegradation reaction is oxidation.

Many reviews have been published on photodegradation and photooxidation degradation of polystyrene(46-50).

Light - induced polymer degradation, or photodegradation, includes the physical and chemical changes caused by irradiation of polymers with ultraviolet or visible light. Thus, the existence of chromophoric groups in the macromolecules is a prerequisite for the initiation of any photochemical reaction(38).

Ketones, quinines, and peroxides are initiators for different reaction degradation or chemical modification occurring in organic compounds(51). They absorb light up to about 380 nm, which causes their excitation or cleavage to radicals. One may initiate polymer degradation and other transformation by abstruction of hydrogen atom from a macromolecule (PH) and formation of polymer alkyl radical ($P^{\cdot}$)(52).

Photodegradation may occur in the absence of oxygen (chain breaking or cross-linking) and the presence of oxygen (photooxidative) degradation. The photooxidative degradation process is induced by UV radiation and other catalysts (or both) and can be accelerated at elevated temperatures.

1.2.3. Mechanism of photooxidative degradation of polymers

Photooxidative degradation of polymers, which include processes such as chain scission, crosslinking and secondary oxidative reactions, and takes place via radical processes, similar to thermal oxidation reactions(53-55).

Two mechanisms have been proposed to explain the photooxidation of polymers. One proceeds through direct reaction of singlet oxygen with the substrate while the other involves the production of radicals and subsequent reaction with oxygen(56-57).

1.2.3.1. The singlet oxygen mechanism of oxidation

It is generally accepted that reactive singlet oxygen $(\mathbf{O_2}^*)^1$ react with polymeric molecule (PH) to form charge transfer complex before formation of hydroperoxide:

$$PH + (O_2^*)^1 \longrightarrow PH^{+} \ldots O_2^{-} \longrightarrow PH^{\cdot} + O_2^{\cdot} \longrightarrow POOH \qquad (1.3)$$

Formation of a hydroperoxide by oxidation of an olefin containing allylic hydrogen, and which could further decompose and lead to formation of a terminal carbonyl group.

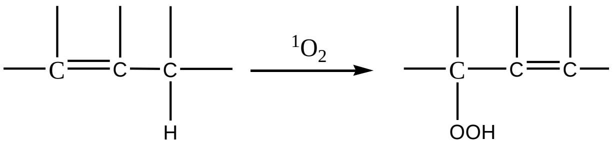

$$-C=C-\underset{H}{C}- \xrightarrow{{}^1O_2} -\underset{OOH}{C}-C=C- \qquad (1.4)$$

1.2.3.2. The free radical mechanism of oxidation

The radical mechanism of photooxidation of polymers proceeds through a chain reaction similar to that for homogeneous liquid phase oxidations(58, 56).

$$
\begin{array}{lllll}
\text{Initiation:} & \text{Polymer} & \rightarrow & R^{\cdot} & \\
\text{Propagation:} & R^{\cdot} + O_2 & \rightarrow & RO_2^{\cdot} & \\
 & RO_2^{\cdot} + PH & \rightarrow & ROOH + R^{\cdot} & \\
 & ROOH & \rightarrow & RO^{\cdot} + {}^{\cdot}OH & \\
 & & & \downarrow & \\
 & & & \beta\text{- Scission} & \\
\text{Termination:} & 2\,RO_2^{\cdot} & \rightarrow & \text{non radical products} &
\end{array}
$$

1.2.4. Steps of Photodegradation

Photooxidative degradation includes the following steps:(59-60) Initiation, Propagation and Termination, These steps are illustrated in the figure (1.3):

(i)Chain initiation:

$$\left.\begin{array}{l}\text{Hydroperoxide (POOH)}\\ \text{Carbonyl compounds (c=o)}\end{array}\right\} \xrightarrow[M^{+2},\,M^{+3}]{\text{heat , hv}} P^{\cdot},POO^{\cdot},OH^{\cdot},HO_2^{\cdot} \quad \text{Free radicales}$$

(ii)Chain propagation:

$$P^{\cdot} + O_2 \xrightarrow[M^{+2},\,M^{+3}]{\text{heat , hv}} POO^{\cdot}$$

$$POO^{\cdot} + PH \xrightarrow[M^{+2},\,M^{+3}]{\text{heat , hv}} POOH + P^{\cdot}$$

$$POOH \longrightarrow PO^{\cdot} + {}^{\cdot}OH$$

$$2POOH \longrightarrow PO^{\cdot} + O\,H + H_2O$$

$$PO^{\cdot} + PH \longrightarrow POH + P^{\cdot}$$

$$HO^{\cdot} + PH \longrightarrow H_2O + P^{\cdot}$$

(iii)Chain termination:

$$\left.\begin{array}{l}P^{\cdot} + P^{\cdot}\\ P^{\cdot} + POO^{\cdot}\\ POO^{\cdot} + POO^{\cdot}\\ \vdots\\ \text{e.t.c}\end{array}\right\} \longrightarrow \text{non radical products}$$

Where P. is polymer radical, M+2 is metal ion, and PH is polymer molecule.

Figure (1.3) General Oxidation & Photooxidation in Polymer (61)

1.2.4.1. Photoinitiation step

Internal and /or external chromophoric groups absorb light and produce low molecular weight radicals ($R^{\cdot}$) and /or polymeric macro radicals ($P^{\cdot}$) as follows:(62)

$$\mathbf{PH} \longrightarrow \mathbf{P^{\cdot} + H^{\cdot}} \qquad (1.5)$$

This reaction may be initiated by physical factors such as: UV radiation, heat, ionization, ultrasonic or mechanical effects or by chemical factors (direct reaction with O_2 or atomic oxygen, catalysis or singlet O_2 $[O_2^{*}]^{1}$ excited state.

The "hydroperoxide" (POOH) is the most important initiator in the photooxidative process. The formation of hydroperoxide and its photolysis illustrate the formation of other effective functional groups such as carbonyl during β-scission of the alkoxy radical(37).

Whatever the initial mechanism of radical formation, hydroperoxides are produced after reaction with oxygen. These are thus key intermediates in the oxidation of polymers(63).

In addition to the polymer oxidation initiation a second major contributor to the photodegradation of polymers is ketone photolysis, which proceeds through two major reactions called Norrish I (radical generation and no chain cleavage) and Norrish II (chain cleavage). On exposure to light, these ketone groups absorb photons of appropriate energy, break carbon–carbon bonds, and scission the polymer backbone(40, 48)as shown in scheem(1.1) and (1.2)(37):

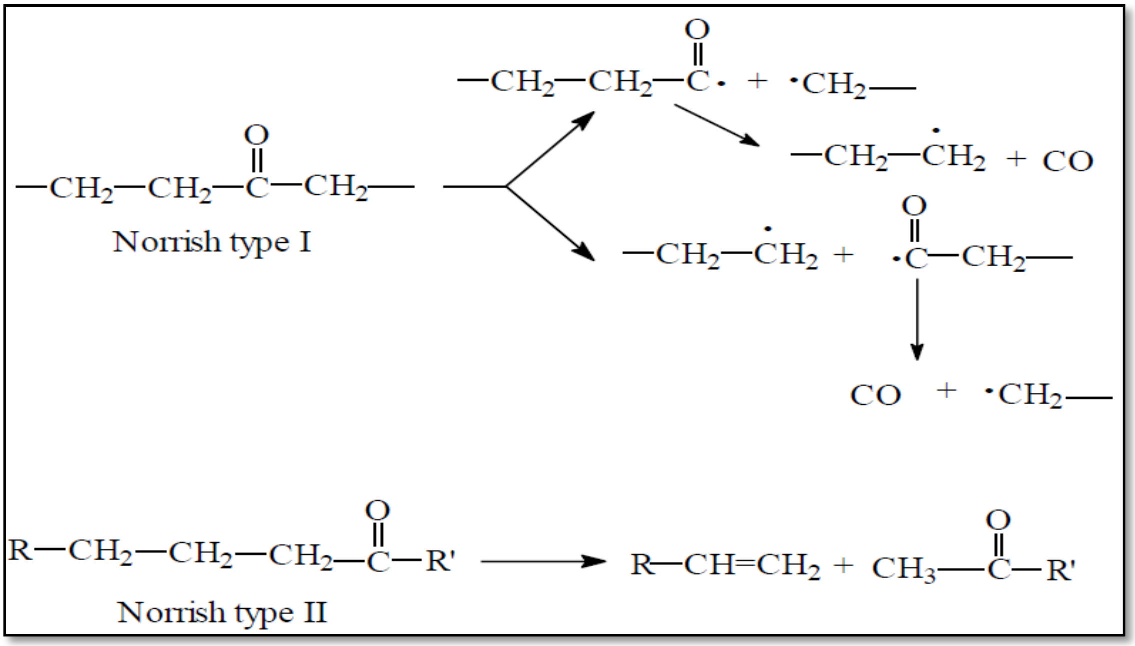

Scheme (1.1) The β Scission in Polymer Molecule [(37)]

Generally, the overall processes of photooxidative degradation are given in Scheme (1.2)[(64)]

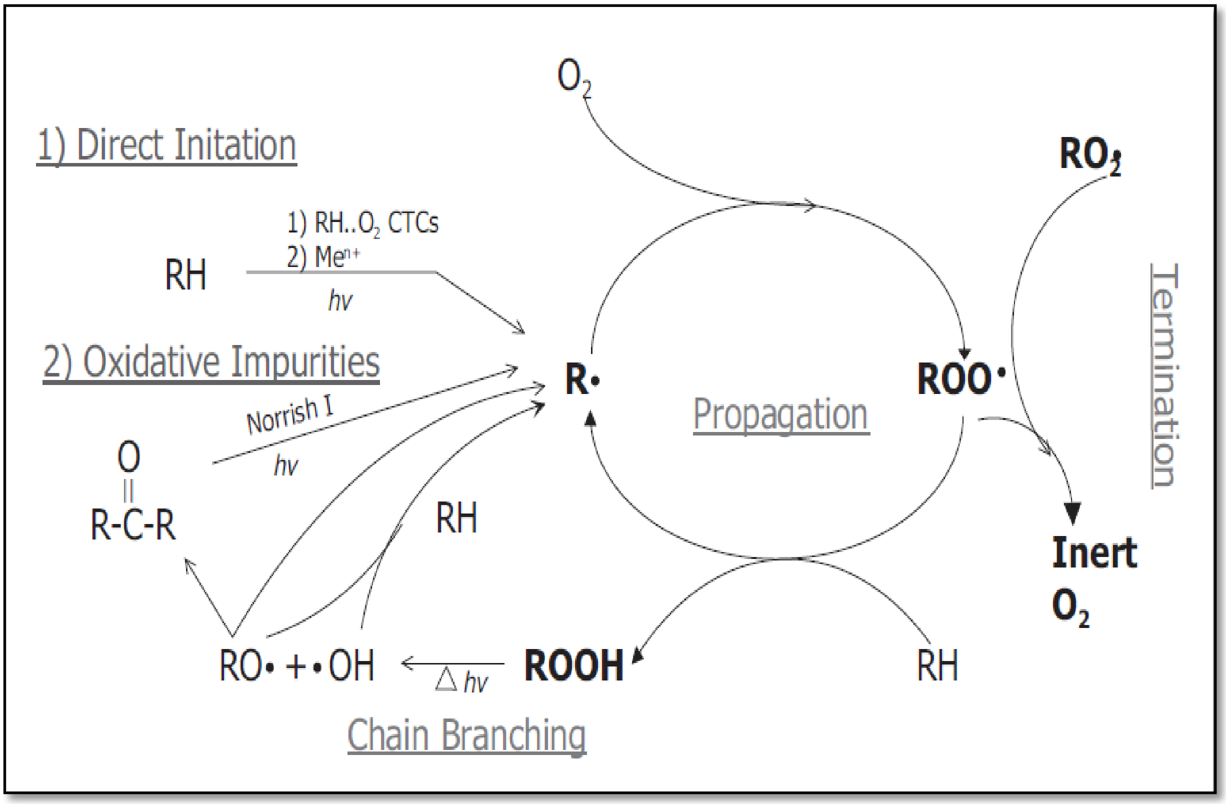

Scheme (1.2) Photooxidation mechanism of polymers RH most labile hydrogen[(65)]

1.2.4.2. Propagation step

This step can be divided into six different steps(66-67):

A) Subsequent reaction, of low molecular radicals ($R^{\cdot}$) and polymer alkyl radical ($P^{\cdot}$) in a chain process similar to the abstraction of hydrogen from polymer molecule:

$$\mathbf{PH + R^{\cdot}(P^{\cdot}) \rightarrow {}^{\cdot}PH + P^{\cdot}} \qquad (1.6)$$

B) Reactions of polymer macro radicals with oxygen, during which polymer peroxy radicals ($POO^{\cdot}$) are formed.

$$\mathbf{P^{\cdot} + O_2 \rightarrow POO^{\cdot}} \qquad (1.7)$$

C) Abstraction of hydrogen from another polymer molecule by polymer alkylperoxy radical, with the formation of hydroperoxide group.

$$\mathbf{POO + {}^{\backslash}PH \rightarrow POOH + {}^{\backslash}P^{\cdot}} \qquad (1.8)$$

D) Photodecomposition of hydroperoxide groups with the formation of polymer alkyloxy ($PO^{\cdot}$), polymer peroxy ($POO^{\cdot}$), and hydroxyl radicals ($HO^{\cdot}$).

$$\mathbf{POOH \rightarrow PO^{\cdot} + {}^{\cdot}OH} \qquad (1.9)$$

$$\mathbf{2POOH \rightarrow PO^{\cdot} + POO^{\cdot} + H_2O} \qquad (1.10)$$

E) Abstraction of hydrogen from another polymer molecule by polymer alkyloxy radical with the formation of hydroxyl function groups in polymer. The formation of (OH) group during photolysis is clearly indicated by IR spectrum.

$$\mathbf{PO^{\cdot} + PH \rightarrow POH + {}^{\cdot}P} \qquad (1.11)$$

F) Dispropertionation reaction (scission process) of polymer alkyloxy radicals with the formation of aldehyd or ketone end groups and end polymer alkyl radicals.

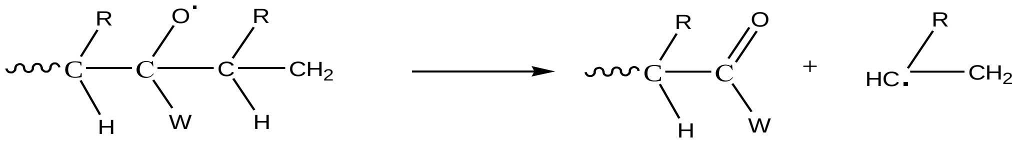

where W = H aldehyde
W = R Ketone

(1.12)

The formation of (C=O) group during photolysis is clearly indicated by IR spectrum.

There are many points concerning the mentioned propagation steps which are:

- Formation of propagating radicals ($POO^{\cdot}$) by reaction (1.7), in a semi-rigid polymer system is very low (ca.1%)(68)because of efficient polymer alkyl radicals ($P^{\cdot}$) recombination before O_2 react with them. Polymer alkylperoxy radicals ($POO^{\cdot}$) are strongly resonance stabilized, and they are stable at room temperature in polymer matrix. They are selective electrophilic species abstracting 3^{o} hydrogen in preference to 2^{o} or 1^{o} (69-71).

- The light quanta produced by sun irradiation are energetically sufficient to cleave PO–OH and also P–OOH, but hardly POO–H bonds, which have the dissociation energies of 42 kcal/mol (PO–OH), 70 K cal/mol (P – OOH) , and 90 kcal/mol (POO–H) (72). The large differences in bond dissociation energy between PO – OH and P – OOH means that reaction with formation PO• and •OH radicals will predominate during light irradiation.

1.2.4.3. Termination step

The radicals formed in the degradation of polymers can be terminated by numerous different combination reactions between two polymer radicals, in which inactive products are formed:

$$\mathbf{POO^{\cdot} + POO^{\cdot} \rightarrow POOP + O_2} \quad (1.13)$$

$$\mathbf{POO^{\cdot} + P^{\cdot} \rightarrow POOP} \quad (1.14)$$

$$\mathbf{P^{\cdot} + P^{\cdot} \rightarrow P - P} \quad (1.15)$$

When the oxygen pressure is high, the termination reaction follows reaction (1.13) almost fully. At low oxygen pressure other termination reactions take place to some extent. In the degradation of solid polymers when sufficient oxygen content cannot be maintained reaction (1.15) becomes significant. Polymer radicals can couple mutually as in reaction (1.14) and form crosslinks with polymer peroxy radicals(73).

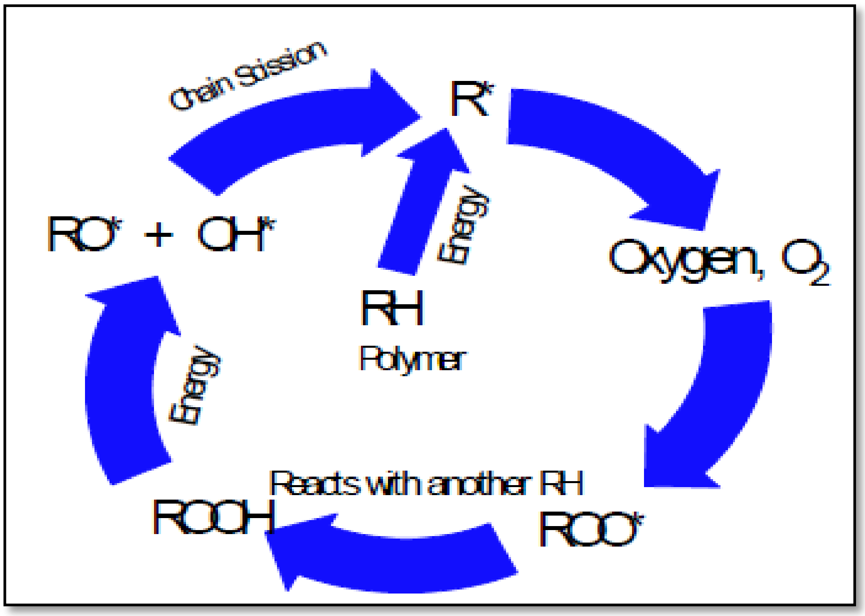

Scheme (1.3) Photooxidation Cycle for Polymers

1.3. Polystyrene (PS)

Polystyrene (PS) is a multipurpose polymer that is used in varied applications. General purpose polystyrene is clear and hard which is used in packaging, laboratory ware, and electronics(74).

1.3.1. History of polystyrene

Edward Simon accidently discovered polystyrene in 1839 in Germany. From the resin of Turkish sweetgum tree, he obtained an oily substance, which thickened into jelly in air; he described it as styrol oxide. In 1845 John Blyth and August Hofmann observed that the same changes occur in styrol in the absence of oxygen. They named it as metastyrol. In the thesis of Hermann Staudinger (1881–1965) it was reported that a chain reaction occurs in styrol resulting in the formation of macromolecules which was later called polystyrene. In Germany in 1931 started producing polystyrene(75).

1.3.2. Synthesis of polystyrene

Polystyrene is manufactured by the addition polymerization of the styrene monomer unit. Styrene is an aromatic monomer, and polystyrene is an aromatic polymer(73). The main manufacturing route to styrene is the direct catalytic dehydrogenation of ethyl benzene as in equation 1.16:

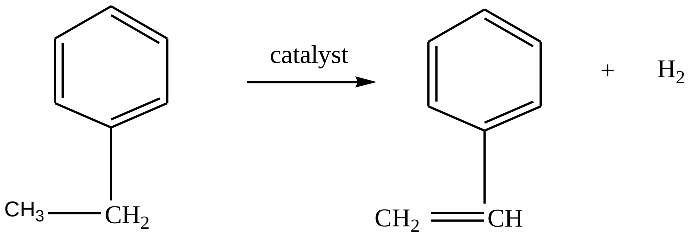

(1.16)

The overall reaction describing the styrene polymerization was shown in equation 1.17:

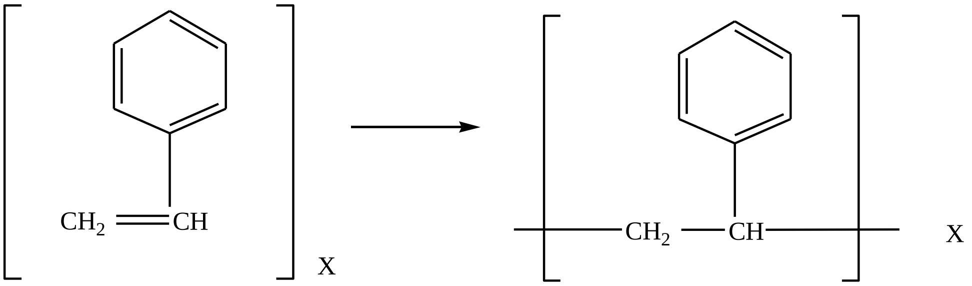

(1.17)

1.3.3. Types of polystyrene

On the basis of structure polystyrene can be classified into three forms. The polystyrene containing all of the phenyl groups on one side is of the planer zig – zag mechanism termed as isotactic polystyrene. If the phenyl groups are randomly distributed then it is called atactic polystyrene. The polystyrene containing phenyl groups on alternating sides of the chain is described as syndiotactic polystyrene (sPS)(76-77). (See Figure 1.4).

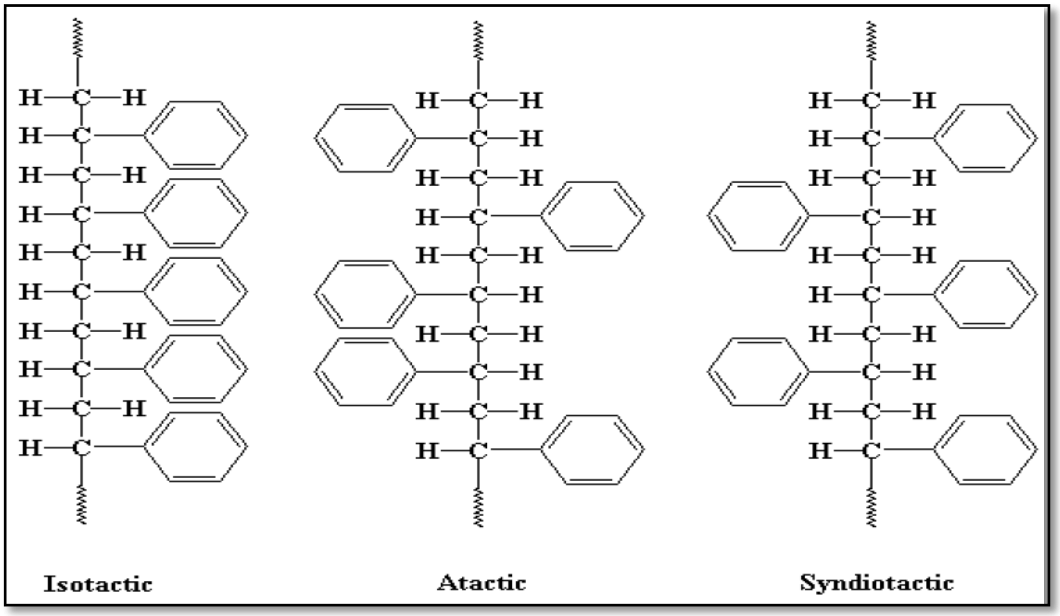

Figure (1.4) Types of Polystyrene(75)

1.3.4. Uses of polystyrene

The low cost and the good performance of Polystyrene products have increased the utilization of this polymer in buildings and other applications. PS is a type of plastic that is used for a variety of functions including in rigid items such as coat hangers, DVD cases, printer cartridges and it is used(78)for packaging , insulation materials, and in electronics, construction, house and medical ware and disposable food services(79). One of the important uses of PS is in the manufacture of cover signal lamps of some automobiles(80).

Figure (1.5) Products made from Polystyrene

Figure (1.6) Uses of PS as insulation in buildings

1.3.5. Degradation of polystyrene

Polymers are weathered due to environmental factors such as light and temperature, it loss it’s mechanical and tensile properties. Photodegradation of PS causes discoloration (yellowing), cross-linking, and chain scission(66)due to oxidation and effect of UV light and heat(81).UV light induces the production of radicals by oxidation.

1.3.6. Consumption of polystyrene in the world

The following pie chart shows world consumption of polystyrene, (see Figure 1.7):

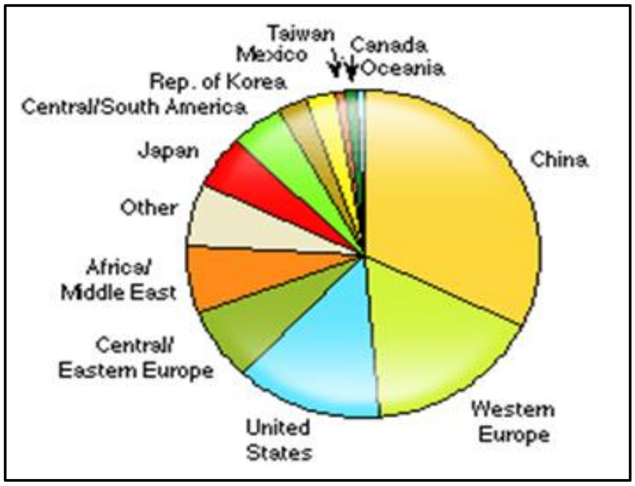

Figure (1.7) World Consumption of Polystyrene–2010

Asia is the overall leader in production and consumption of polystyrene, with 53% of total world production and 47% of total consumption of it in 2010. Of all Europe countries, France, Poland, Austria and Germany reported the highest consumption of PS. The lowest consumption was registered in Greece, Hungary, Italy and Spain.

1.3.7. Photooxidative degradation of polystyrene by radical processes

All commercial organic polymers degrade in air when exposed to sunlight. Thus the life of thermoplastics for outdoor applications becomes limited due to weathering(82).

When polystyrene is subjected to UV irradiation in the presence of air, it undergoes a rapid yellowing and embrittlement, the yellow discoloration is an important adverse effect of the ageing of polystyrene(83-85).

Irradiation of polystyrene by UV. and visible light with wavelength (λ< 400) nm., leads to the formation of radicals(86). The end groups of PS or ketonic impurities also absorb the light of wave lengths longer than 300 nm(87-88).

Absorption of light quanta by benzene rings is the first step producing excitation of the rings at excited singlet states which are transformed by intersystem crossing (ISC) to the triplet sate:

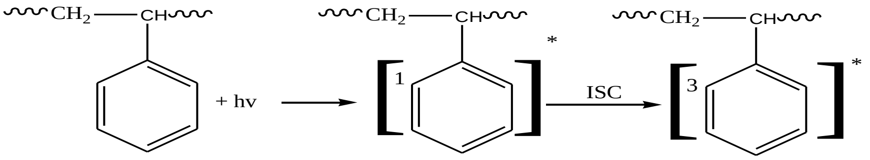

(1.18)

The secondary step in the reaction of triplet state of benzene, which occurs by one of the following two modes:

(1) Triplet energy of the excited benzene ring may be used for the dissociation of $C_6H_5 - C$ bond.

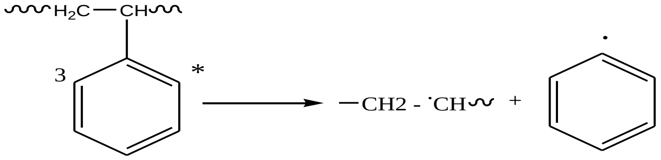

(1.19)

(2) Triplet energy excitation can be transferred by intramolecular energy transfer processes to the C – H or C – C bonds.

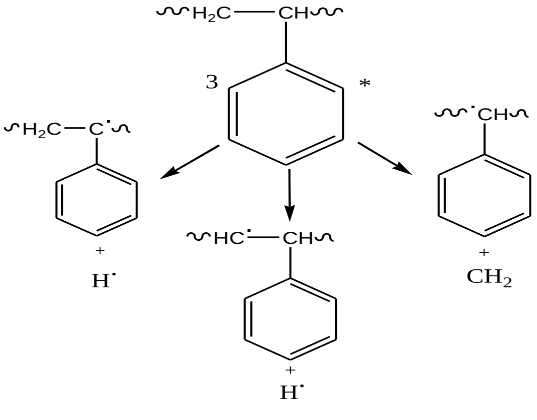

(1.20)

This mechanism proceeds through the following fundamental steps: initiation, propagation, and termination(89,90):

1.3.7.1. Initiation:

When PS is irradiated with UV radiation the phenyl ring is excited, after that resulting in cleavage of C–H bond, leading to polymer free radical formation (R·), and when two macro radicals are near to each other cross-linking may occur:

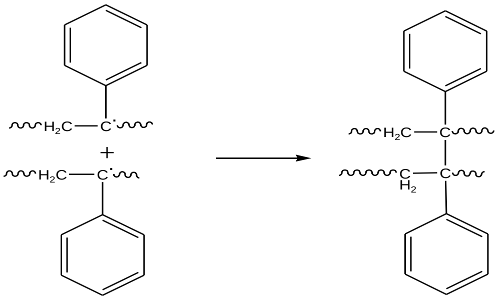

(1.21)

On the other hand, macroradicals may disproportionate leading to chain scission:

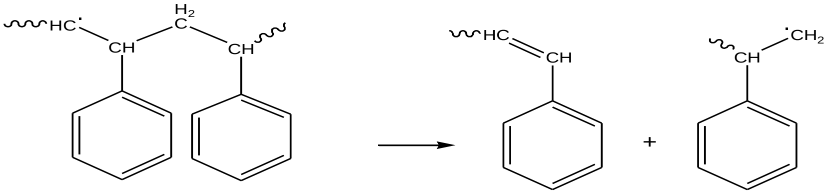

(1.22)

1.3.7.2. Propagation reaction:

Polystyrene alkyl radicals (R·) can easily react with molecular oxygen to produce peroxy radicals(91).

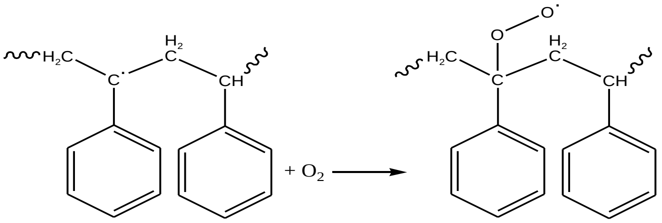

(1.23)

A polymer peroxy radical can react with the surrounding polystyrene molecule and abstract hydrogen atom:

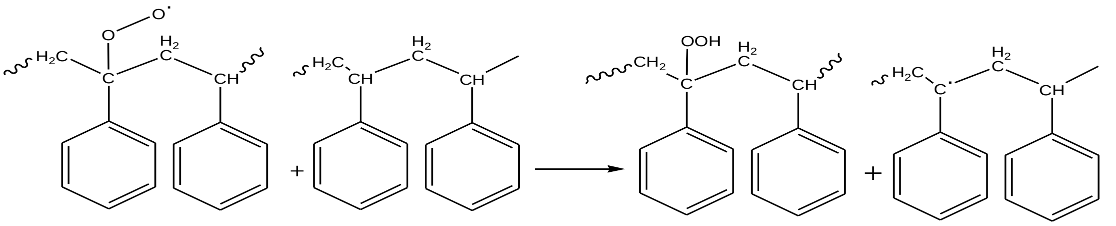
(1.24)

On exposure to light the polymer hydroperoxides can decompose according to the following reactions:

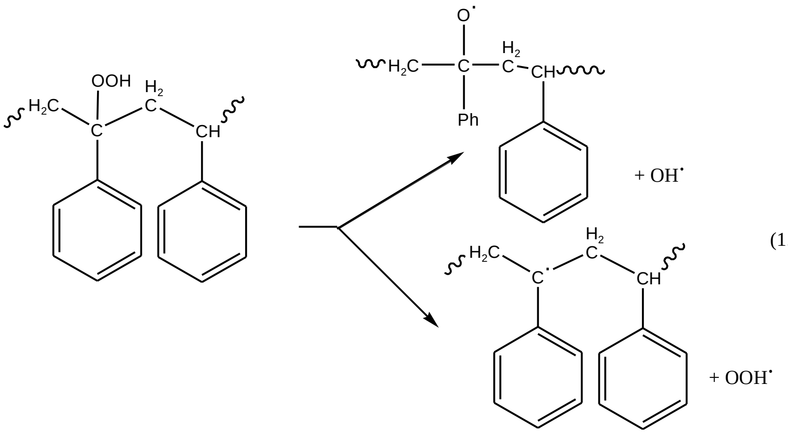
(1.25)

The produced Alkoxy polymer radicals it may decompose by β-scission reaction and to form a cetophenone and chain aliphatic ketone$^{(92, 83)}$.

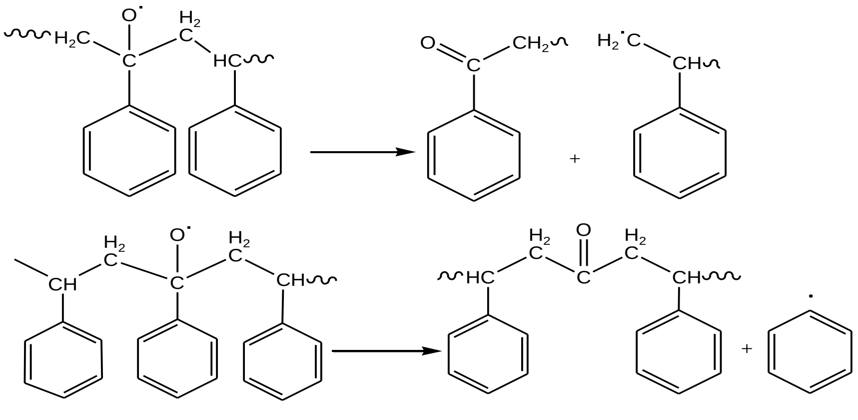
(1.26)

The general process for photodegradation of polystyrene was shown in Figure(1.8)(93) :

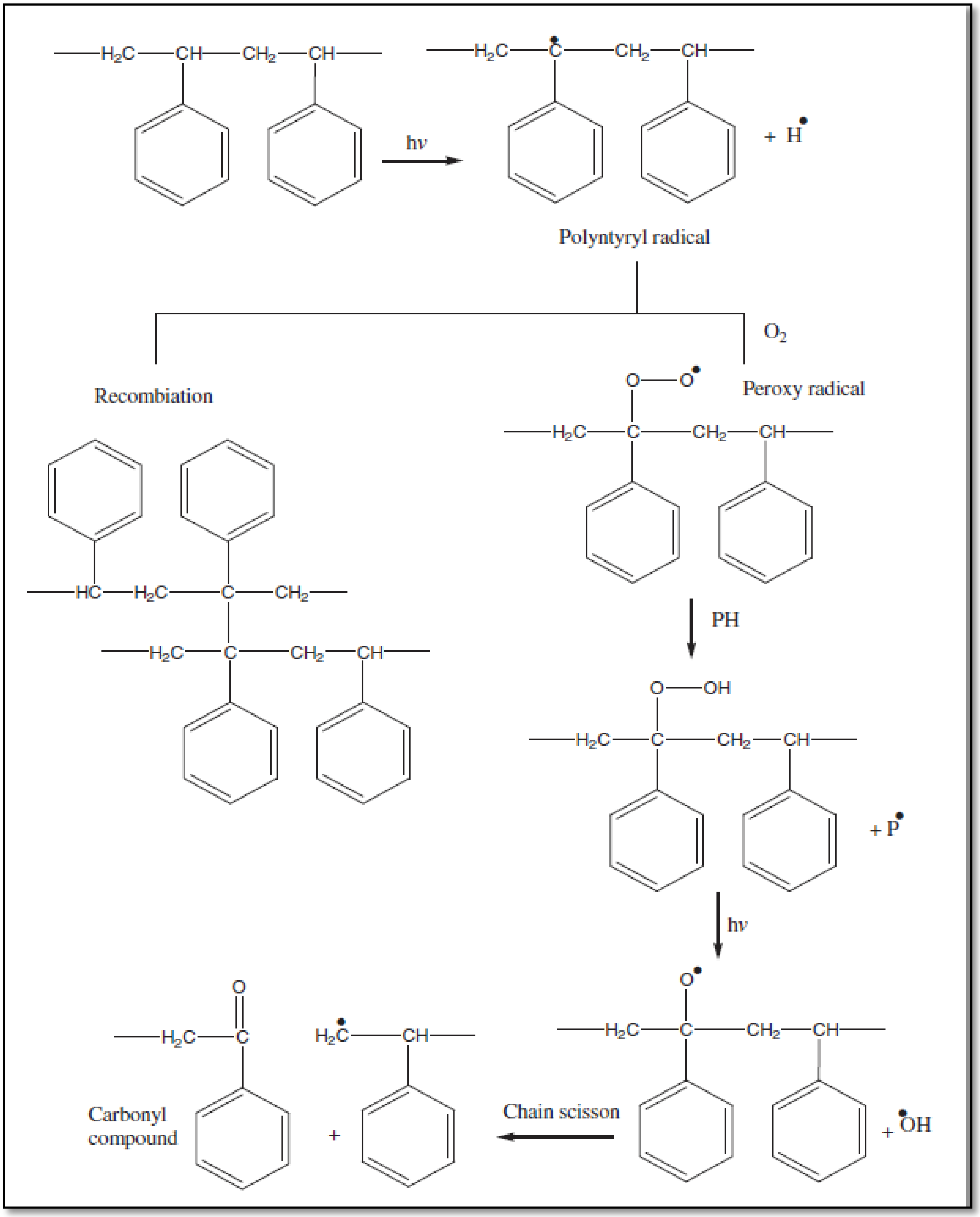

Figure (1.8) The general process for photodegradation of polystyrene (93)

1.4. Types of Photostabilization system in Polymers

It is well known that all commonly used plastics degrade under the influence of sunlight. Almost all synthetic polymers require stabilization against the adverse effects; it became necessary to find ways to prevent, or at least reduce, the damage caused by the environmental parameters such as light, air and heat. That is why the photostability of polymers is one of the most important considerations for application. The photostabilization of polymers involves the retardation or elimination of photochemical process in polymers and plastics that occur during irradiation.

The following stabilizing systems have been developed which depend on the action of stabilizer: (a) light screeners, (b) UV absorbers, (c) excited state quenchers, (d) peroxide decomposers and (e) radical scavengers. Of these, it is generally believed that types c, d and e are the most effective(71, 93).

Practice shows that when the polymer contains a photostabilizer, the oxidation rate is much reduced. Stabilizers reduce but do not completely prevent oxidation.

1.4.1. Ultraviolet Stabilizers

Ultraviolet Stabilizers additives for plastic which prevent the photodegradation or photocrosslinking caused by ultraviolet light. The UV absorber and screener operate by absorbing the incident UV radiation preventing it from reaching the bulk of the polymer and converting the energy thus acquired into a less damaging form such as heat(94).

It has been shown that urethane and silylated derivatives of hydroxybenzophenones are effective photostabilizers(95). These compounds can act as(96-98): Light screeners, excited state quenchers, Free radical scavengers, or Hydroperoxide decomposers. Hydroxy benzophenones and hydroxyphenyl bezotriazoles are the most extensively studied UV absorbers (99).

The UV stabilizer can be classified into(66):

(i) Pigments.
(ii) Metal chelates.
(iii) Carbon black.
(iv) Salicylates.
(v) Hydroxy phenyl benzotriazoles.
(vi) Hydroxy benzophenones.

Ultraviolet stabilizers can be classified according to their mechanisms of action in the photostabilization process into:

(i) UV absorber and light screeners.
(ii) Quenchers.
(iii) Hydroperoxide decomposers.
(iv) Radical scavengers.
(v) Singlet oxygen, ($^1O_2$), quenchers.

There is some of UV. absorber as shown in Figure (1.9)(36,100).

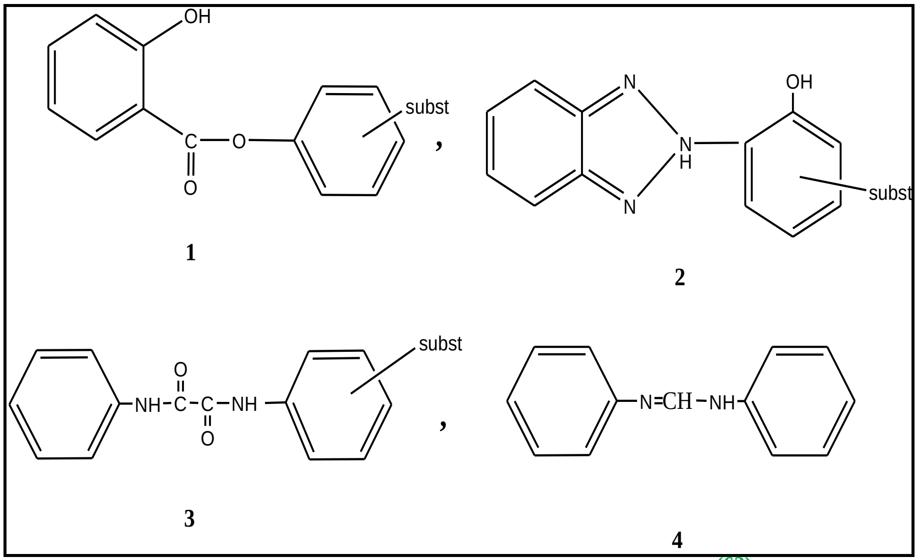

Figure (1.9) Examples of UV. absorbers (62)

1.4.2. Pigments

Pigments are insoluble inorganic and organic compounds of complex structure, such as:

(i) Powder metal (aluminum) is excellent reflector to UV light.
(ii) Fe_2O_3, Fe_3O_4, ZnO,TiO_2… are inorganic pigment excellent UV screener.
(iii) Organic pigments such as azo and anthraquenone display good UV light absorption.

Pigments used as additives*(101)*, are incorporated into polymers, coating, inks, etc…. for:

(i) Cost reduction. (ii) Reinforcement (iii) Hardening.
(iv) Improving slip and skid resistance. (v) Color effect. (vi) Storage stability.

A pigment as a light screener should be: (100)

(i) Light stable (ii) Heat stable (iii) Low cost and non-toxic

1.4.3. Carbon black

Carbon black is one of the most efficient light absorbers. It consists of very fine particles fused together to form primary aggregates. Carbon black absorbs UV radiation more efficiently than conventional pigments, carbon black are efficient light stabilizers for polymers such as polyethylene. Their high efficiency as light stabilizers is probably due to their ability to act as inner filters for UV radiation, and as radical scavengers, because many of the carbon blacks contain stable radicals(102)and quenchers of singlet and triplet states of polymers. The effectiveness of carbon blacks is dependent upon(103)the type of carbon black, the particle size and the degree of dispersion in the polymer phase.

An optimum concentration of carbon black is 3-5%. Higher than this concentration, the polymer looses it tensile strength and other mechanical properties(104).

The micro structure of carbon black particles is illustrated in Figure (1.10) (104).

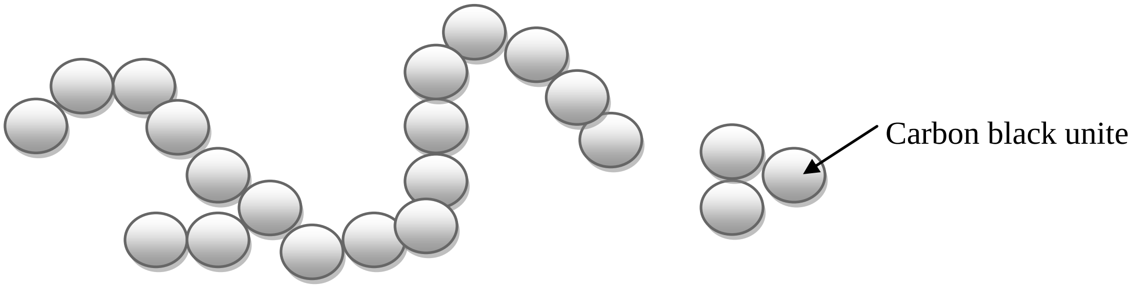

Figure (1.10) The Micro Structure of Carbon Black Particles (105)

1.4.4. Quenchers

Quenchers deactivate excited states (singlet and/or triplet) of chromophoric groups in polymers before bond scission can occur by two mechanisms (106-107).

1. Energy transfer process.
2. Chemical and/or physical deactivation.

So the Quenchers must be capable of dissipating most of the excepted energy harmlessly, without destroying the polymer bonds or it's structure.

The quenching process is successful only if the quencher molecule is within quenching distance of the excited (singlet and/or triplet) of the chromophoric group. High diffusion constants in a polymer matrix, (i.e.) good mobility of quencher and/or excited chromophoric group and long lifetime of excited chromophoric group, may therefore enlarge the apparent action sphere of the quencher(108).

Nickel chelates are very effective quenchers of the triplet state of carbonyl groups in polyolefins. These chelates have been tested for photostabilization of poly butadiene(109), polystyrene(110), poly (2,6-dimethyl-1,4-phenyloxide) and poly urethanes(111-112).

Nickel chelates can photostabilize a polymer by one or more of the following mechanisms:

(i) Quenching of the excited state of carbonyl groups.
(ii) Quenching of the singlet oxygen ($^1O_2$)(113).
(iii) Decomposing of hydroperoxides (OOH) radical, to non radical inactive species(99).
(iv) Scavenging of free radicals (alkylperoxy ($ROO^·$) and alkyloxy ($RO^·$)(114).

1.4.5. Hydroperoxide decomposer

These compounds operate by reacting directly with polymeric hydroperoxide (ROOH). The decomposition of hydroperoxide in polymer to non radical derivatives was first demonstrated(115). Compounds that belong to this type are organic phosphites and some Nickel chelates. They function by reducing hydroperoxide stochiometrically as presented in the Figure (1.11).

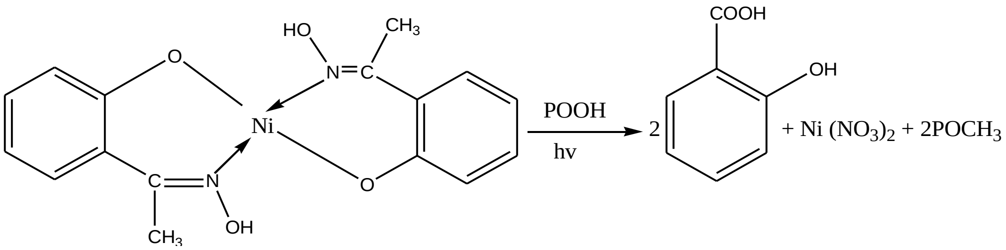

Figure (1.11) Example of Hydroperoxide Decomposer

1.4.6. Hindered amine peroxide decomposer

Hindered amine light stabilizers (HALS) have been found to be remarkably effective in performing both radical trapping and hydroperoxide decomposition. These are one of the most effective photostabilizers for polymers and have been used in a large number of commercial polymers(116).

The mechanism of (HALS) activity includes scavenging of $R^{\cdot}$, ROO and deactivation of hydroperoxides (ROOH), which are based on a complex of chemical transformations. Nitroxide the key intermediate formed from (HALS). Therefore HALS of different structure are able to interconvert in cyclic pathways, destroying species which could lead to polymer degradation and coating species which protect the polymer against degradation(116).

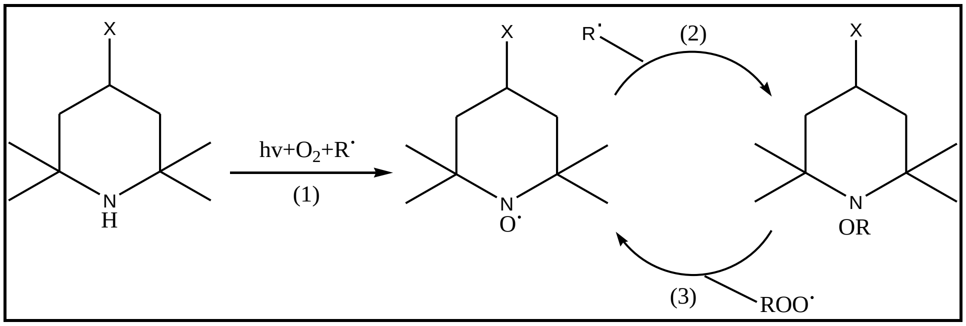

Figure (1.12) The General Cycle for Protecting the Polymer Against Degradation by HALS(116)

It has been generally accepted that hindered piperidine (e.g., 2,2,6,6-tetramethyl piperidine, which is the simplest model compound for HALS), during UV irradiation in the presence of oxygen (air) and radicals ($R^{\cdot}$), produces hindered piperidinoxy radicals according to the reaction **1**(71): Piperindoxy radicals react with alkyl radicals ($R^{\cdot}$) to give a substituted hydroxypiperidine as shown in reaction **2** in Figure(1.12). For the reaction of nitroxyl with (POOH) precedes via the formation of an intermediate (hydroxylamine) which reacts with ($PO^{\cdot}$) to generate the nitroxyl as reaction **3** as in Figure (1.12)(117). HALS reduces the photooxidation by acting as radical scavengers(118).

1.4.7. Radical scavengers

The scavenging of radical intermediates is another possibility for polymer stabilization, analogous to that used in thermal degradation. Quinones react with alkyl radicals to form radicals that do not initiate polymer oxidation.

The radicals scavengers operate by interfering with the propagating step in the oxidative chain and this can be achieved by two routes:
(i)Reaction of propagating radicals ($P^{\cdot}$, $PO^{\cdot}$ $POO^{\cdot}$).
(ii)Reaction with resulting hydroperoxide which are the source of chain branching through the propagating process(40).

1.5. Photostabilization of Polystyrene

The photostabilization process may be accomplished with commercial light stabilizers in addition to chalate complexes. The nature of the photostabilizer and polymer will determined the process and efficiency of photoprotection of the polymer film. The route by which photodegradation occurs and the importance of the impurities remaining after either polymerization or processing have to be known to determine the most satisfactory method of stabilization(110).

Complexes of 2-thioacitic acid benzothiazol have been used as additives to increase the photostabilization of polystyrene(119).

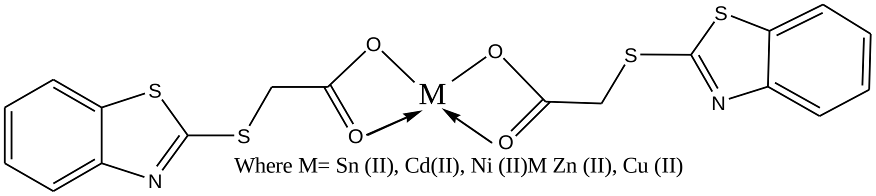

Where M= Sn (II), Cd(II), Ni (II)M Zn (II), Cu (II)

Two methods have been used to monitor the extent of photodegradation of polystyrene films. The first was by using FTIR spectra. The progress of photodegradation at different irradiation times was followed by observing the changes in carbonyl and hydroxyl peak intensities; this is called band index method. The second method involves measuring the average molecular weight using viscometry technique. These additives stabilize PS film through UV absorption or screening, and by peroxide decomposers, or radical scavengers(119).

The photochemical and photophysical protection for polystyrene by commercial UV absorbers such as 2-hydroxy-4-methoxybenzophenone and Tinuvin 327 involves triplet energy transfer from excited polymer carbonyl impurities groups in addition to UV screening(110).

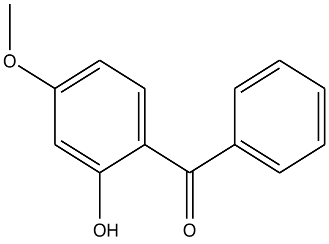

2-hydroxy-4-methoxybenzophenone

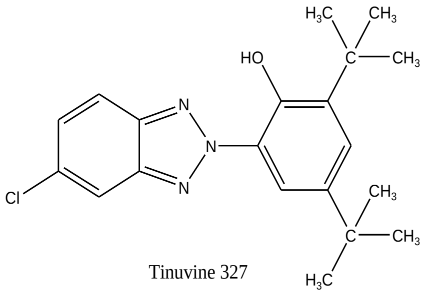

Tinuvine 327

Other categories of UV absorbers (hydroxyl phenyl pyrazole) have been shown to be able to act as photostabilizers to prevent oxidation or degradation of polystyrene(120).

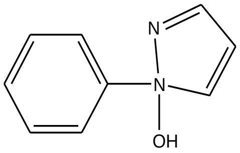

hydroxyl phenyl pyrazole

Many commercial light stabilizers have been developed in an attempt to overcome the problem of photodegeradation of PS articles. The presence of various concentrations of Tinuvin 1577(121), thiadiazole compounds(93), 2-(2-Hydroxy-5-methylphenyl)benzotriazole(122), hydroxyphenyltriazine(123)and 2,5-Dimercapto-1,3,4-thiadiazole(124)additive effectively inhibits the surface photooxidation of PS.

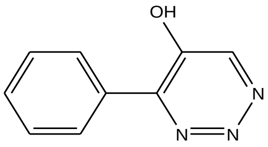

hydroxyphenyltriazine

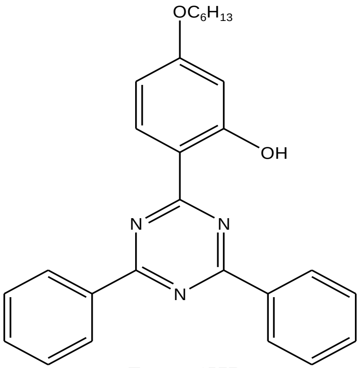

Tinuvin 1577

The photooxidation of PS decreased with addition of high molecular weight of HALS (linear peroxide amine type of new polymeric HALS) and the photostabilization efficiency was similar or better than that of Cyabsorb 3529(125).

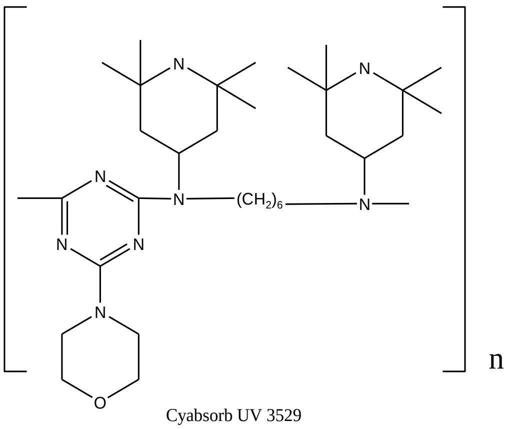

Cyabsorb UV 3529

The photostabilizing effect of 2,3 dihydro-(5-mercapto-1,3,4-oxadiazol-2-yl)-phenyl-2-(substituted)-oxazepine- 4,7-dione compounds in PS has been reported. These additives stabilize PS films through UV absorption or screening, peroxide decomposition and radical scavenging$^{(126)}$.

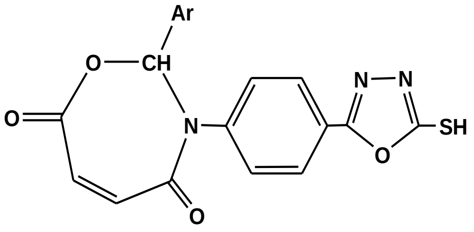

Uracil derivatives have been used as photostabilizers for PS. The results reveal a higher stabilizing efficiency for the materials investigated$^{(127)}$.

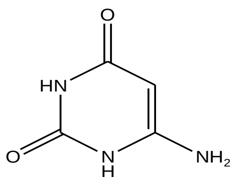

6 aminouracil

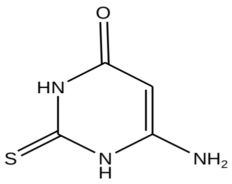

6 aminothiouracil

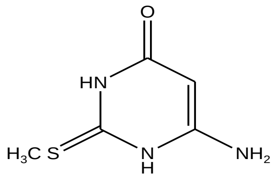

6 amino-s-methyluracil

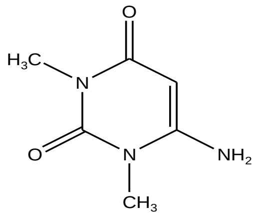

1,3-dimrthyluracil

The protection of polystyrene films by UV absorbers including Ni(II) chelate complexes has been studied. Acetylactonate of Ni(II), Cu(II), and Co (III) complexes are more efficient than the corresponding Fe(III) complex for the photostabilization of PS(128).

Photostabilization of PS films by anthraquinone derivatives and their complexes with copper(II), oxovanadium(IV) and nickel(II) ions has also been studied(129). In this work four methods have been used to monitor the degradation of polystyrene. There are: FTIR spectroscopy, UV- visible spectroscopy, solution viscosity and weight loss. The two anthraquinone derivatives and complexes provide good stabilization. Nickel and copper complexes provide better resistance to degradation than the uncomplexed anthraquinones(130).

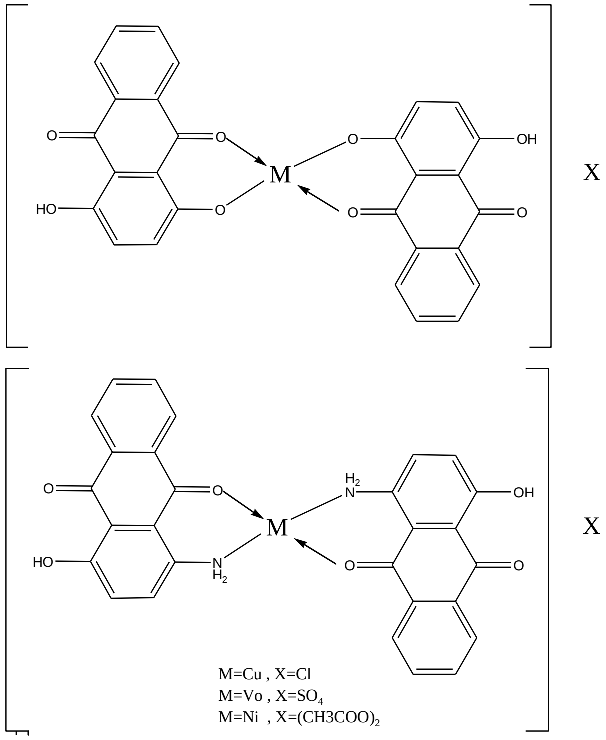

M=Cu , X=Cl
M=Vo , X=SO_4
M=Ni , X=$(CH3COO)_2$

1.6. Aim of the present work:

The aim of present research is to synthesize, characterize and study the activity of new types of transition metal complexes that might act as photostabilizer of polystyrene. These compounds are new types of 4-amino-5-(pyridyl)-4H-1,2,4-triazole -3-thiol complexes of Ni(II), Cu(II), Zn(II), Cd(II), Sn(II).

These compounds might possess the properties of UV absorption, peroxide decomposer and radical scavenger, which lead to photostablization of PS.

Chapter Two

2

EXPEREMENTAL

2.1. Chemicals

All of the reagents and starting materials used in the present work are of reagent grade and were used without further purifications unless otherwise noted. Table (2.1) shows all the utilized chemicals in the experimental course of the thesis.

Table (2.1) Chemicals and their manufacturers

No.	Compound	Formula	Mwt	Purity	Supplied from
1.	Isonicotinic acid	$C_6H_7N_3O$	137.06	96%	BDH
2.	Carbon disulfide	CS_2	76	99%	Scharlau
3.	Potassium hydroxide	KOH	56	99%	Fluka
4.	Diethyl ether	$(CH_3CH_2)_2O$	74.7	95%	BDH
5.	Ethanol	CH_3CH_2OH	46.07	99%	Scharlau
6.	Hydrazine hydride	$N_2H_4.4H_2O$	96.5	98%	Thomas BAKER
7.	Cupper acetate	$(CH_3CO_2)_2Cu$	181.5	98%	BDH
8.	Nickel nitrite	$Ni(NO_3)_2$	291	99%	BDH
9.	Tine chloride	$SnCl_2$	190	99%	Fluka
10.	Zinc acetate dihydrate	$(CH_3CO_2)_2Zn.2H_2O$	219.5	98%	Fluka
11.	Cadmium acetate	$(CH_3CO_2)_2Cd.2H_2O$	266.5	98%	Fluka
12.	Methanol	CH_3OH	32.03	99%	Scharlau
13.	Dimethyl sulfooxide	DMSO = $(CH_3)_2SO$	78.13	98%	Merck
14.	Chloroform	$CHCl_3$	119.38	99%	Hopkin and Williams
15.	Polystyrene	PS = $(C_8H_8)_n$	n(133)	97%	BDH

2.2. Instruments

2.2.1. Melting point

The melting points were determined on electro thermal capillary apparatus, Coslab melting point. In laboratories of Chemistry department / College of Science / Al-Nahrain University and in Ibn Sina state company.

2.2.2. Fourier Transform Infrared Spectroscopy (FT-IR)

The FT-IR spectra in the range (4000-200) cm^{-1} cut were recorded as KBr and by using CSI disc on FT-IR.8300 Shimadzu Spectrophotometer. In laboratories of Chemistry department / College of Science / Al-Nahrain University and in Ibn Sina state company.

2.2.3. Ultraviolet-Visible Spectroscopy (UV-Vis)

The UV-visible spectra were measured using Shimadzu UV-Vis. 160 A-Ultra-violet Spectrophotometer in the range (200-1000) nm. in laboratories of Chemistry department / College of Science / Al-Nahrain University

2.2.4. Magnetic susceptibility measurements

The magnetic susceptibility values of the prepared complexes were obtained at room temperature using Magnetic Susceptibility Balance of Johnson Matthey (England) . In laboratories of Chemistry department / College of Science / Al-Nahrain University

2.2.5. Conductivity measurements

Conductivity measurements were carried out by using WTW conductivity meter, by using ethanol as solvent and 10^{-3} g. laboratories of Chemistry department / College of Science / Al-Nahrain University

2.2.6. Nucleir Magnetic Resonance (NMR)

^{1}H NMR spectra were obtained with Bruker spectrophotometer model ultra shield at 300 MHz in DMSO- d6 solution with the TMS as internal standard. In AL-Albait University/ Amman/ Jordan.

2.2.7. Microscope

Morphlogical observations were obtained by using MEIJI TECHNO (Japan) microscope, the magnification ratio is 400 times. In Chemistry department / College of Science / Al-Nahrain University.

2.3. Synthesis

2.3.1. Synthesis of 4 amino-5-(pyridyl)-4H 1,2,4 triazole -3-thiol (Ligand)(130)

A mixture of the isonicotinic acid (1 g), (0.0072 mol) and (0.44 g), (0.008 mol) from potassium hydroxide, was dissolved in (10 cm^{3}) absolute ethanol with stirring. After the mixture was dissolved then (2 cm^{3}), (0.014 mol) from carbon disulfide was added slowly - Add excess from KOH and CS_2 - at room temperature which the color of mixture immediately change from white to orange color. The reaction mixture was stirred for 10 hours. Dry ether (10 cm^{3}) was added and a yellow precipitate was then collected by filteration, washed with ether and dried. The salt was obtained in almost quantitative yield and was employed to the next step.

Excess of hydrazine hydride (20 cm^{3}) was added to the yellow precipitate (potassium salt), and it was refluxed for 10 hos. by using water path with stirring until the evaluation hydrogen sulfide; it was ceased by lead acetate paper. During reflex the color of reaction changed to dark green, producing a clear homogenous solution.

After cooling the reaction mixture was filtered. Then the filterate diluted by 10 cm^3 of water and then was acidified by concentrated hydrochloric acid the resultant white precipitate collected by filtration and dried at room temperature. Yield (62 %) according to potassium's salt, m.p. (210-214).

2.3.2. Synthesis of Ligand's Complexes(131)

(0.23 g) from cupper(II) acetate, (0.24 g) from tine (II) chloride, (0.28 g) from zinc (II) acetate dihydrate, (0.34 g) from cadmium(II) chloride and (0.37 g) from nickel (II) nitrite was dissolved in (5 cm^3) ethanol and was added to (5 cm^3) ethanolic solution of (0.5 g) from ligand.

The molar ratio [2: 1] from [ligand: metal] was carried out. After reflux for 2 hours, crystalline colored precipitate was formed.

The precipitate was filtered and dried at room temperature. Then the precipitate was washed by hot methanol to yield a purified precipitate.

2.4 Experimental Technique

2.4.1. Films preparation(132)

A solution of polystyrene (5% w/v) in chloroform was used to prepare (40µm) thickness of polymer filmS. The films were prepared by evaporation technique at room temperature for 24 hours, to remove the possible residual chloroform solvent.

After Polystyrene solution was prepared, then poured it into glass's sinks. This sinks was made by glue the laboratory glass's slides onto a piece of regular glass, to obtain small sinks, their volume is (4 cm^3), which is illustrated in Figure (2.1).

Figure (2.1) picture of glass's sinks

After the evaporation of solvent, that's led to formation of PS films. The thickness of these films is about (40 µm), these films were paste onto cartoon papers, these papers contain hole in dimension (2x2). Modified PS can be prepared by mixing of (0.5%) by weight complexes to the solution containing polystyrene.

2.4.2. Incident Light Intensity Measurement

The intensity of the incident light (I_o) was measured by the use of potassium Ferrioxalate actinometer methods as described by Hatchard and Parker(133).

The actinometer solution (6 x 10^{-3} M) was prepared by dissolving (3.00 g) of $K_3 [Fe(C_2O_4)_3].3H_2O$ in (800 cm^3) of distilled water, then (100 cm^3) of (1 N) H_2SO_4 was added and the whole solution was diluted to one liter with distilled water. The actinometer solution absorbed 100% of incident light at λ= 365nm.

The light intensity measurement involves irradiation of the actinometer solution for known period of time (3 min.); ferrous ion concentration was estimated spectrophotometrically using (0.1 %) 1-10-phenathroline as complexing agent.

According to the Hatchard and Parker, Ferric ions are reduced to Ferrous ion:

$(Fe^{3+} \longrightarrow Fe^{2+})$. ………………..(2.1)

Thus the phenathroline complex is formed with $Fe^{+2,}$ which strongly absorbed at 510nm. For Fe^{2+} formation equation(2.1) the quantum yield (Q) is known and equal (1.24), so the intensity of light can be calculated, after a calibration curve for Fe^{+2} was obtained using the following solution:

i. $4*10^{-4}$ M of $FeSO_4$ in 0.1 N H_2SO_4.
ii. 0.1% w/v phenanthroline monohydrate in water.
iii. Buffer solution was prepared from mixing (600 ml) 1N CH_3COONa and (360 ml) of 1N H_2SO_4 dilute to 1L. Solutions of different concentrations of Fe^{+2} were prepared from solution (i) by taking different amount in 25 ml. volumetric flask, to each **a-** (2 ml) phenanthroline solution was added, **b-** (5ml) of buffer solution, **c-** 0.1 N H_2SO_4 was added to make the acid

equivalent to ($10cm^3$) of 0.1 N H_2SO_4 and diluting the whole solution to ($25cm^3$) with distilled water. The volumetric flasks were covered with aluminum foil, and kept in the dark for (30 min). Then the optical densities were measured at λ=510 nm.

The plot of absorbencies verses Ferrous ion concentration was straight line, the obtained slope gives the extinction coefficient of $FeSO_4$ solution, which is equal to ($\varepsilon = 1.21 \text{ X } 10^4 \text{ mol}^{-1}. \text{ dm}^3. \text{ cm}^{-1}$).

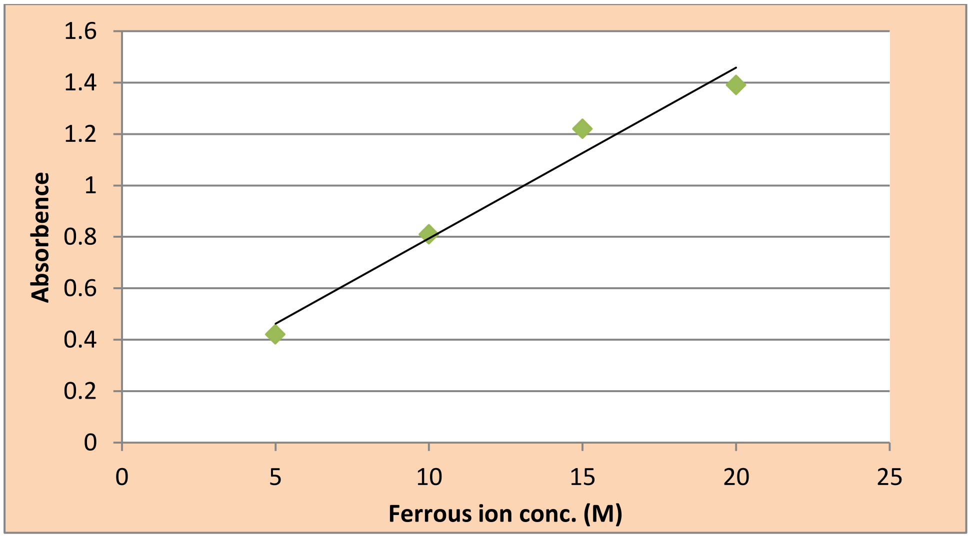

Figure (2.3) Calibration curve

In order to determine the light intensity, (3 cm^3) of actinometer solution was put in irradiation cell. The cell was irradiated in the same position used for irradiation samples.

After illumination, (1 cm^3) of irradiated solution was transferred to volumetric flask (25 cm^3), (2 cm^3) of solution (ii) phenanthroline monohydrate in water and (0.5 cm^3) of solution (iii) (Buffer solution) then complete the volume to (25 cm^3) with distilled water.

Blank solution was prepared by mixing 1cm^3 of unirradiated mixture Ferrioxalate solution with other components. The solution was allowed in the dark for (30 min). and then the optical density was measured at (λ=510 nm.). The intensity of incident light was calculated using the following relation: (134)

$$I_o = \frac{A \times V_1 \times 10^{-3} \times V_3}{Q_\lambda \times \varepsilon \times V_2 \times t} \text{ einstein dm}^{-3}\text{ sec}^{-1} \qquad (2.2)$$

I_o= Intensity of incident light.

A= Absorbance at λ= 510.

V_1= Initial volume.

V_2= Volume used of irradiation solution.

V_3= Final volume (25cm^3).

Q_λ= Quantum yield (1.24).

ε= Molar extinction coefficient (slope of calibration curve).

t= Irradiation time in seconds.

2.4.3. Accelerated testing technique

UV- Light was used for irradiation of PS films, giving wavelength range between (250 to 380 nm) and the maximum wavelength light intensity is at 6.2 X 10^{-9} Ein Dm^{-3} S^{-1}. The polymer film samples were fixed parallel to each other and the lamp of the UV. incident radiation is vertically incident on the samples. The distance between the polymer films and the source was (10 cm).

2.5. Photodegradation Measuring Methods

2.5.1. Measurement of the Photodegradation Rate of Polymer Films using Infrared Spectrophotometery(135)

The photodegradation of polymer film samples were followed using Shimadzu Spectrophotometer. The absorption spectra of the film samples were recorded in the range of (4000-400) cm^{-1}. The position of carbonyl absorption is assigned at 1730 cm^{-1}, and hydroxyl is assigned in 3400cm^{-1}(136).

The photodegradation during different irradiation times were followed by observing changes in carbonyl and hydroxyle peaks. Then carbonyl (I_{CO}) and hydroxyle (I_{OH}) indices were calculated by comparison of the FTIR absorption peak at 1730 cm^{-1} and 3400 cm^{-1} with reference peak at 1450 cm^{-1}, respectively. This method is called band index method(136)which includes:

$$Is = \frac{As}{Ar} \text{..................}(..2.3)$$

As = Absorbance of peak under study.
Ar = Absorbance of reference peak.
Is = Index of the group under study.

The percentage transmittance (%T) is change into absorbance (A) using Beer-Lambent law as in the following equation. (2.4):

$$\left.\begin{aligned} A &= \log(100/\%T) \\ A &= \log 100 - \log\%T \\ A &= 2 - \log\%T \end{aligned}\right\} \text{..............}(2.4)$$

Actual absorbance, the difference between the absorbance of base line and top peak (A Top Peak – A Base Line), is calculated using the Base Line method.

2.5.2. Measurement of the Photodegradation Rate of Polymer Films Using Ultraviolet-Visible Spectrophotometer(137)

The ultraviolet-visible spectrophotometer type Shimadzu UV-VIS. 160 was used to measure the changes in the Uv-visible spectrum during irradiation time for each compound at maximum absorption band (λ_{max}). The absorption spectrum was measured in the range of (200-400nm), and the (λ_{max}) at each absorption was also recorded for different irradiation times.

The infinite irradiation time was considered and the infinite absorption (A_∞) was assumed to be after the infinite irradiation time.

To determine the photodegradation rate constant for photostabilizer (K_d), the first order equation was used:

$$\ln(a-x) = \ln a - K_d\, t \;\ldots\ldots\ldots\ldots\ldots..(2.5)$$

Where a, represent the stabilizer concentration before irradiation, x represents the change in stabilizer concentration after irradiation time (t).

If A_o represents the absorption intensity of the polymer film containing stabilizer before irradiation, A_t represents the absorption intensity after t time of irradiation, then:

$a = A_o - A_\infty$

$x = A_o - A_t$

$a - x = A_o - A_\infty - A_o + A_t = A_t - A_\infty$ ………… (2.6)

Substitution of a and (a - x) from equation (2.6) in (2.5) gives:

$\ln(A_t - A_\infty) = \ln(A_o - A_\infty) - K_d t$ …………… (2.7)

Thus a plot of $\ln(A_t - A_\infty)$ versus irradiation time (t) gives straight line with a slope equal (K_d) which indicates that photodecomposition of the additives is first order.

2.5.3. Determination of Viscosity Average Molecular Weight by Using Viscometer Method(138)

The viscosity property was used to determine the molecular weight of polymer, using the Mark- Houwink relation·

$[\eta] = KM_v^\alpha$...............(2.8)

$[\eta] =$ intrinsic viscosity.

K, α = are constants dependent upon the polymer-solvent system at a particular temperature.

The intrinsic viscosity of a polymer solution was measured with an Ostwald U-tube viscometer. Solutions were made by dissolving the polymer in a solvent (gm/100 ml) and the flow times of polymer solution and pure solvent are t and t_o respectively. Specific viscosity (η_{sp}) was calculated as follows:

$$\eta_{re} = \frac{t}{t_o} \text{....................(2.9)}$$

η_{re} = Relative viscosity .

$$\eta_{sp} = \eta_{re} - 1 \quad \text{…..………………..(2.10)}$$

The single – point measurements were converted to intrinsic viscosities by the relation (2.11).

$$[\eta] = \left(\sqrt{2}/c\right)\left(\eta_{sp} - \ln\eta_{re}\right)^{1/2} \qquad \text{.....................(2.11)}$$

C = Concentration of polymer solution (gm/100ml).

Molecular weights of PS with and without additives were calculated from intrinsic viscosities measured in Chloroform solution.

$$[\eta] = 4.17 \text{ X } 10^{-4} M_v^{0.66} \qquad \text{------------(2.12)}$$

The most common solution viscosity terms are: relative viscosity, specific viscosity, inherent viscosity and intrinsic viscosity(139).

The quantum yield of main chain scission (ϕ_{cs}) was use to viscosity measurement using the following relation.

$$Q_{cs} = (CA/\overline{M}_{v,o})\left[\left([\eta_o]/[\eta]\right)^{1/\alpha} - 1\right]/I_o t \text{..............} (2.13)$$

Where:

C = concentration.

A = Avogadro’s number.

$(M_{v,o})$ = the initial viscosity - average molecular weight.

$[\eta_o]$ = Intrinsic viscosity of polymer before irradiation.

$[\eta]$= Intrinsic viscosity of polymer after irradiation.

α = Exponent in the relation: $[\eta] = KM^{\alpha}$.

I_o = Incident intensity.

t = Irradiation time in second.

2.5.4. Measurement of the Photodegradation by Weight loss (140)

The stabilizing efficiency was determined by measuring the % weight loss of photodegraded PS films in absence and in presence of additives by applying the following equation:

$$\textbf{Weight loss \%} = [(W_1 - W_2) / W_1]\ 100 \qquad (2.14)$$

Where W_1 is the weight of the original films (PS blank and modified PS) before irradiation and W_2 is the weight of the sample after irradiation.

2.5.5. observation of the Photodegradation by Morphology Study(141)

To examine the surface morphology of the irradiated polymer films, the lab. microscope was used for this purpose; it shows the top surface of the irradiated films.

The surface morphology of films of the non irradiated PS blank and PS in the presence of the five types of additives, Irradiated for 0 h, 100 h, 200 and 300 h was studied.

Chapter Three

3

RESULTS & DISCUSSION

3.1 Identification of prepared complexes

The steps of synthesis of 4-amino-5-(pyridyl)-4H 1,2,4 triazole -3-thiol (ligand) is showed in Scheme (3.1)

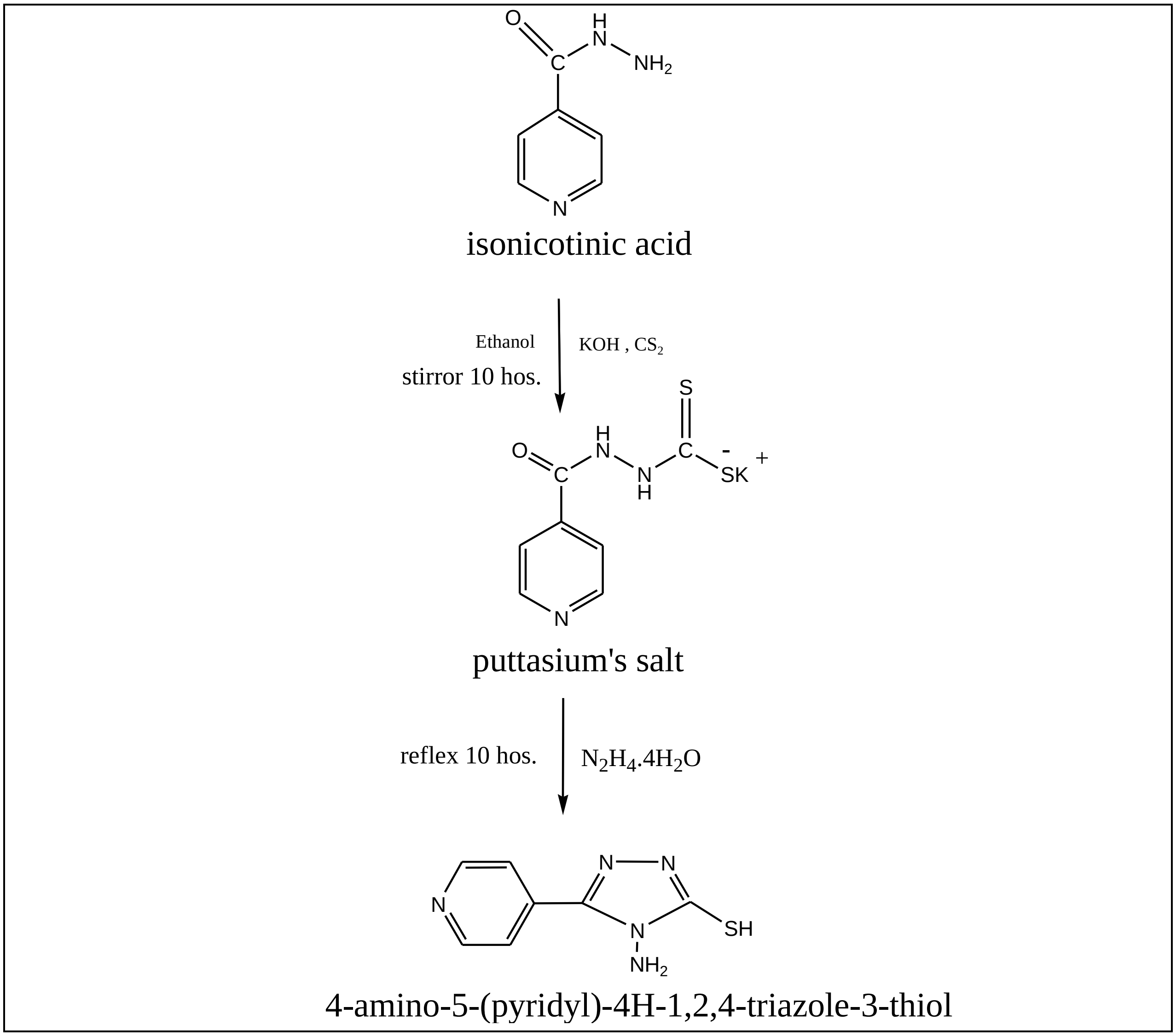

Scheme (3.1) The chemical steps for synthesis of ligand

The steps of preparation of the complexes can be shown in Scheme (3.2):

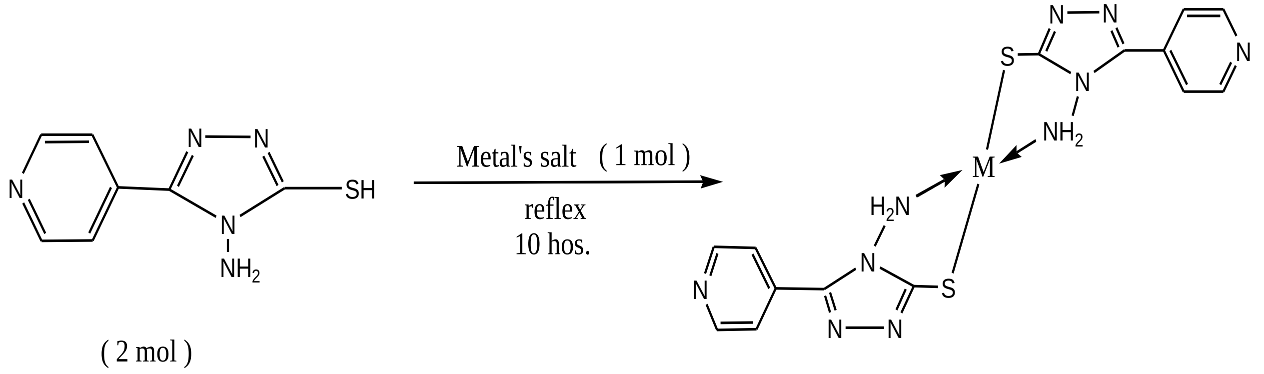

Scheme (3.2) The chemical steps for synthesis of Complexes

3.1.1 Physical properties of prepared complexes

Melting points and physical properties of all the compounds studied are tabulated. The physical analytical data, melting point, molecular weight of (L) and its complexes are tabulated in Table (3.1).

Table (3.1) Physical data of prepared complexes

Compounds	**Color**	**M.P. C^{o}**	**Mwt $g.mol^{-1}$**	**Yield**
L	White	212-214	193	62%
$Ni(L)_2$ 1	Green	240-242	442.7	77%
$Cu(L)_2$ 2	Dark green	222-224	447.5	81%
$Zn(L)_2$ 3	Pale yellow	178-180	449.4	75%
$Cd(L)_2$ 4	White	255-257	496.4	41%
$Sn(L)_2$ 5	Yellow	230-232	502.7	10%

3.1.2. Characterization of prepared complexes by Infra-Red spectroscopy

The infra-red spectrophotometer technique was used to characterize the prepared compounds through the assignment of stretching vibration bands. The FTIR spectrum of this ligand (L) showed some characteristic stretching bands at: 3250 cm^{-1} and 3213 cm^{-1}, 2736 cm^{-1}, 1645 cm^{-1}, 673 cm^{-1} assigned to NH_2, S-H, C=N of triazole ring, and the last one is for stretching of C-S bond, respectively(142-145).

The tatumerisum form could occur in triazole ring(7), see Figure (3.1). It is responsible to expect deprotonation of ligand molecule before complexation, the complete disappearance of the band due to υ(S-H) in the spectra of complexes unambiguously support this view. After deprotonation, the ligand can link with the metal ion at either by N or S atom of thioamid group. Bonding at S atom is more favorable because such a thing would result in a stable five membered chelate(146).

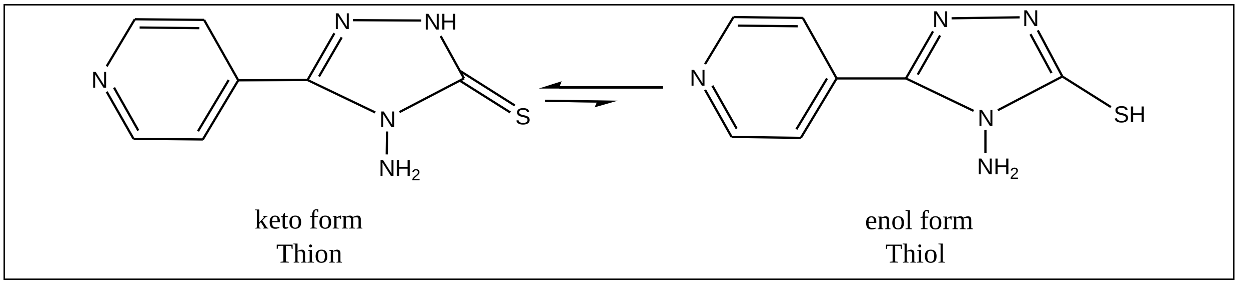

Figure (3.1) tatumerisum form in triazole

The exceptional case is that the υ(C = N) of complexes **1–5** were found to be shifted to a lower wave number compared to the ligand indicated the coordination with the ligand(147). The frequencies of NH_2 bands were shifted due to complexation. The band of S-H in the ligand was disappeared when complexation occur, but the bands of C-S also shifted to the higher frequency result from complexation of the metal ion to the ligand through sulfate, and the band of C = N is shifted to the lower frequency due to complexation, and the other bands such as C = C (1590-1660) cm^{-1}, C-H aromatic (3010-3080) cm^{-1} were didn't show any shifting because they aren't participate in the complexation(148).

Another new bands was appeared which were supported by the appearance frequencies of M-S, M-N(149-151). The major IR bands and their probable assignment are given in Table (3.2):

Table (3.2) key infrared data of L and complexes1-5

Compounds	**υ NH_2**	**υ -S-H**	**υ C=N**	**υ C-S**	**υ M-N**	**υ M-S**
L	3250, 3213	2736	1645	673	-	-
$Ni(L)_2$ 1	3280, 3228	-	1643	690	530	459
$Cu(L)_2$ 2	3321, 3286	-	1620	694	532	428
$Zn(L)_2$ 3	3329, 3286	-	1640	694	529	432
$Cd(L)_2$ 4	3298, 3245	-	1639	693	528	451
$Sn(L)_2$ 5	3200, 3165	-	1643	690	528	432

The FTIR spectrum of ligand and its complexes was shown in Figures (3.2) - (3.7).

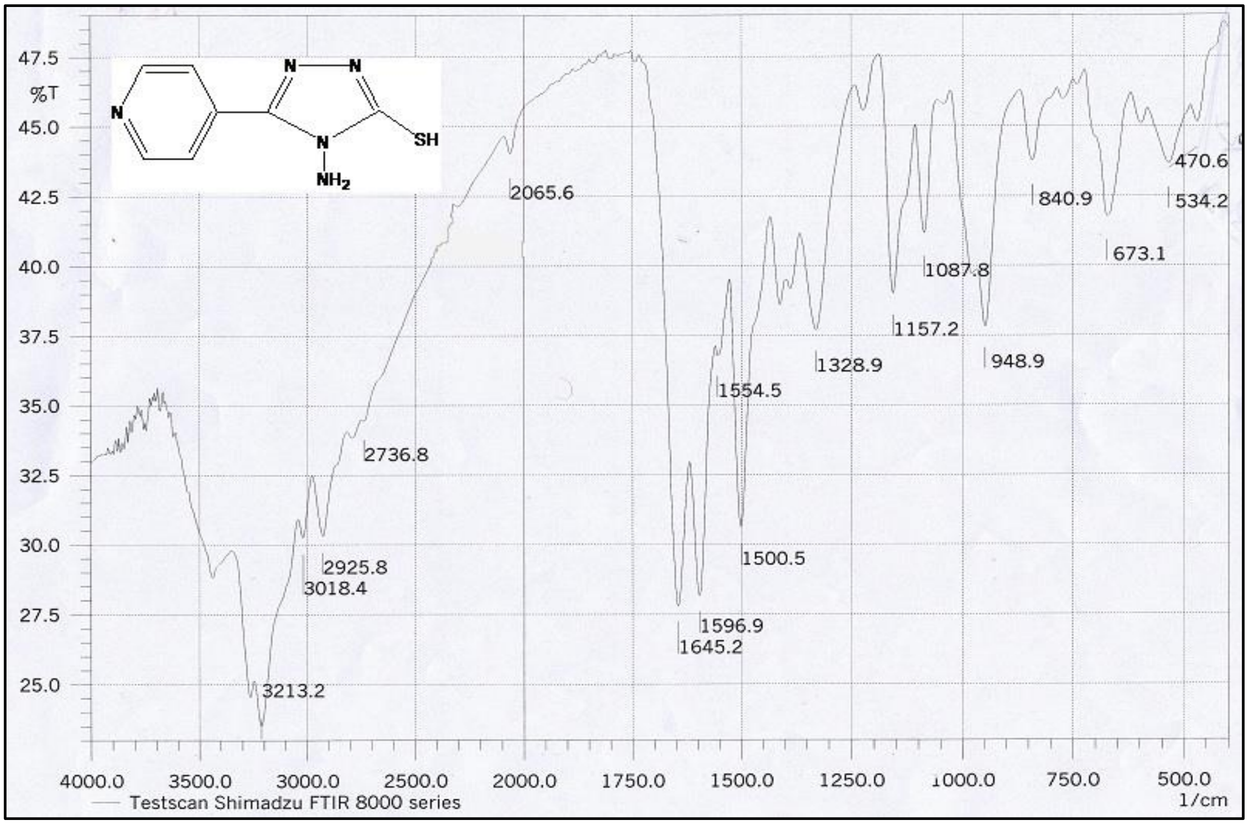

Figure (3.2) FTIR spectrum of ligand

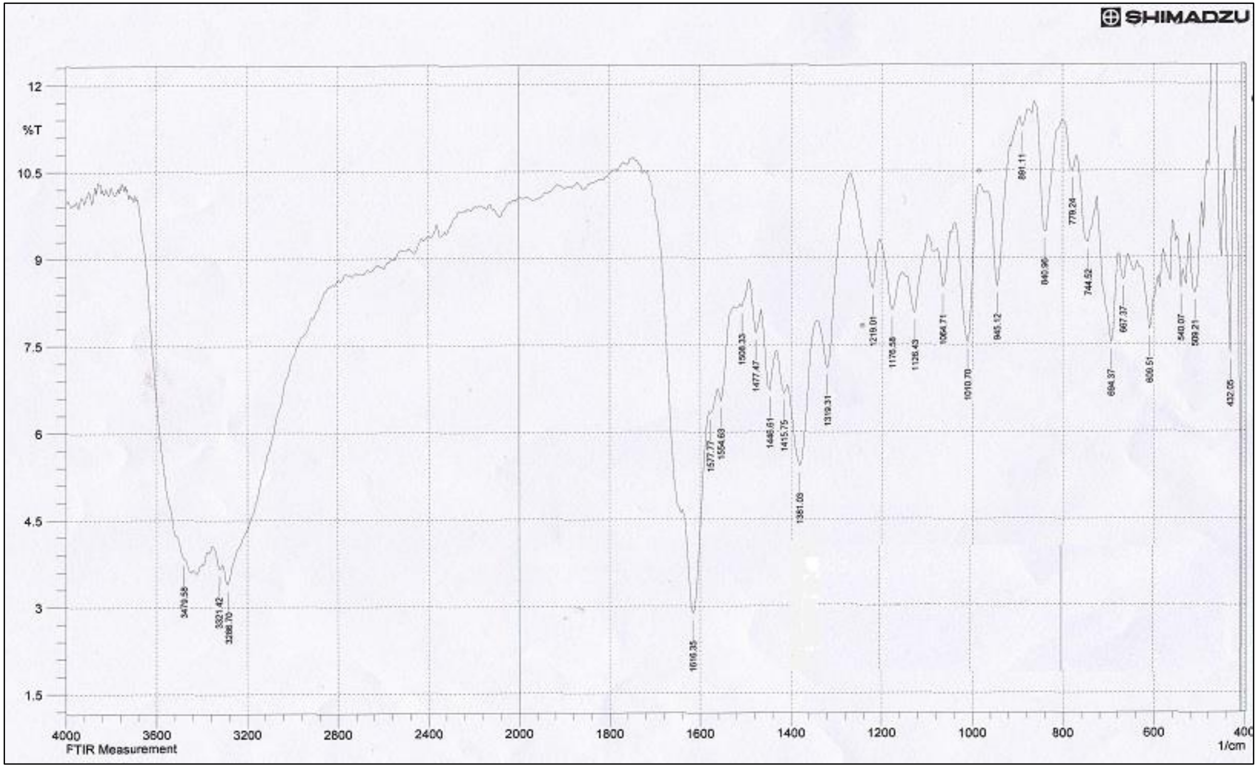

Figure (3.3) FTIR spectrum of Cu(L)$_2$

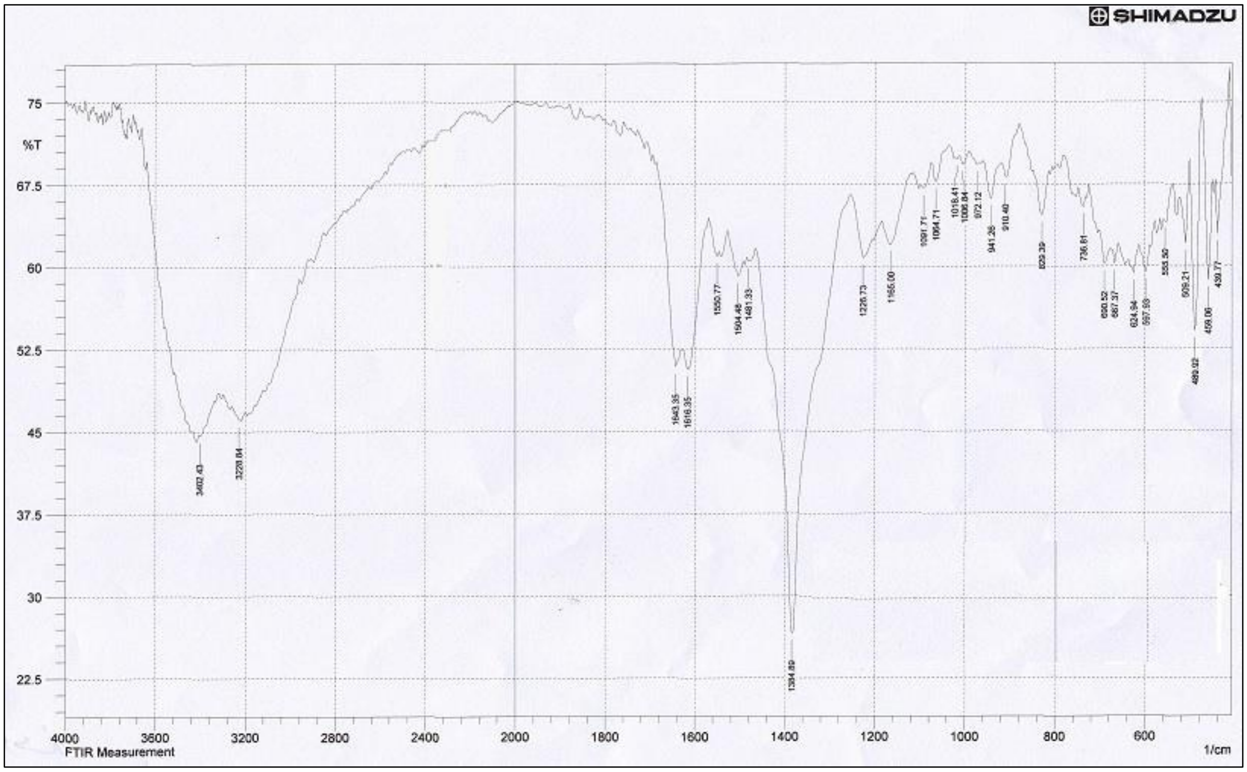

Figure (3.4) FTIR spectrum of Ni(L)$_2$

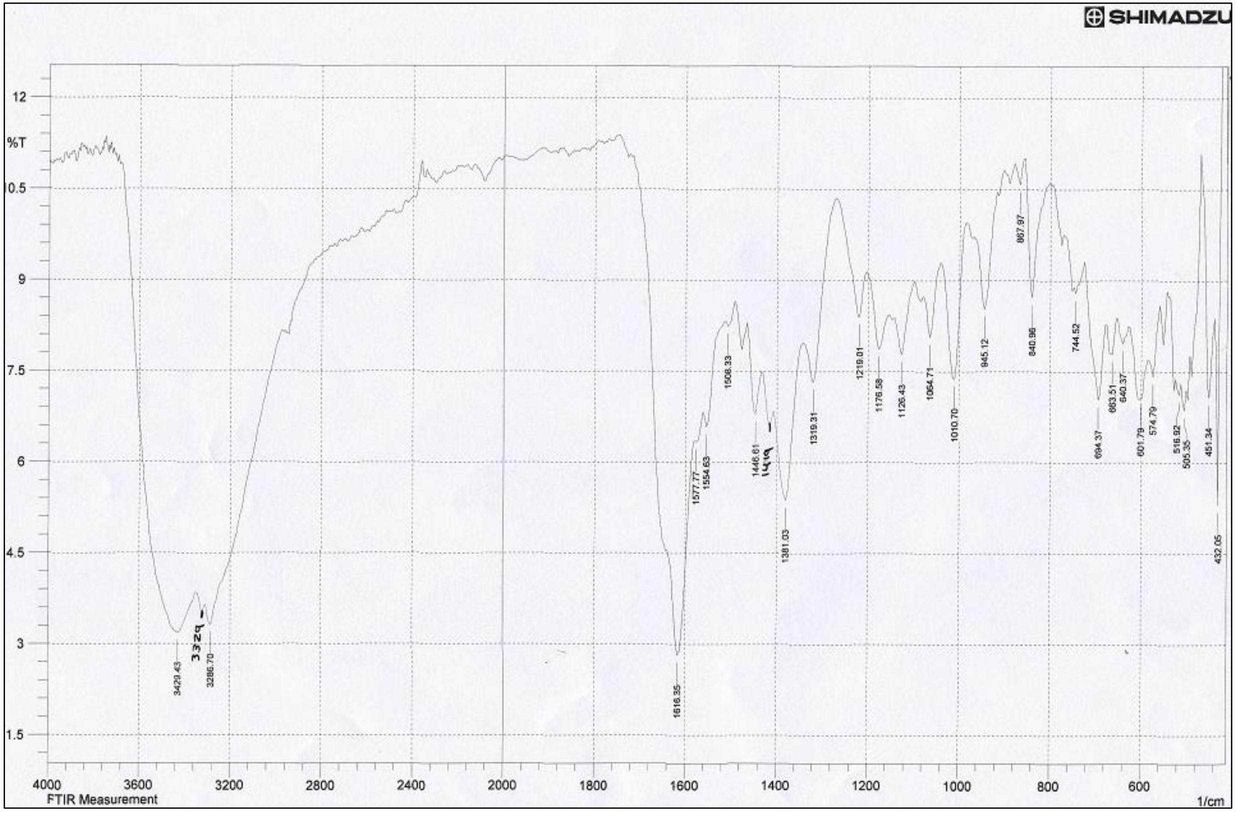

Figure (3.5) FTIR spectrum of Zn(L)$_2$

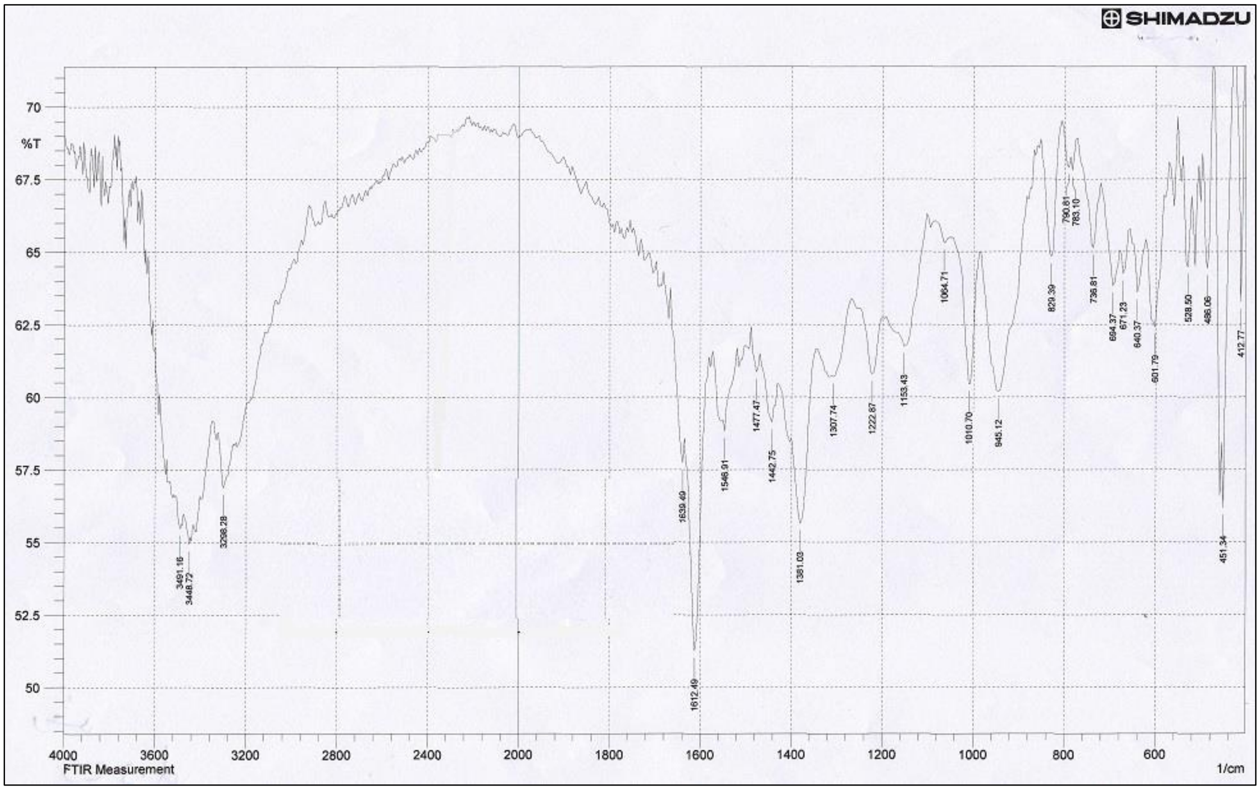

Figure (3.6) FTIR spectrum of Cd(L)$_2$

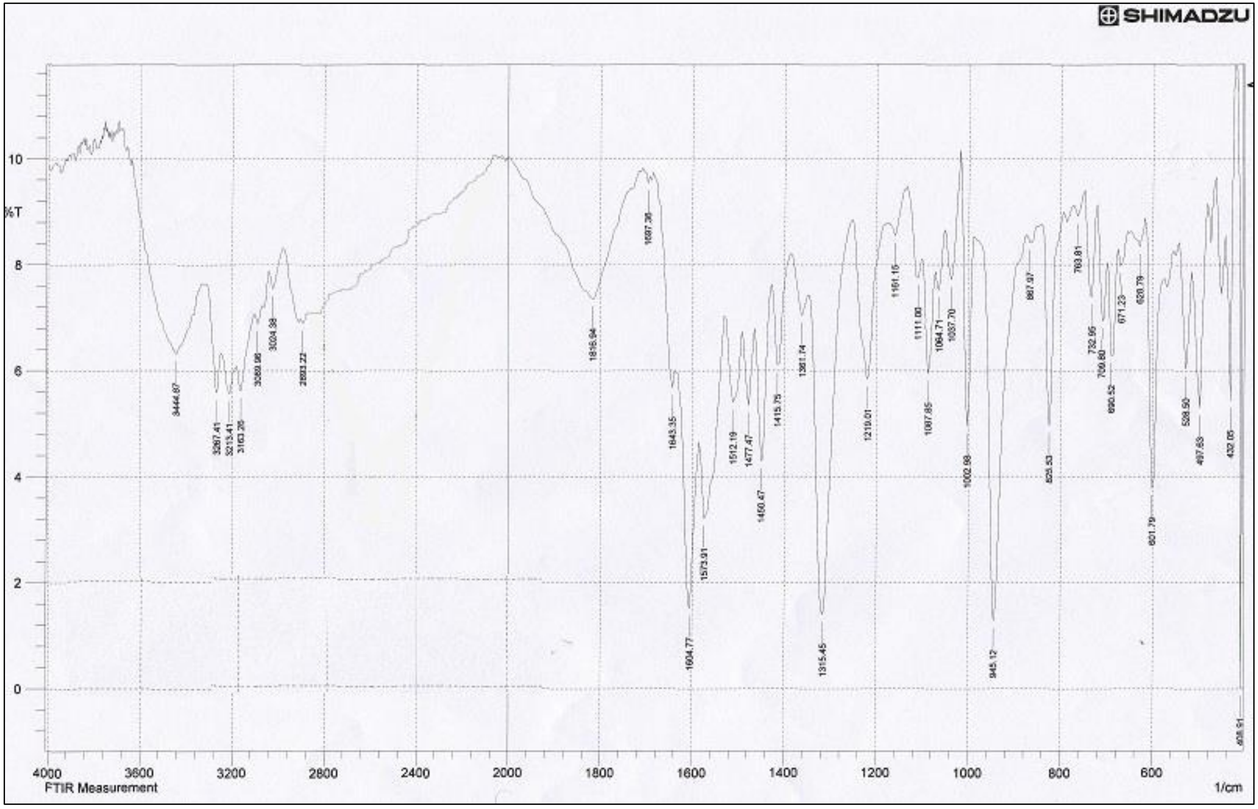

Figure (3.7) FTIR spectrum of Sn(L)$_2$

3.1.3. Characterization of prepared complexes by Nuclear magnetic resonance

The data of ^{1}H NMR and ^{13}C NMR of 4-amino-5-(pyridyl)-4H-1,2,4-triazole-3-thiol and its complexes displayed good solubility in DMSO. The proton nuclear magnetic resonance spectral data gave additional support for the composition of the complexes. The observed changes are evidences of complexation had happened because the chemical shift of a compound is heavily depended on its electronic environment$^{(152-154)}$.

Note: for all ^{1}H NMR spectra, the peaks at 2.5 for the solvent (DMSO-d6).

Ligand:

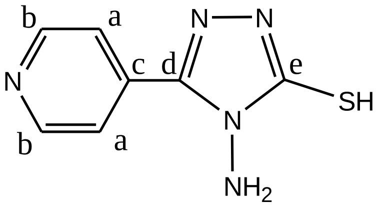

^{1}H NMR data (ppm), δ_{H}(300 MHz, DMSO-d$_6$): Figure (3.8) shows signals at 5.301 (2H, s, NH$_2$), 8.014,8.025-8.744,8.755 (4H, d,d, CH aromatic ring) and 10.189 (1H, s, SH). ^{13}C NMR Figure (3.9) shows chemical shift at 121.564 (carbon a), 150.133 (carbon b), 132.891 (carbon c), 147.308 (carbon d) and 167.551 (carbon e).

Complex 1:

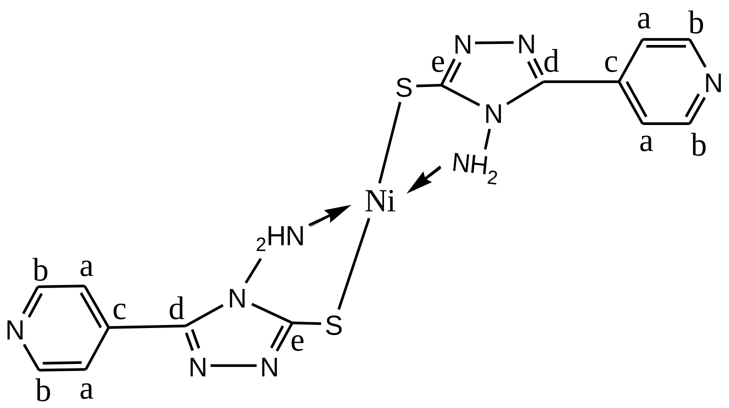

^{1}H NMR data (ppm), δ_H(300 MHz, DMSO-d$_6$): Figure (3.10) shows the signals at 3.314 (2H, s, NH_2) (this peak is shifted to lower field due to its attachment to the Nickel atom), 7.945,8.014-8.739,8.678 (4H, d,d, CH aromatic ring). ^{13}C NMR Figure (3.11) shows chemical shift at 125.001 (carbon a), 149.583 (carbon b), 134.991 (carbon c), 155.683 (carbon d) and 183.548 (carbon e).

Complex 3:

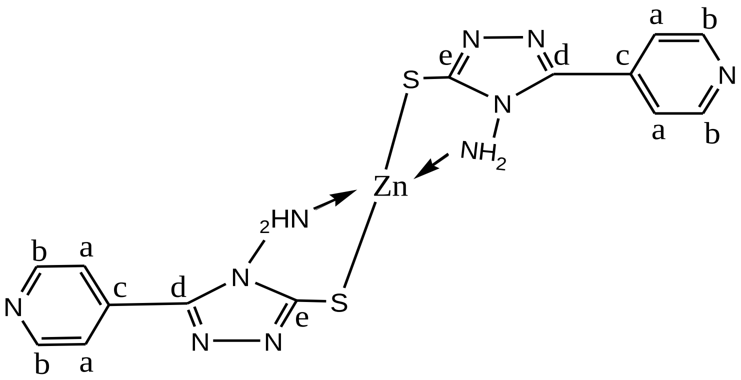

^{1}H NMR data (ppm), δ_H(300 MHz, DMSO-d$_6$): Figure (3.12) shows the signals at 3.354 (2H, s, NH_2) (this peak is shifted due to its attachment to the metal atom), 8.024-8.702 (4H, m, CH aromatic ring). ^{13}C NMR Figure (3.13) shows chemical shift at 121.705 (carbon a), 149.322 (carbon b), 134.035 (carbon c), 158.297 (carbon d) and 180.114 (carbon e).

Complex 4:

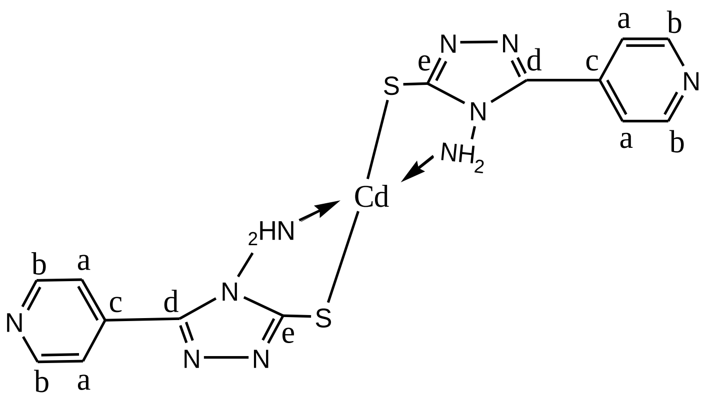

^{1}H NMR data (ppm), δ_H(300 MHz, DMSO-d_6): Figure (3.14) shows the signals at 3.270 (2H, s, NH_2) (for the reason mentioned above), 7.901,7.952-8,625,8.690 (4H, d,d, CH aromatic ring). ^{13}C NMR Figure (3.15) shows chemical shift at 120.992 (carbon a), 149.603 (carbon b), 134.036 (carbon c), 150.297 (carbon d) and 187.329 (carbon e).

Table (3.3),(3.4) show the ^{1}H NMR, ^{13}C NMR data of L and metal complexes 1,3 and 4 in DMSO-*d*6 Chemical shift, d (ppm).

Table (3.3) ^{1}H NMR data of L and metal complexes 1,3 and 4 in DMSO-*d6* Chemical shift, σ (ppm)

Compounds	σ (C-H aromatic) ppm	σ (NH_2) ppm	σ (S-H) ppm
L	(8.014,8.025-8.744,8.755)d,d	(5.301)s	(10.189)s
Ni(L)$_2$ 1	(7.945,8.014-8.739,8.678)d,d	(3.314)s	-
Zn(L)$_2$ 3	(8.024-8.702)m	(3.354)s	-
Cd(L)$_2$ 4	(7.901,7.952-8,625,8.690)d,d	(3.270)s	-

Where s = singlet

d,d = doublet of doublet

Table (3.4) ^{13}C NMR data of L and metal complexes 1,3 and 4 in DMSO-*d6* Chemical shift, σ (ppm)

Compounds	Carbon a	Carbon b	Carbon c	Carbon d	Carbon e
L	121.564	150.133	132.891	147.308	167.551
$Ni(L)_2$ 1	125.001	149.583	134.991	155.683	183.548
$Zn(L)_2$ 3	121.705	149.322	134.035	158.297	180.114
$Cd(L)_2$ 4	120.992	149.603	134.036	150.297	187.329

The ^{1}H NMR and ^{13}C NMR spectrum of ligand and its complexes is shown in Figures (3.8) - (3.15).

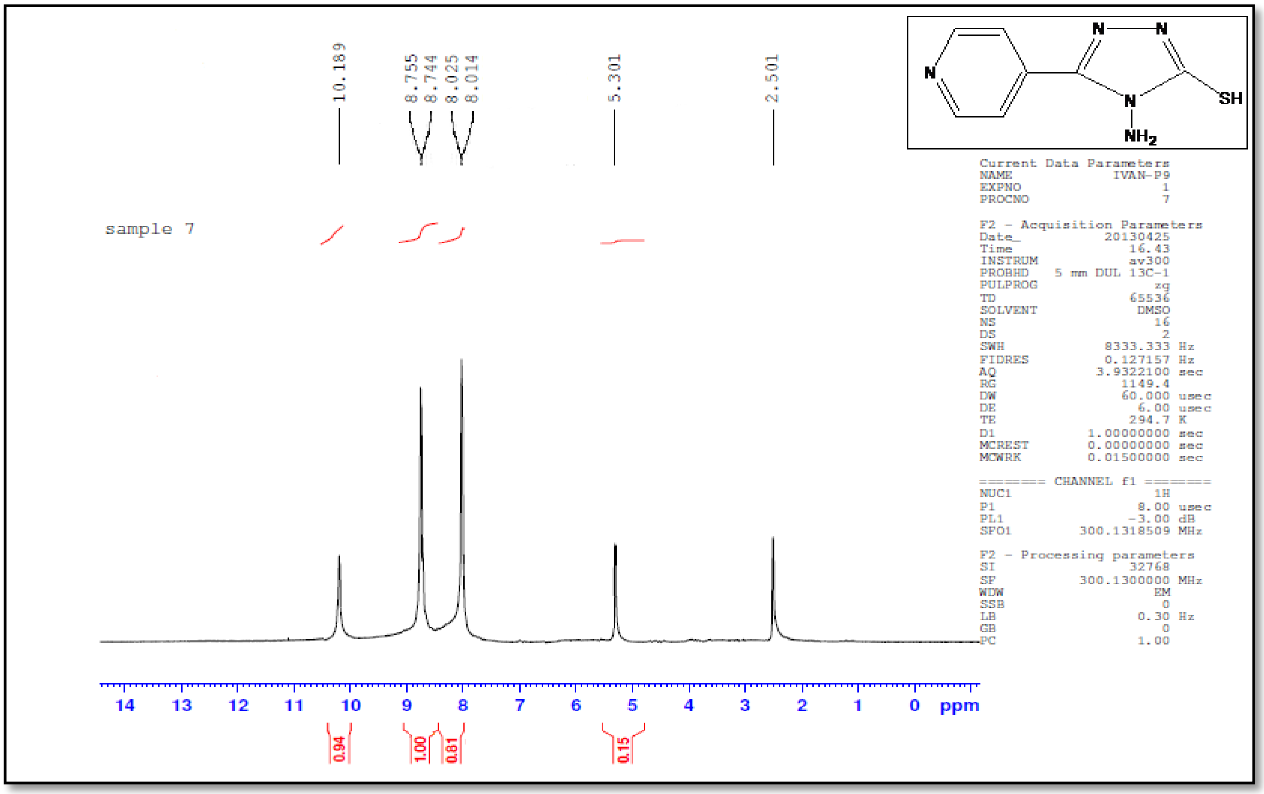

```
Current Data Parameters
NAME              IVAN-P9
EXPNO                   1
PROCNO                  7

F2 - Acquisition Parameters
Date_            20130425
Time                16.43
INSTRUM             av300
PROBHD   5 mm DUL 13C-1
PULPROG                zg
TD                  65536
SOLVENT              DMSO
NS                     16
DS                      2
SWH              8333.333 Hz
FIDRES           0.127157 Hz
AQ              3.9322100 sec
RG                 1149.4
DW                 60.000 usec
DE                   6.00 usec
TE                  294.7 K
D1             1.00000000 sec
MCREST         0.00000000 sec
MCWRK          0.01500000 sec

======= CHANNEL f1 =======
NUC1                   1H
P1                   8.00 usec
PL1                 -3.00 dB
SFO1          300.1318509 MHz

F2 - Processing parameters
SI                  32768
SF            300.1300000 MHz
WDW                    EM
SSB                     0
LB                   0.30 Hz
GB                      0
PC                   1.00
```

Figure (3.8) ^{1}H NMR spectrum of ligand (L)

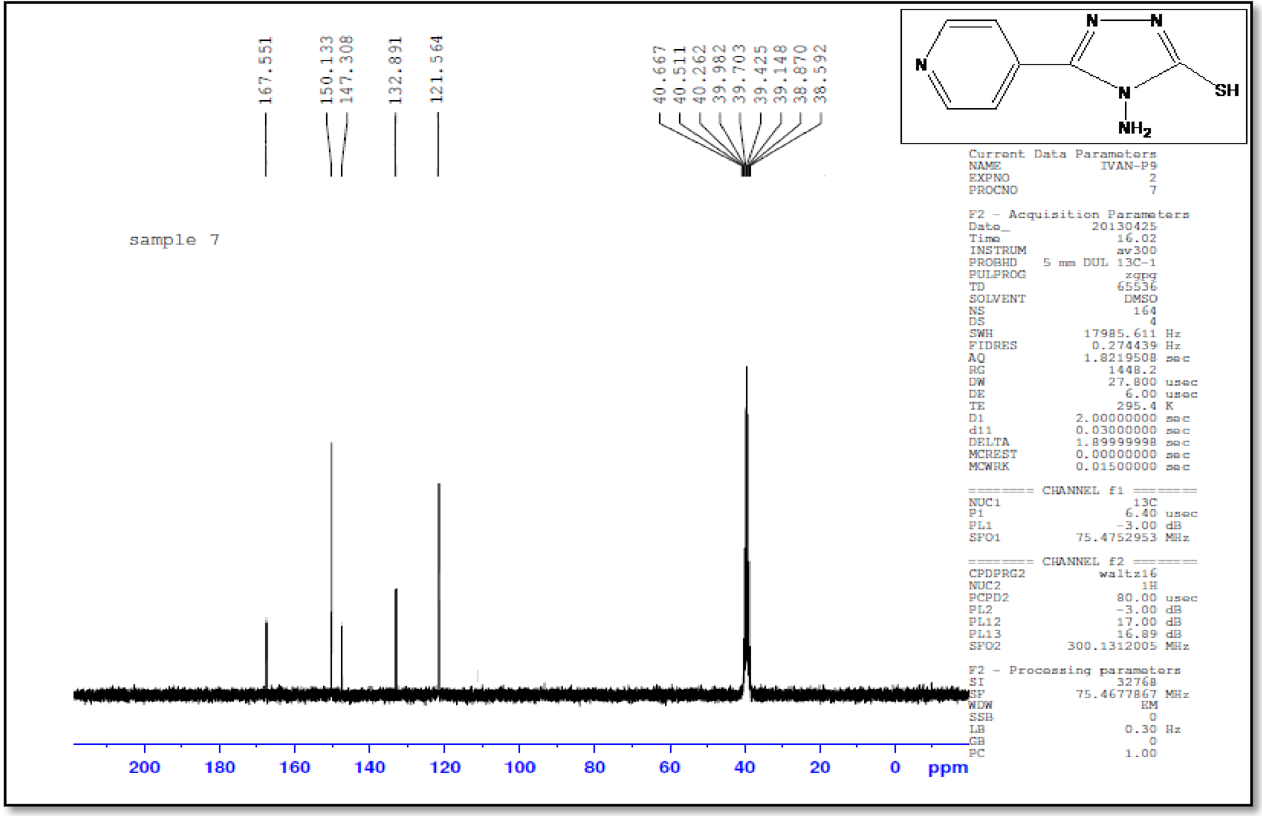

```
Current Data Parameters
NAME              IVAN-P9
EXPNO                   2
PROCNO                  7

F2 - Acquisition Parameters
Date_            20130425
Time                16.02
INSTRUM             av300
PROBHD   5 mm DUL 13C-1
PULPROG              zgpg
TD                  65536
SOLVENT              DMSO
NS                    164
DS                      4
SWH             17985.611 Hz
FIDRES           0.274439 Hz
AQ              1.8219508 sec
RG                 1448.2
DW                 27.800 usec
DE                   6.00 usec
TE                  295.4 K
D1             2.00000000 sec
d11            0.03000000 sec
DELTA          1.89999998 sec
MCREST         0.00000000 sec
MCWRK          0.01500000 sec

======== CHANNEL f1 ========
NUC1                  13C
P1                   6.40 usec
PL1                 -3.00 dB
SFO1           75.4752953 MHz

======== CHANNEL f2 ========
CPDPRG2           waltz16
NUC2                   1H
PCPD2               80.00 usec
PL2                 -3.00 dB
PL12                17.00 dB
PL13                16.89 dB
SFO2          300.1312005 MHz

F2 - Processing parameters
SI                  32768
SF             75.4677867 MHz
WDW                    EM
SSB                     0
LB                   0.30 Hz
GB                      0
PC                   1.00
```

Figure (3.9) ^{13}C NMR spectrum of ligand (L)

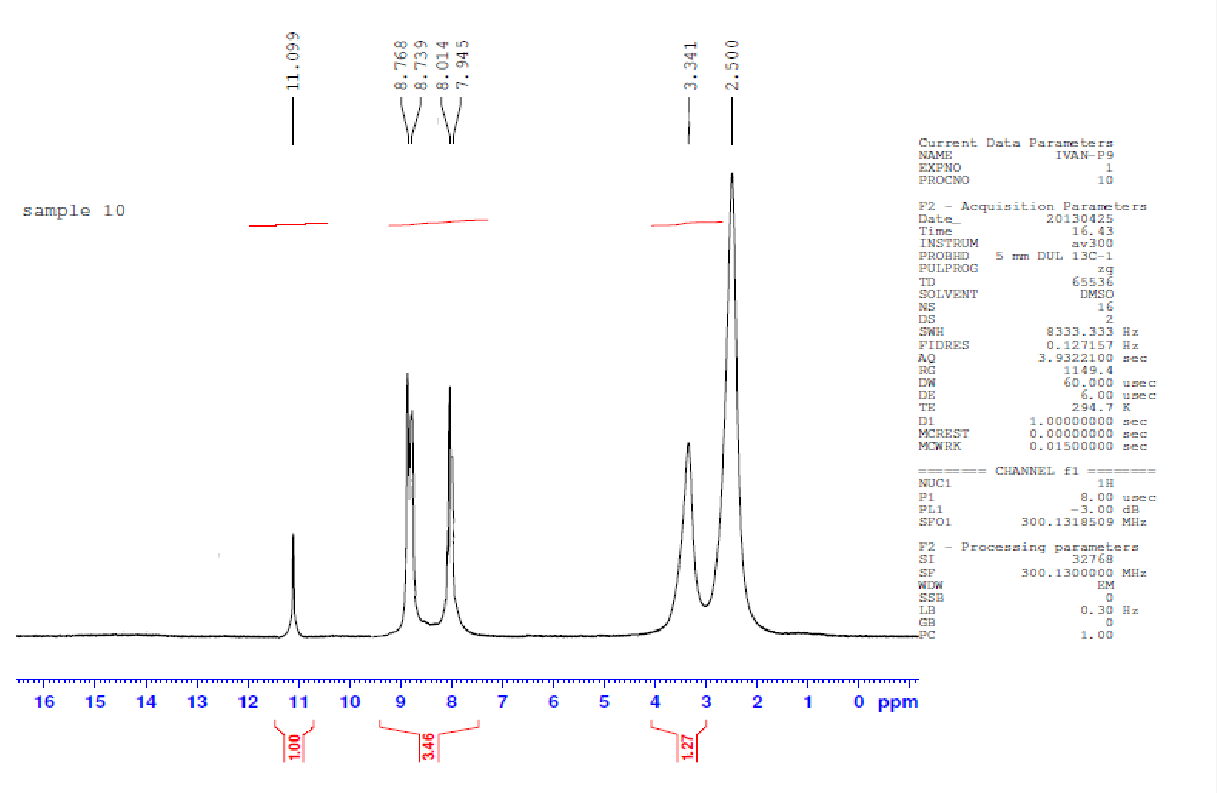

```
Current Data Parameters
NAME             IVAN-P9
EXPNO                  1
PROCNO                10

F2 - Acquisition Parameters
Date_           20130425
Time               16.43
INSTRUM            av300
PROBHD   5 mm DUL 13C-1
PULPROG               zg
TD                 65536
SOLVENT             DMSO
NS                    16
DS                     2
SWH             8333.333 Hz
FIDRES          0.127157 Hz
AQ             3.9322100 sec
RG                1149.4
DW                60.000 usec
DE                  6.00 usec
TE                 294.7 K
D1            1.00000000 sec
MCREST        0.00000000 sec
MCWRK         0.01500000 sec

======= CHANNEL f1 =======
NUC1                  1H
P1                  8.00 usec
PL1                -3.00 dB
SFO1         300.1318509 MHz

F2 - Processing parameters
SI                 32768
SF           300.1300000 MHz
WDW                   EM
SSB                    0
LB                  0.30 Hz
GB                     0
PC                  1.00
```

Figure (3.10) ^{1}H NMR spectrum of $Ni(L)_2$

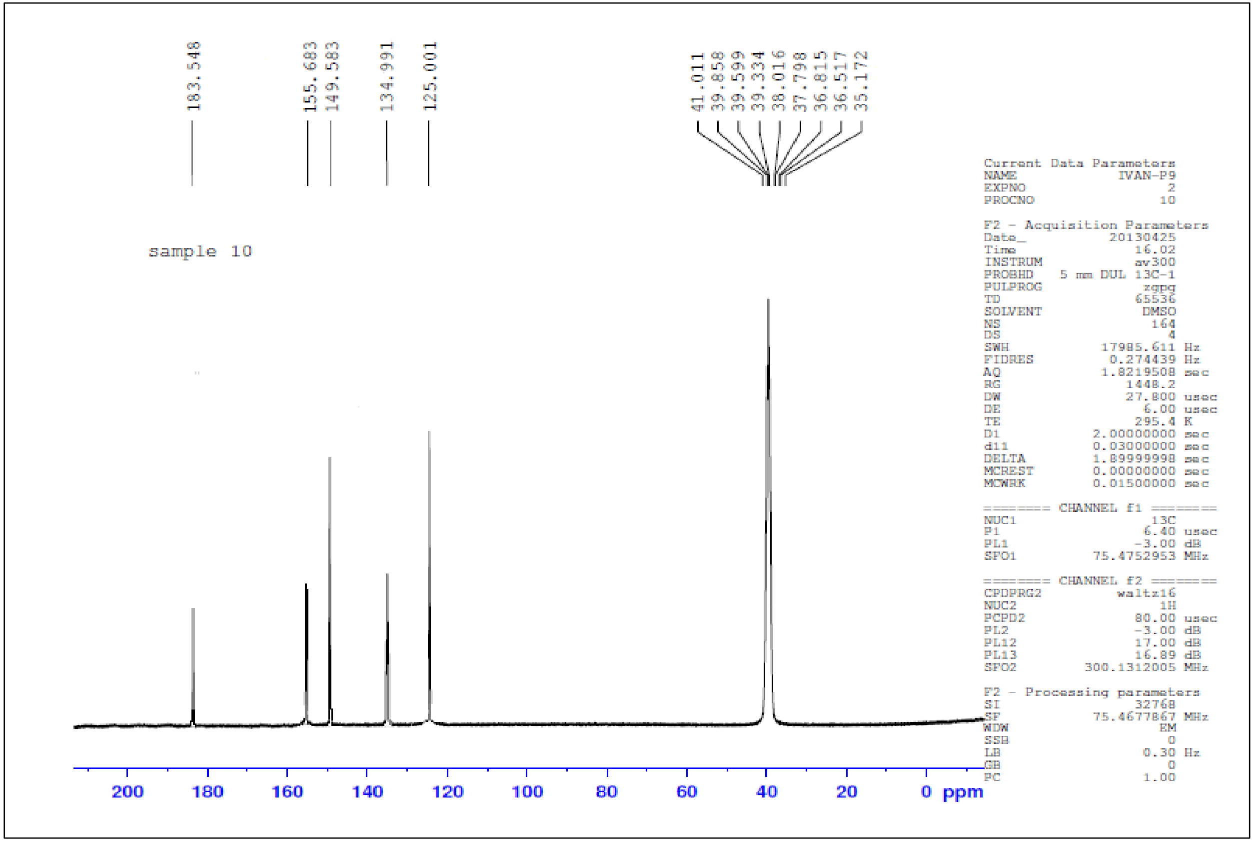

```
Current Data Parameters
NAME             IVAN-P9
EXPNO                  2
PROCNO                10

F2 - Acquisition Parameters
Date_           20130425
Time               16.02
INSTRUM            av300
PROBHD   5 mm DUL 13C-1
PULPROG             zgpg
TD                 65536
SOLVENT             DMSO
NS                   164
DS                     4
SWH            17985.611 Hz
FIDRES          0.274439 Hz
AQ             1.8219508 sec
RG                1448.2
DW                27.800 usec
DE                  6.00 usec
TE                 295.4 K
D1            2.00000000 sec
d11           0.03000000 sec
DELTA         1.89999998 sec
MCREST        0.00000000 sec
MCWRK         0.01500000 sec

======= CHANNEL f1 =======
NUC1                 13C
P1                  6.40 usec
PL1                -3.00 dB
SFO1          75.4752953 MHz

======= CHANNEL f2 =======
CPDPRG2          waltz16
NUC2                  1H
PCPD2              80.00 usec
PL2                -3.00 dB
PL12               17.00 dB
PL13               16.89 dB
SFO2         300.1312005 MHz

F2 - Processing parameters
SI                 32768
SF            75.4677867 MHz
WDW                   EM
SSB                    0
LB                  0.30 Hz
GB                     0
PC                  1.00
```

Figure (3.11) ^{13}C NMR spectrum of $Ni(L)_2$

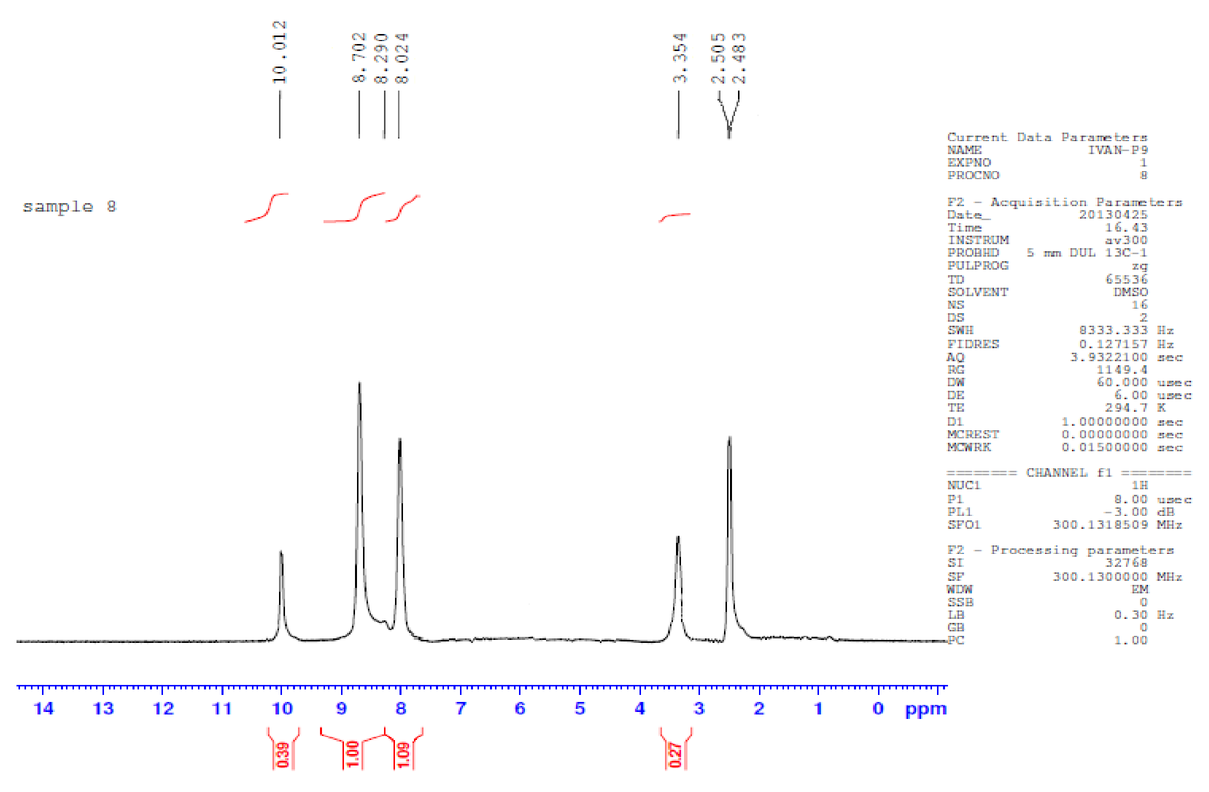

Figure (3.12) ^{1}H NMR spectrum of Zn(L)$_2$

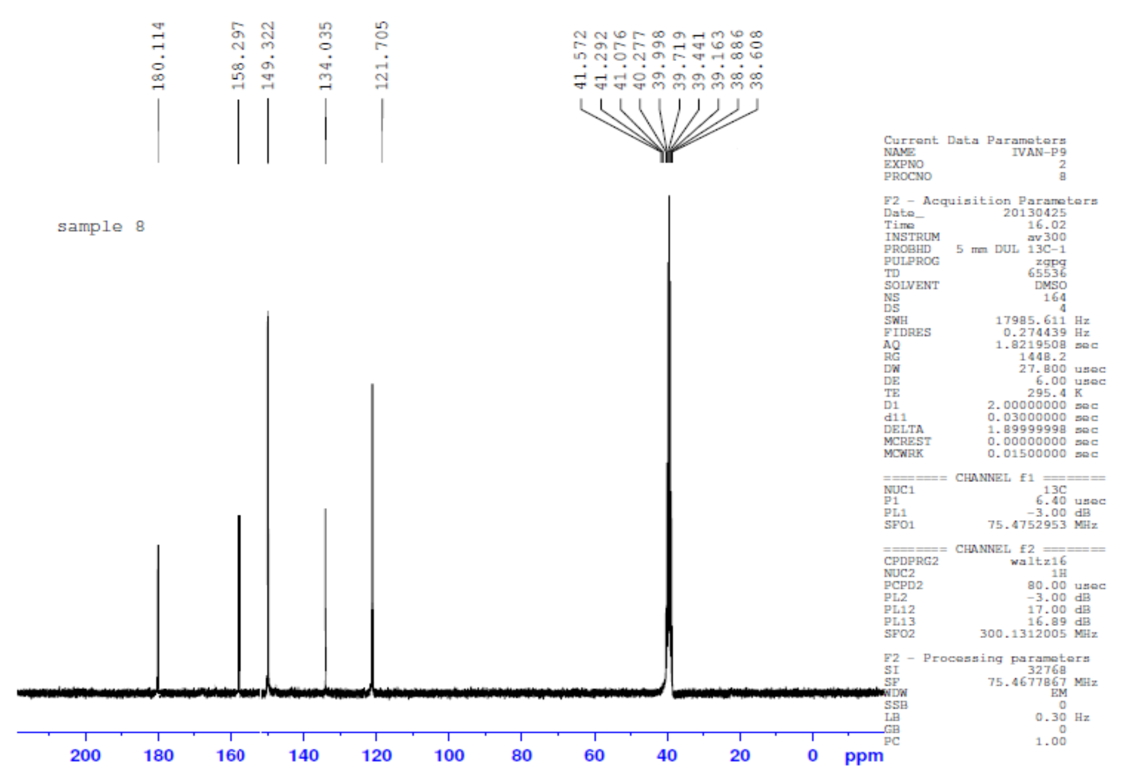

Figure (3.13) ^{13}C NMR spectrum of Zn(L)$_2$

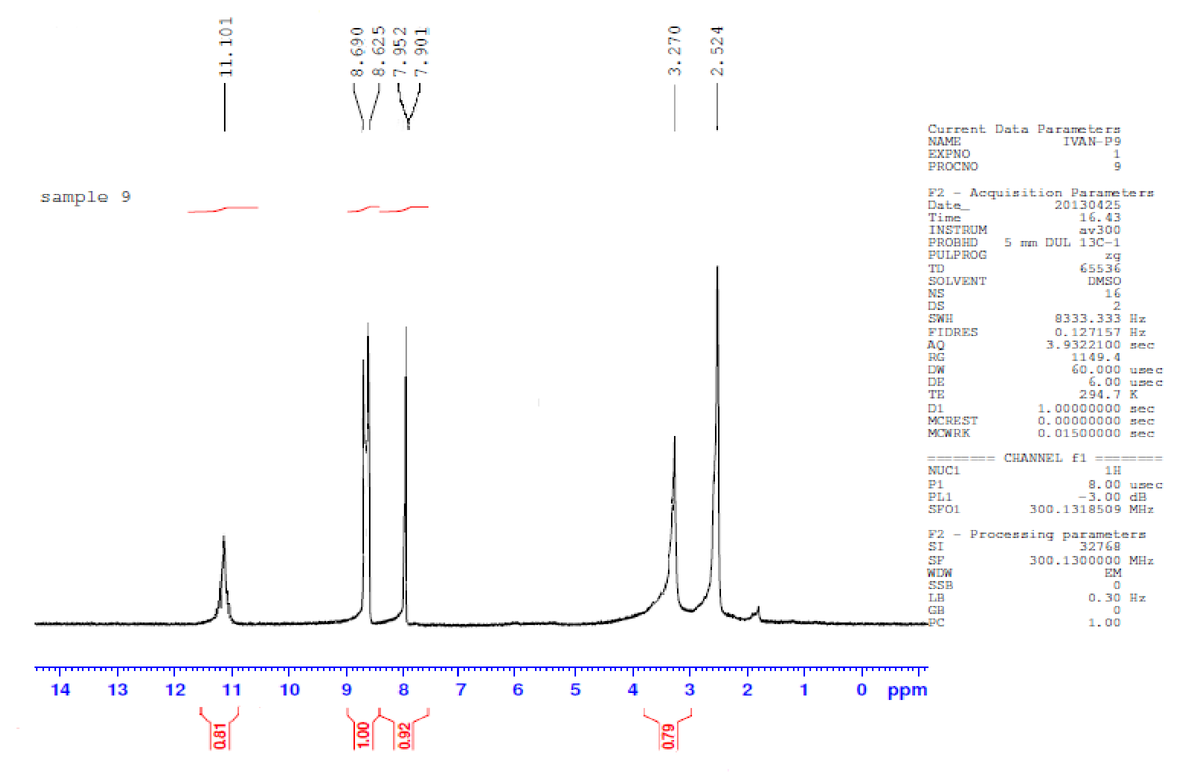

```
Current Data Parameters
NAME             IVAN-P9
EXPNO                  1
PROCNO                 9

F2 - Acquisition Parameters
Date_           20130425
Time               16.43
INSTRUM            av300
PROBHD   5 mm DUL 13C-1
PULPROG               zg
TD                 65536
SOLVENT             DMSO
NS                    16
DS                     2
SWH             8333.333 Hz
FIDRES          0.127157 Hz
AQ             3.9322100 sec
RG                1149.4
DW                60.000 usec
DE                  6.00 usec
TE                 294.7 K
D1            1.00000000 sec
MCREST        0.00000000 sec
MCWRK         0.01500000 sec

======= CHANNEL f1 =======
NUC1                  1H
P1                  8.00 usec
PL1                -3.00 dB
SFO1         300.1318509 MHz

F2 - Processing parameters
SI                 32768
SF           300.1300000 MHz
WDW                   EM
SSB                    0
LB                  0.30 Hz
GB                     0
PC                  1.00
```

Figure (3.14) ^{1}H NMR spectrum of $Cd(L)_2$

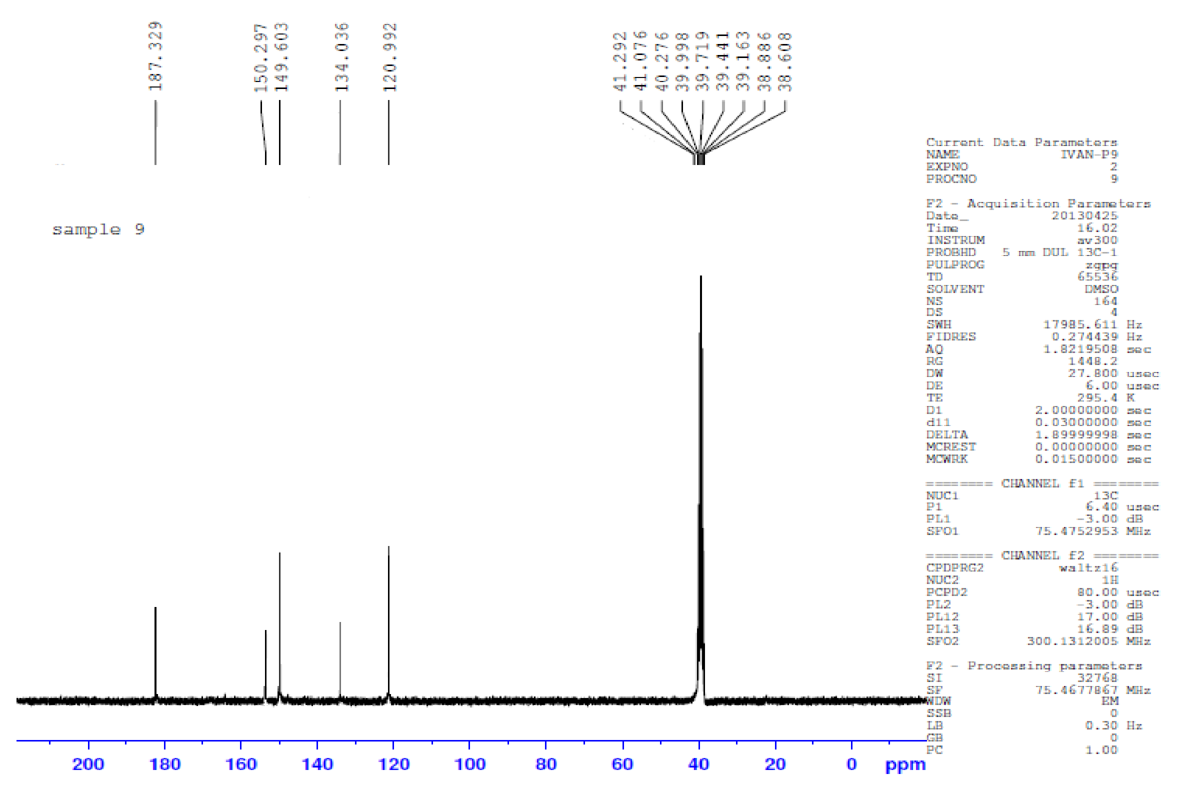

```
Current Data Parameters
NAME             IVAN-P9
EXPNO                  2
PROCNO                 9

F2 - Acquisition Parameters
Date_           20130425
Time               16.02
INSTRUM            av300
PROBHD   5 mm DUL 13C-1
PULPROG             zgpg
TD                 65536
SOLVENT             DMSO
NS                   164
DS                     4
SWH            17985.611 Hz
FIDRES          0.274439 Hz
AQ             1.8219508 sec
RG                1448.2
DW                27.800 usec
DE                  6.00 usec
TE                 295.4 K
D1            2.00000000 sec
d11           0.03000000 sec
DELTA         1.89999998 sec
MCREST        0.00000000 sec
MCWRK         0.01500000 sec

======= CHANNEL f1 =======
NUC1                 13C
P1                  6.40 usec
PL1                -3.00 dB
SFO1          75.4752953 MHz

======= CHANNEL f2 =======
CPDPRG2          waltz16
NUC2                  1H
PCPD2              80.00 usec
PL2                -3.00 dB
PL12               17.00 dB
PL13               16.89 dB
SFO2         300.1312005 MHz

F2 - Processing parameters
SI                 32768
SF            75.4677867 MHz
WDW                   EM
SSB                    0
LB                  0.30 Hz
GB                     0
PC                  1.00
```

Figure (3.15) ^{13}C NMR spectrum of $Cd(L)_2$

3.1.4. Characterization of prepared complexes by Ultraviolet-Visible spectroscopy

The absorption spectra of the ligand (L) and it's complexes were recorded in DMSO solvent in range of 250-900 nm. The electronic spectra of (L) and its complexes were illustrated in Table (3.5). The electronic spectrum of this ligand show 3 bands at (263, 302, 309) nm due to intraligand transition (π-π*), (π-π*), (n-π*) electronic transitions, respectively. From Table (3.5), complexes **1–5** also showed the similar electronic transition but with shifting comparing with the ligand.

For complexes 1 and 2, the electronic transitions of the metal *d* orbitals (*d-d* electronic transition) observed in the Ni (II) and Cu (II) located in the visible region. There are three *d-d* electronic transitions in Ni complexes as in Orgeal diagram assigned to the $^3T_{1(F)} \rightarrow {}^3T_{2(F)}$, $^3T_{1(F)} \rightarrow {}^3T_{1(P)}$ and $^3T_{1(F)} \rightarrow {}^3A_{2(F)}$ transitions, respectively(155-156). But in this study there is one transition appeared at 620 nm. For Cu(II), the bands appeared at 280, 300, 312 and 451 nm were attributed to (π-π*), (n-π*), charge transfer and $^2T_2 \rightarrow {}^2E_2$ respectively(157-159).

But the other complexes (4, 5, 6), were diamagnetic as expected for d^{10} ions, so that no (d-d) transition can be expected in the visible region(160).

Table (3.5) electronic spectra of prepared compounds

Compounds	Absorption nm	Transition
L	263, 302 309	π-π* n-π*
$Ni(L)_2$ 1	262 610	π-π* $^{3}T_{1(F)}\rightarrow {}^{3}T_{1(P)}$
$Cu(L)_2$ 2	280 300 312 451	π-π* n-π* L→ Cu(CT) $^{2}T_{2}\rightarrow {}^{2}E_{2}$
$Zn(L)_2$ 3	264, 300 310	π-π* n-π*
$Cd(L)_2$ 4	262 310	π-π* n-π*
$Sn(L)_2$ 5	265 310	π-π* n-π*

The UV. visible spectrum of ligand and its complexes was shown in Figures (3.16) - (3.21).

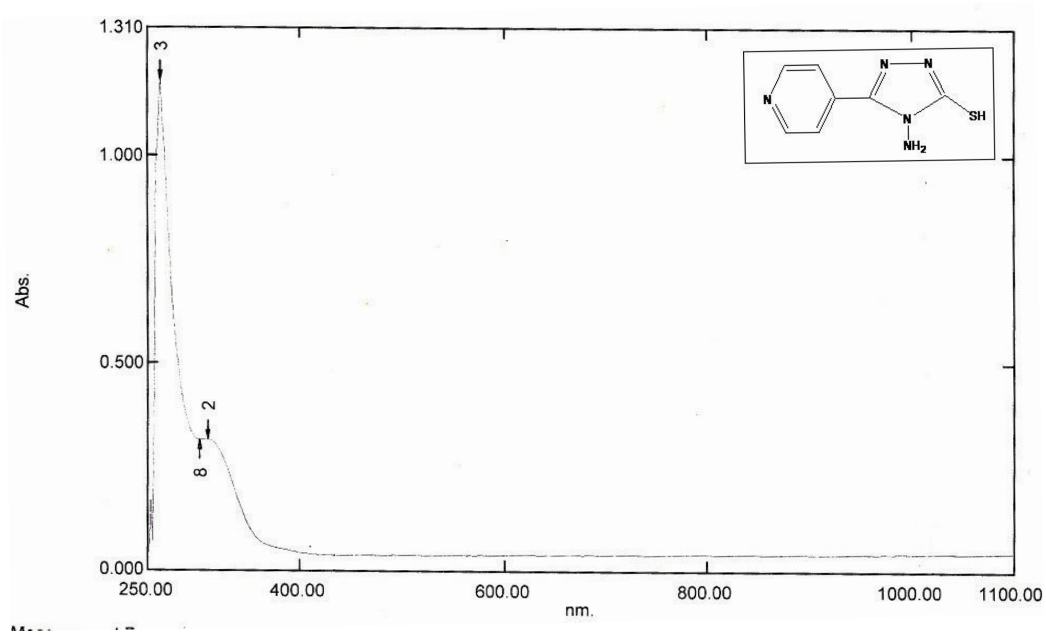

Figure (3.16) The ultraviolet visible spectrum for the ligand in DMSO solvent

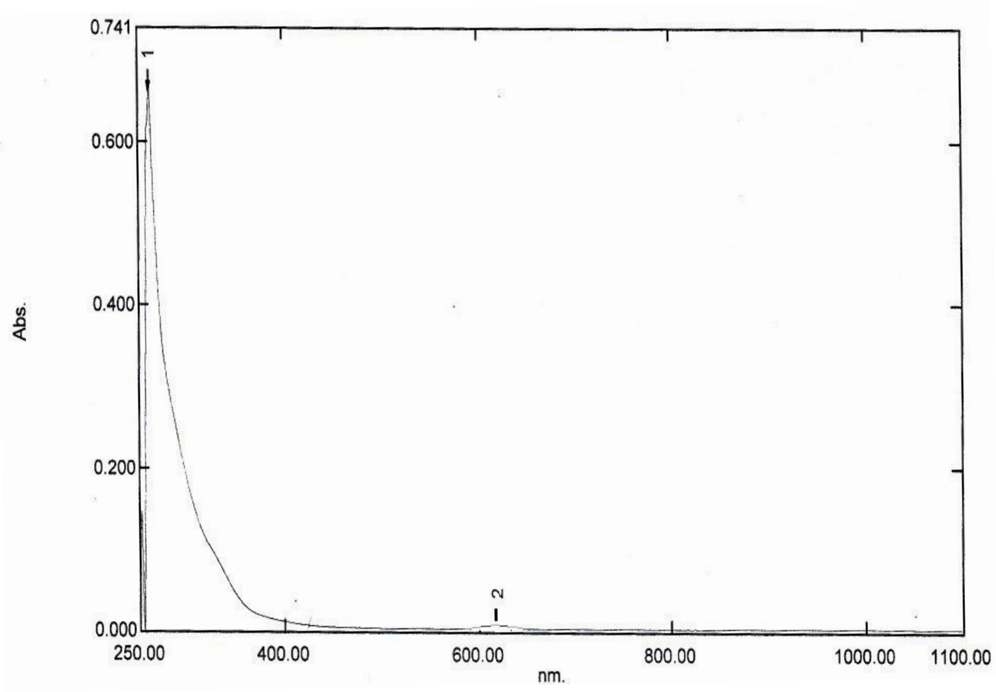

Figure (3.17) The ultraviolet visible spectrum for the Ni(L)$_2$ in DMSO solvent

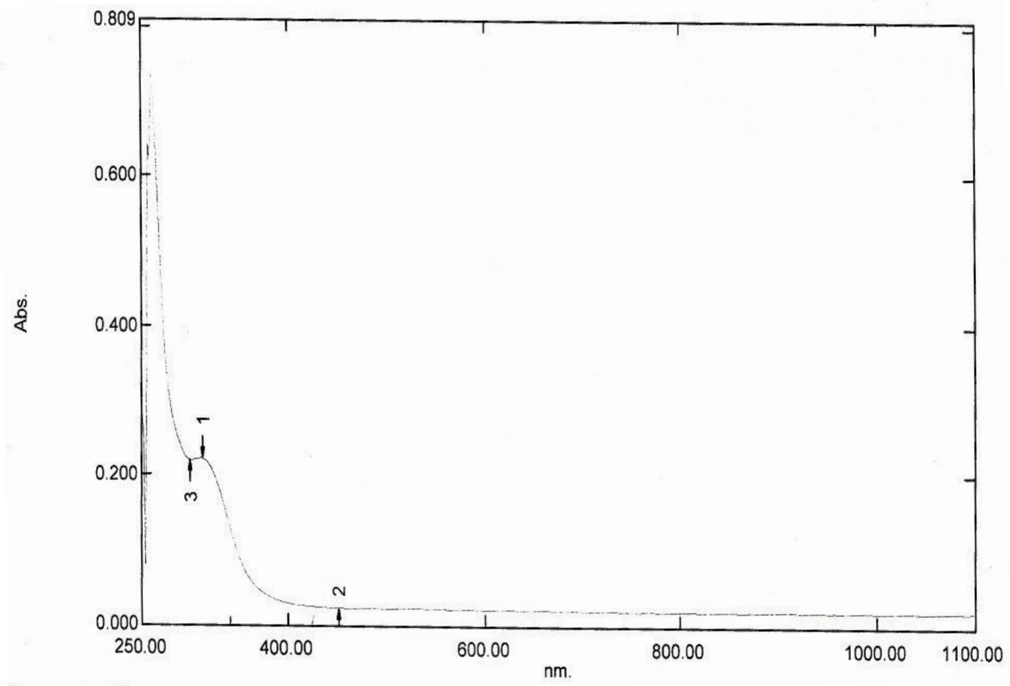

Figure (3.18) The ultraviolet visible spectrum for the Cu(L)$_2$ in DMSO solvent

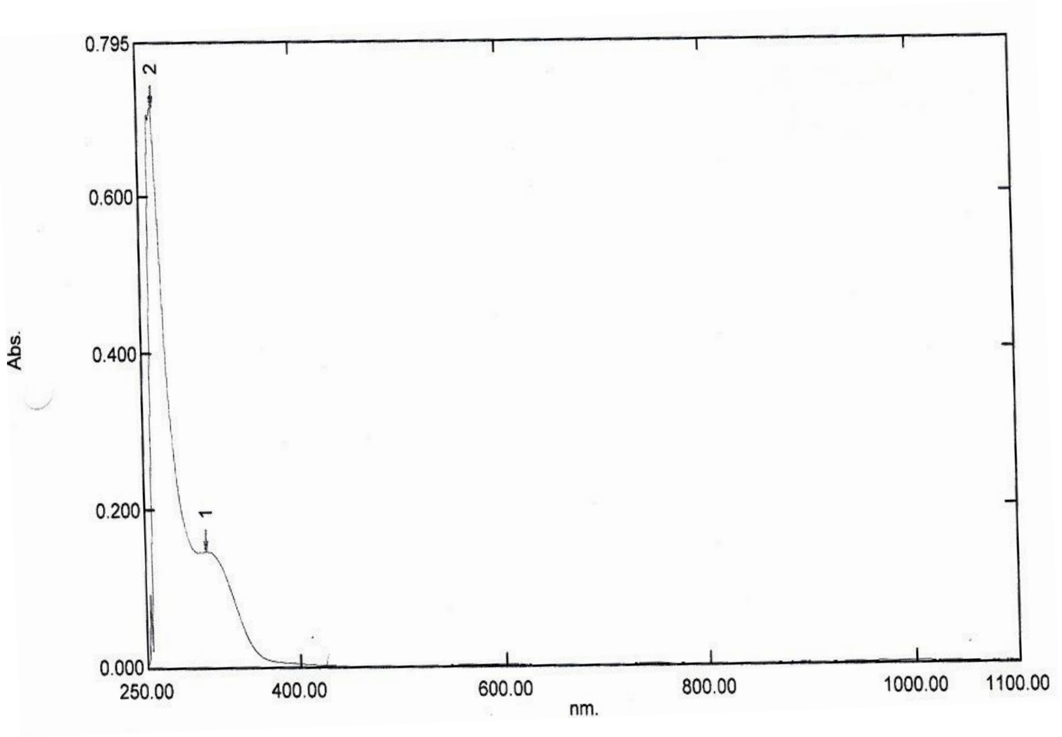

Figure (3.19) The ultraviolet visible spectrum for the $Zn(L)_2$ in DMSO solvent

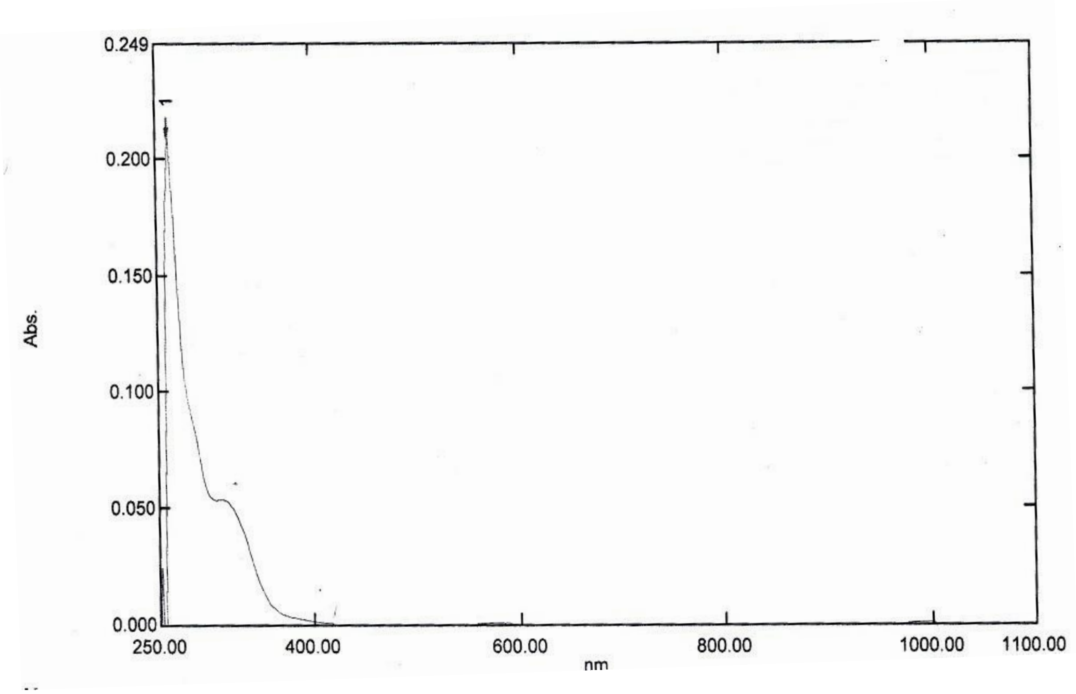

Figure (3.20) The ultraviolet visible spectrum for the $Cd(L)_2$ in DMSO solvent

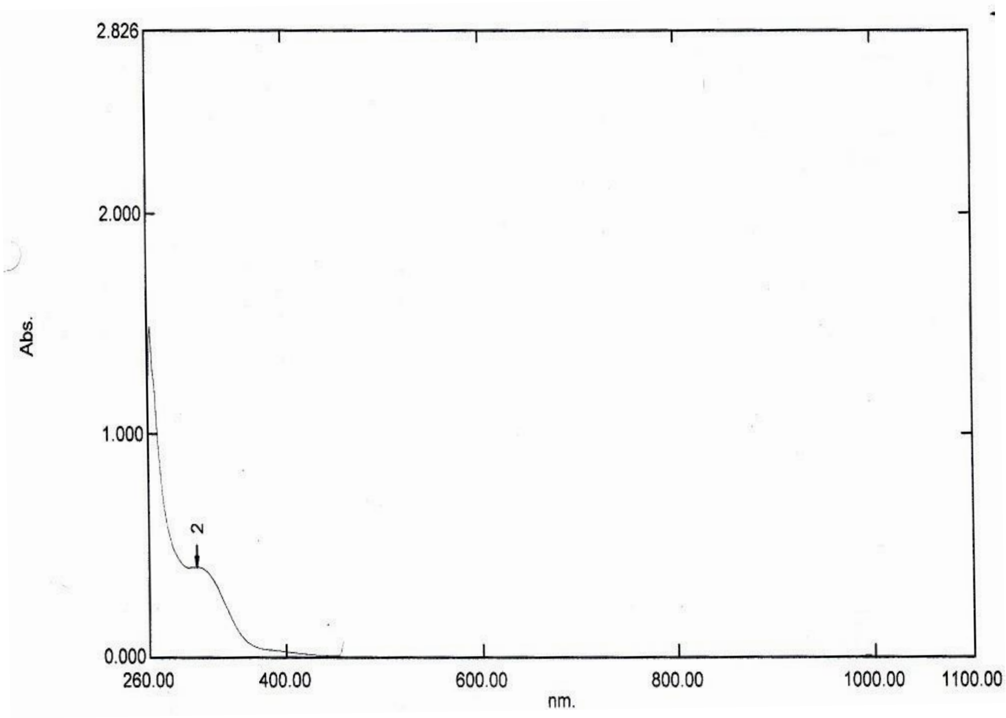

Figure (3.21) The ultraviolet visible spectrum for the $Sn(L)_2$ in DMSO solvent

3.1.5. Magnetic susceptibility and Conductivity measurements

Magnetic measurements are widely used in studying transition metal complexes. The magnetic property is due to the presence of unpaired of electrons in the partially filled d- orbital in the outer shell of these elements.

The resultant magnetic moment of an ion is due to both orbital and spin motions(161). The magnetic moment is given by the following equation:

$$\mathbf{Xg = (C * L / 10^9 M) (R\text{-}R_o)} \quad \ldots\ldots\ldots \quad \mathbf{(3.1)}$$

Where: Xg: magnetic susceptibility

C: constant =1.5

L: length of the tube = 1 cm

M= weight of the sample

R= susceptibility of the tube with the sample

R_o= susceptibility of the empty tube

The value of magnetic susceptibility of the prepared complexes at (25 ºC) temperature is calculated using the following equation:

$$\boldsymbol{\mu_{eff} = 2.83 \sqrt{X_A . T}} \qquad \textbf{B.M ……….. (3.2)}$$

Where: $X_A = X_m + D$

$X_m = X_g . \text{Mwt.}$

Mwt = Molecular weight of complex.

X_g = Mass susceptibility.

D = Pascal`s constant.

X_m = Molar susceptibility which was corrected from diamagnetic.

μ_{eff} = Effective magnetic moment.

T = Temperature in Kelvin (ºC +273).

The magnetic moment value of complex **1** was 1.09 B.M. and referred as paramagnetic. Complex **2** showed that the magnetic moment value is 0.7 B.M. and believed that the Cu (II) metal moiety exhibited distorted square planar geometry (162). Complexes **3–5** are diamagnetic and there were no magnetic moment recorded in this study(160). The Magnetic moment values of prepared complexes **1-5** were illustrated in table (3.6).

Conductivity measurement of these complexes was recorded as a solution in ethanol solvent by dissolving 10^{-3} g in ethanol. This measurement gives an idea if a solution is electrolyte or not. Table (3.6) show the molar conductivity measurements of complexes **1–5**, it was shown that all the prepared complexes were found to be non-electrolyte(163).

Table (3.6) Conductivity measurement and Magnetic moment of L and its complexes

Complexes	Conductivity (µS/cm)	Megnetic moment (BM)
L	-	-
Ni(L)$_2$ 1	3	1.09
Cu(L)$_2$ 2	1	0.7
Zn(L)$_2$ 3	3.4	0
Cd(L)$_2$ 4	2	0
Sn(L)$_2$ 5	12	0

Based on the spectral study, complexes **1–5** exhibited distorted tetrahedral geometry except complex **2** (distorted square planar)(164). The proposed structure of complexes **1–5** is shown below, See Figure (3.22).

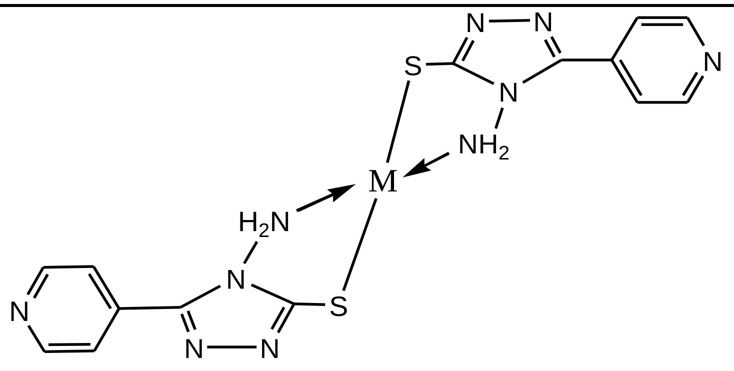

Where M = Ni(II), Cu(II), Zn(II), Cd(II) or Sn(II)

Figure (3.22) The proposed structure of Complexes 1-5

3.2. Photo-activity of Complexes Additives in Polystyrene Films

Initiation of the photooxidative degradation of PS is attributed to be absorption of UV. Light by different internal chromophoric impurities, such as(61):

i) Peroxide groups formed through the polymerization process of styrene monomer, by reaction of oxygen with PS growing radicals.

ii) Pendant acetophenone groups formed as a result of photo or thermal reaction of hydroperoxide groups, at the end of the PS chain.

The film absorbed at wavelength longer than 200 nm, owing to the presence of the aromatic ring in polymer. The carbonyl groups generated during the photooxidation process of PS(165). These groups absorb light when they irradiated with light of wavelength between (250-380) nm. and activated to the singlet and triplet excited state which enhanced various successive photooxidation reaction(165), Figure (3.23) shows FTIR spectrum for PS film (40 μm.) thickness.

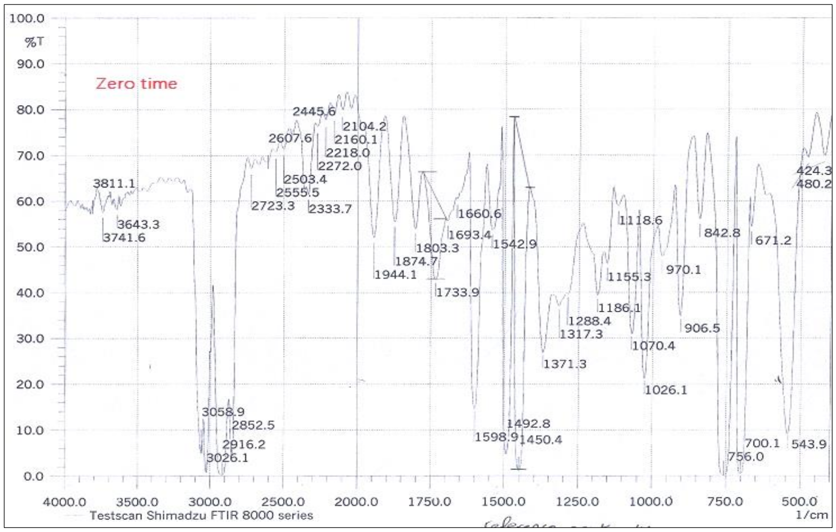

Figure (3.23) FTIR Spectra of poltstyrene film

The hydroperoxide groups can be formed directly (CT) complex via excitation by UV. light radiation. (61)

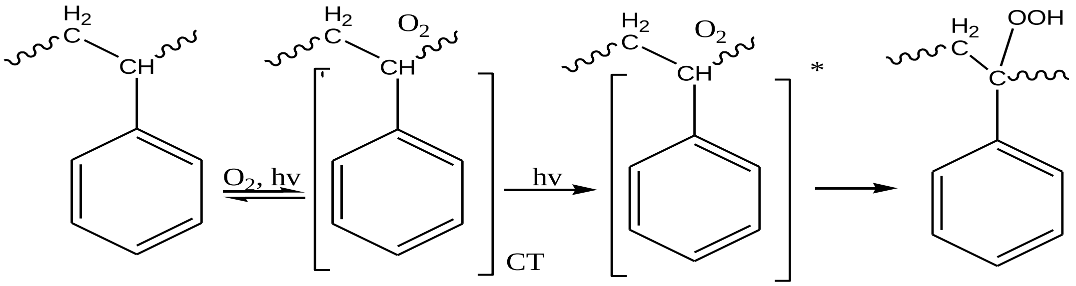

(3.3)

Photodecomposition of hydroperoxide group results in the formation of acetophenone derivative and two types of aliphatic ketones that absorbed at 1720 cm^{-1}.

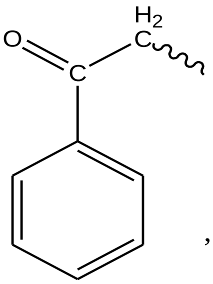

,

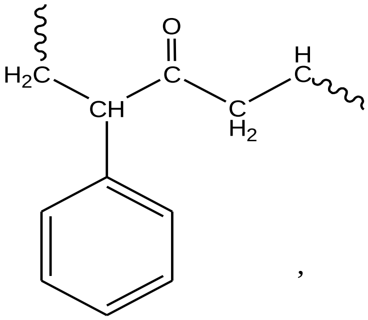

,

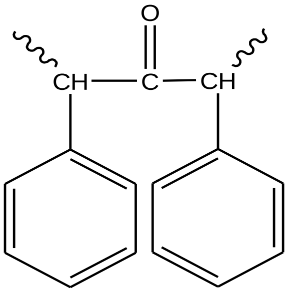

As shown in equation (3.3), acetophenone groups can be formed by thermal or photodecomposition of polystyrene hydroperoxide. It can also be formed by thermal or photodecomposition of polymeric peroxide during free radicals polymerization process.

The control PS film becomes slightly yellow in color during irradiation. Yellow coloring of PS sample can result from the formation of many different chromophoric groups. It is generally accepted that acetophenone end group form during UV. irradiation of PS is most probable, are responsible for yellowing coloration of the polymer(166).

3.2.1. Photochemical Study of the PS films by infra-red spectroscopy

The irradiation of PS films with light of wavelength, λ=365 nm led to a clear changes in their infrared spectrum.

The photo activity of triazole additives in PS films has been tested and their efficiency in preventing the photooxidation reaction has been examined by spectroscopic methods.

The IR spectra recorded throughout irradiation show an increase in absorbance due to formation of oxidized products so the appearance of intense bands in the range between 1690 and 1730 cm^{-1} refers to the formation of carbonyl groups are used to follow the extent of polymer degradation during irradiation. Appearance of a broad band in the range of (3200-3600) cm^{-1} is attributed to the formation of hydroxyl group(136). These absorption are calculated as carbonyl index (I_{CO}) and hydroxyl index (I_{OH})(167). **(See chapter 2).**

Therefore, one should expect that growth of hydroxyl index is the measure of the degradation. As seen from Table (3.7) and Figure (3.24) that the presence of $Cu(\mathbf{L})_2$, $Zn(\mathbf{L})_2$, $Ni(\mathbf{L})_2$, $Cd(\mathbf{L})_2$ and $Sn(\mathbf{L})_2$ show lower growth rate of hydroxyl index with irradiation time with respect to the PS without additives (control).

Table (3.7) Hydroxyl index (I_{OH}) with irradiation time for PS films in (40µm) thickness containing 0.5% w\w from the additives

Additives	Irradiation time (hours)						
	0	50	100	150	200	250	300
PS (blank)	0.345	0.457	0.533	0.600	0.651	0.68	0.723
PS+Ni(L)$_2$	0.240	0.36	0.412	0.457	0.477	0.500	0.540
PS+Cu(L)$_2$	0.191	0.264	0.309	0.352	0.376	0.388	0.430
PS+Zn(L)$_2$	0.208	0.311	0.360	0.415	0.435	0.436	0.480
PS+Cd(L)$_2$	0.267	0.38	0.436	0.48	0.517	0.537	0.577
PS+Sn(L)$_2$	0.300	0.412	0.465	0.537	0.554	0.598	0.632

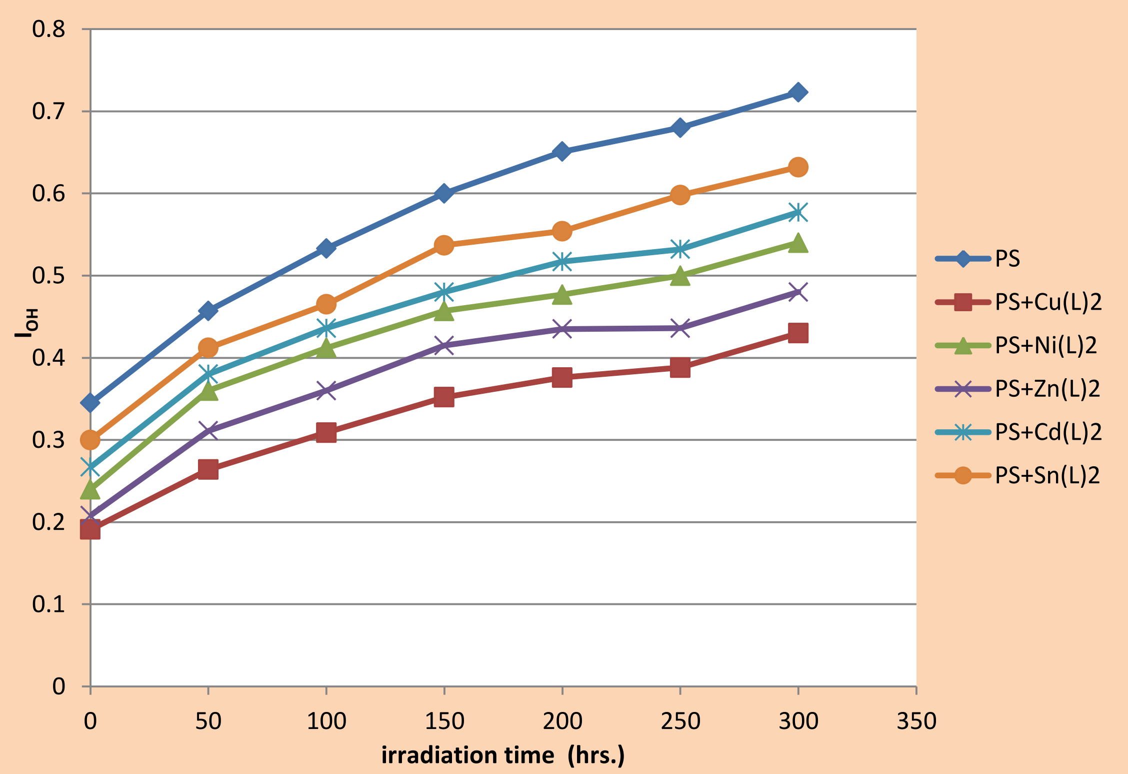

Figure (3.24) The relationship between the (I_{OH}) and irradiation time for PS films (40µm) thickness containing 0.5%w\w from the additives

So these additives might be considered as photostabilization of polystyrene films. The induction period shown by these additives is clear.

The good photostabilizer show a longer induction period. Therefore, from Figure (3.24), the $Cu(L)_2$ is the most active photostabilizer, followed by $Zn(L)_2$, $Ni(L)_2$, $Cd(L)_2$ and $Sn(L)_2$, are less active.

It was mentioned before that several types of carbonyl compounds are produced during photodegradation of PS. Therefore, carbonyl index (I_{CO}) was monitored with irradiation time and the presence and the absence of these additives. Results are shown in Table (3.8) and Figure (3.25).

Table (3.8) Carbonyl index (I_{CO}) with irradiation time for PS films in (40µm) thickness containing 0.5%w\w from the additives

Additive	Irradiation time (hours)						
	0	50	100	150	200	250	300
PS (blank)	0.425	0.618	0.729	0.764	0.787	0.802	0.819
PS+Ni(L)$_2$	0.361	0.434	0.468	0.494	0.499	0.510	0.523
PS+Cu(L)$_2$	0.327	0.360	0.381	0.403	0.407	0.410	0.420
PS+Zn(L)$_2$	0.343	0.349	0.420	0.440	0.444	0.442	0.447
PS+Cd(L)$_2$	0.384	0.504	0.542	0.565	0.586	0.590	0.582
PS+Sn(L)$_2$	0.412	0.542	0.611	0.631	0.661	0.660	0.665

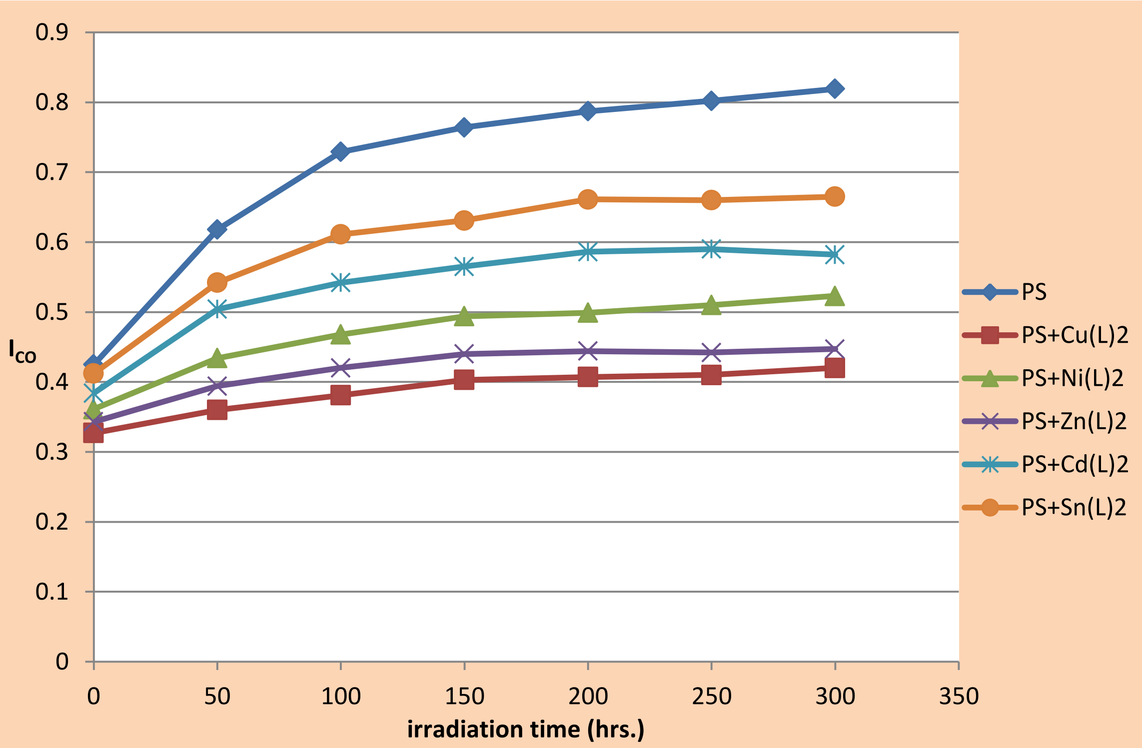

Figure (3.25) The relationship between the (I_{CO}) and irradiation time for PS films (40µm) thickness containing 0.5%w\w from the additives

Again the results confirmed that all these additives are photostabilizer for PS films. However, from the rate of carbonyl index (I_{CO}) growth, and from the Figure (3.25), the $Cu(L)_2$ is the most active photostabilizer, followed by $Zn(L)_2$, $Ni(L)_2$, $Cd(L)_2$ and $Sn(L)_2$, are less active.

In unstabilized PS films the carbonyl absorbance increased slowly during the first 50 hours and after this period the rate of formation of carbonyl groups increase quickly.

It is generally accepted that the action of the additives in the photostabilization are either UV. absorber, peroxide decomposer or radical scavengers.

Therefore the action of these additives in the PS films might be attributed to the UV. absorption and dissipate the the UV. energy to harmless heat energy. This is also suggested for benzotriazol(167)and aromatic Schiff base photostabilizer.

The irradiation of PS films with the UV. light lead to clear change in their FTIR spectrum as shown in Figures (3.26), (3.27), (3.28) and (3.29).

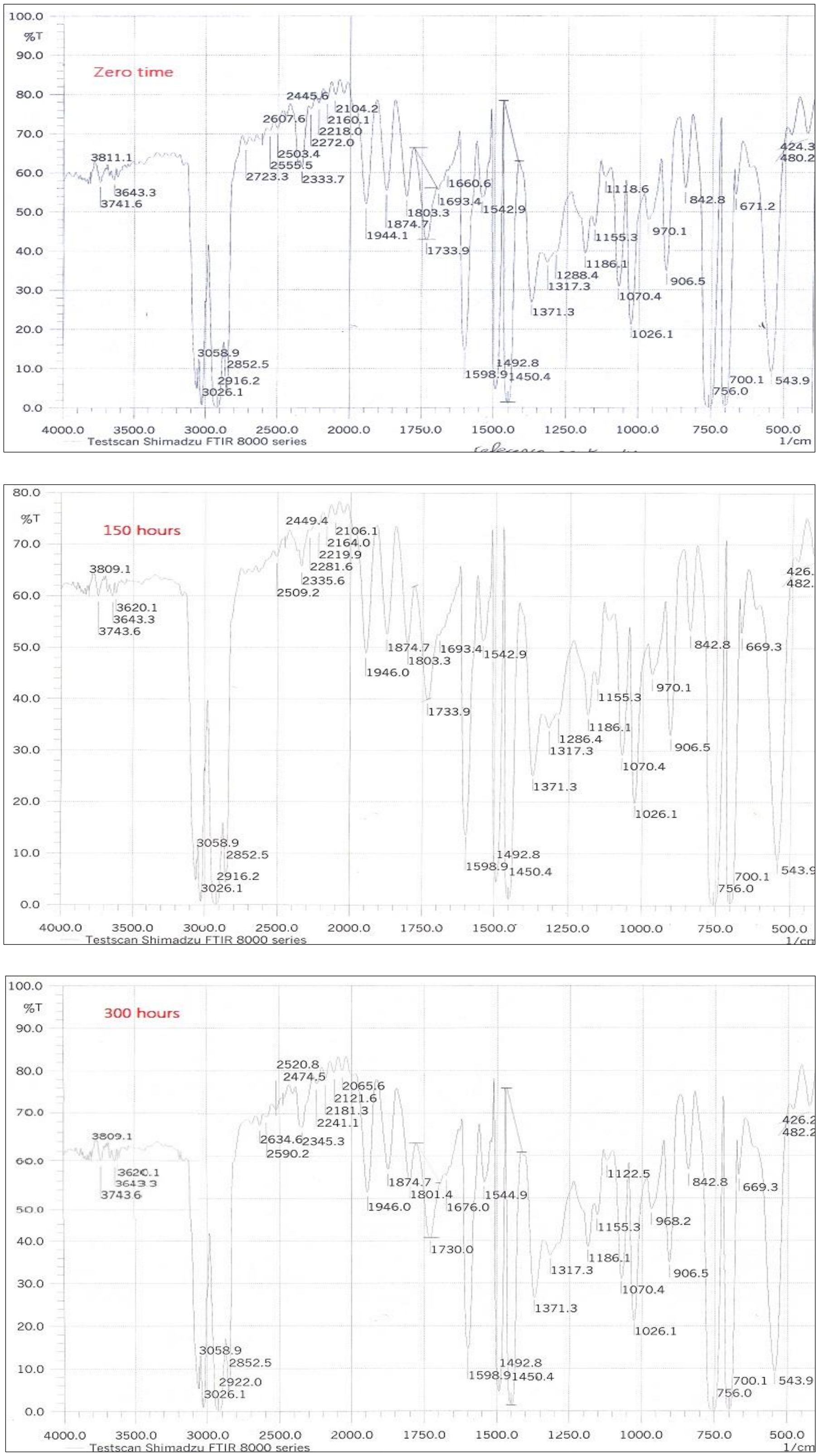

Figure (3.26) FTIR spectrum of PS blank films at different irradiation time

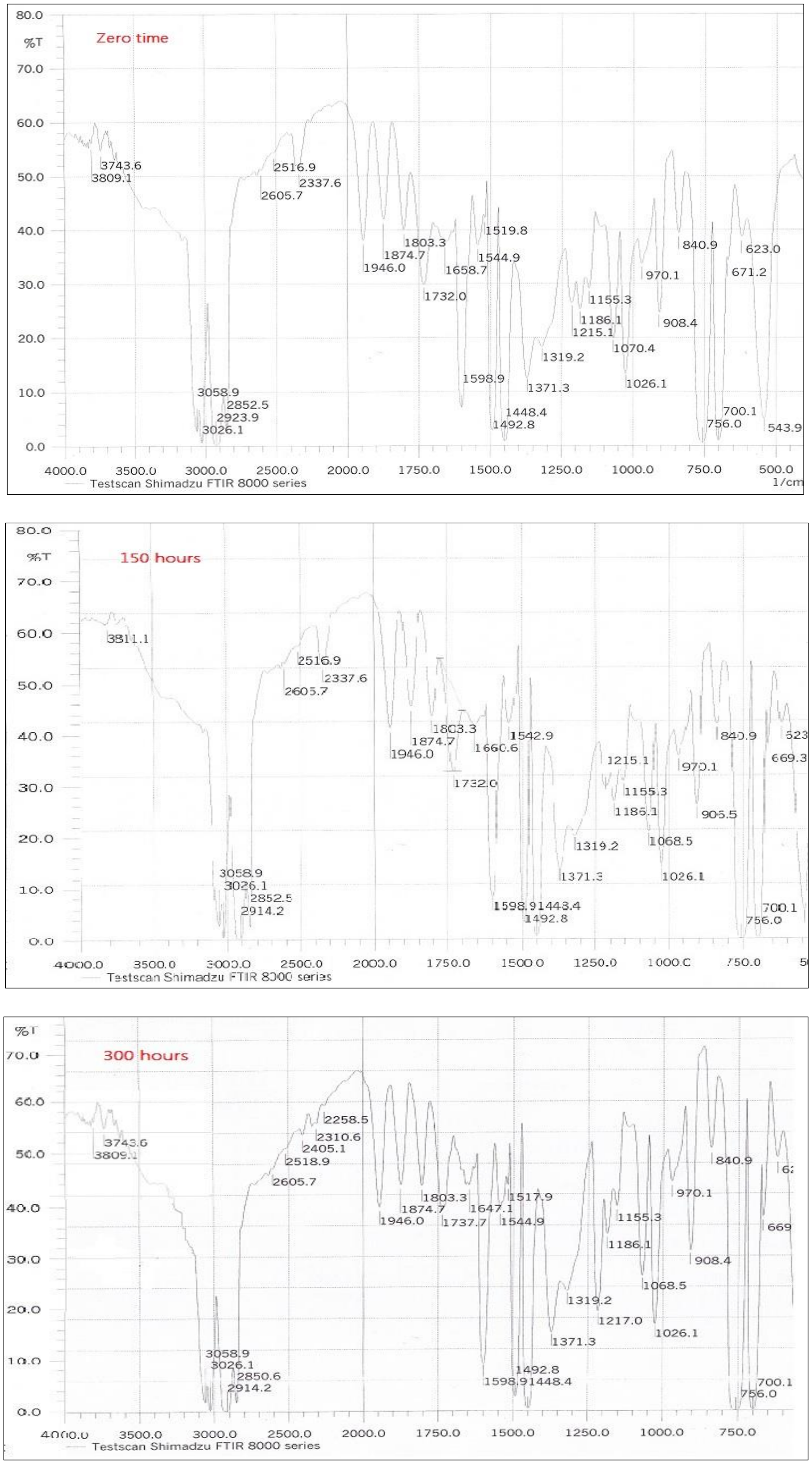

Figure (3.27) FTIR spectrum of (PS +Ni(L)$_2$)films at different irradiation time

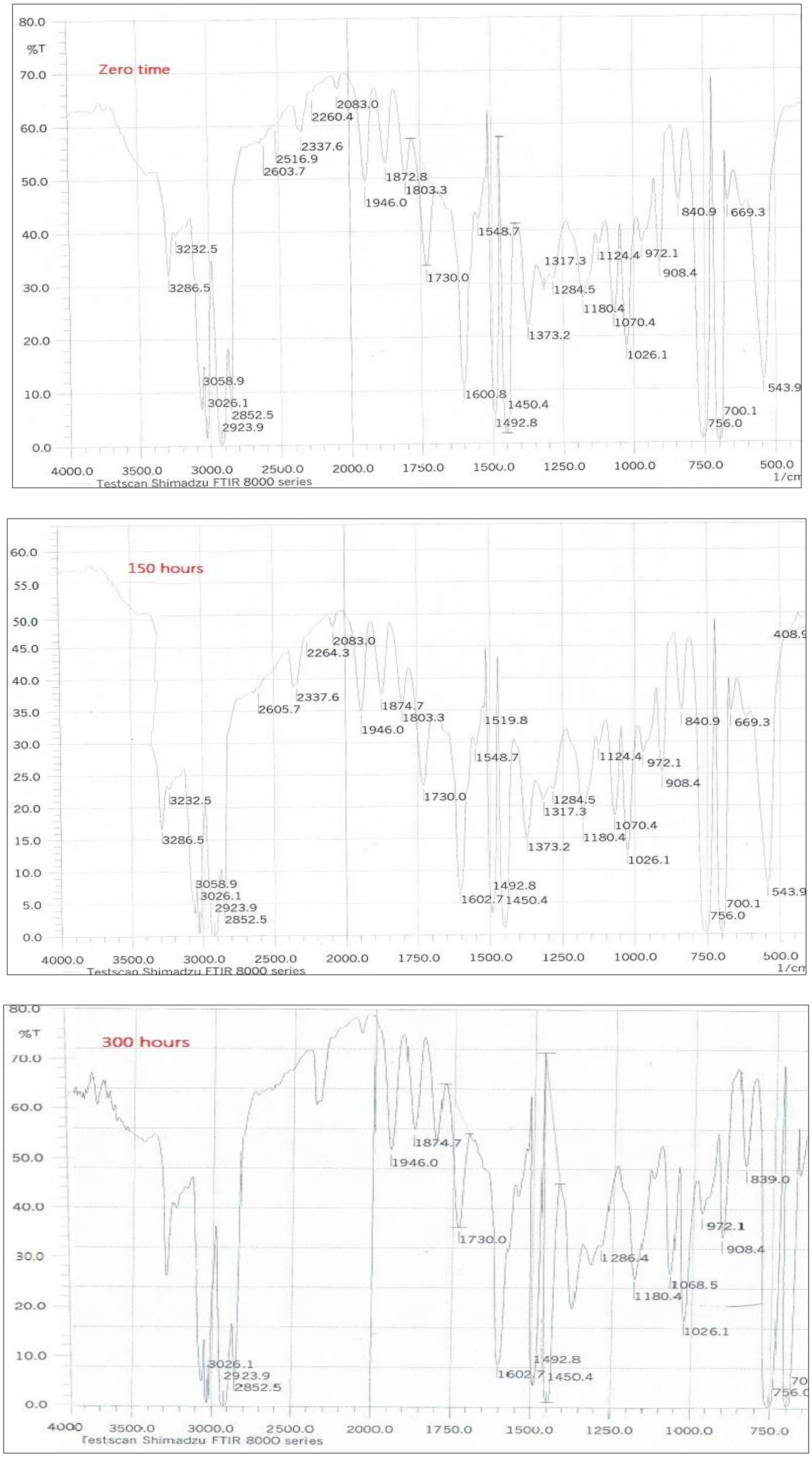

Figure (3.28) FTIR spectrum of (PS +Zn(L)$_2$)films at different irradiation time

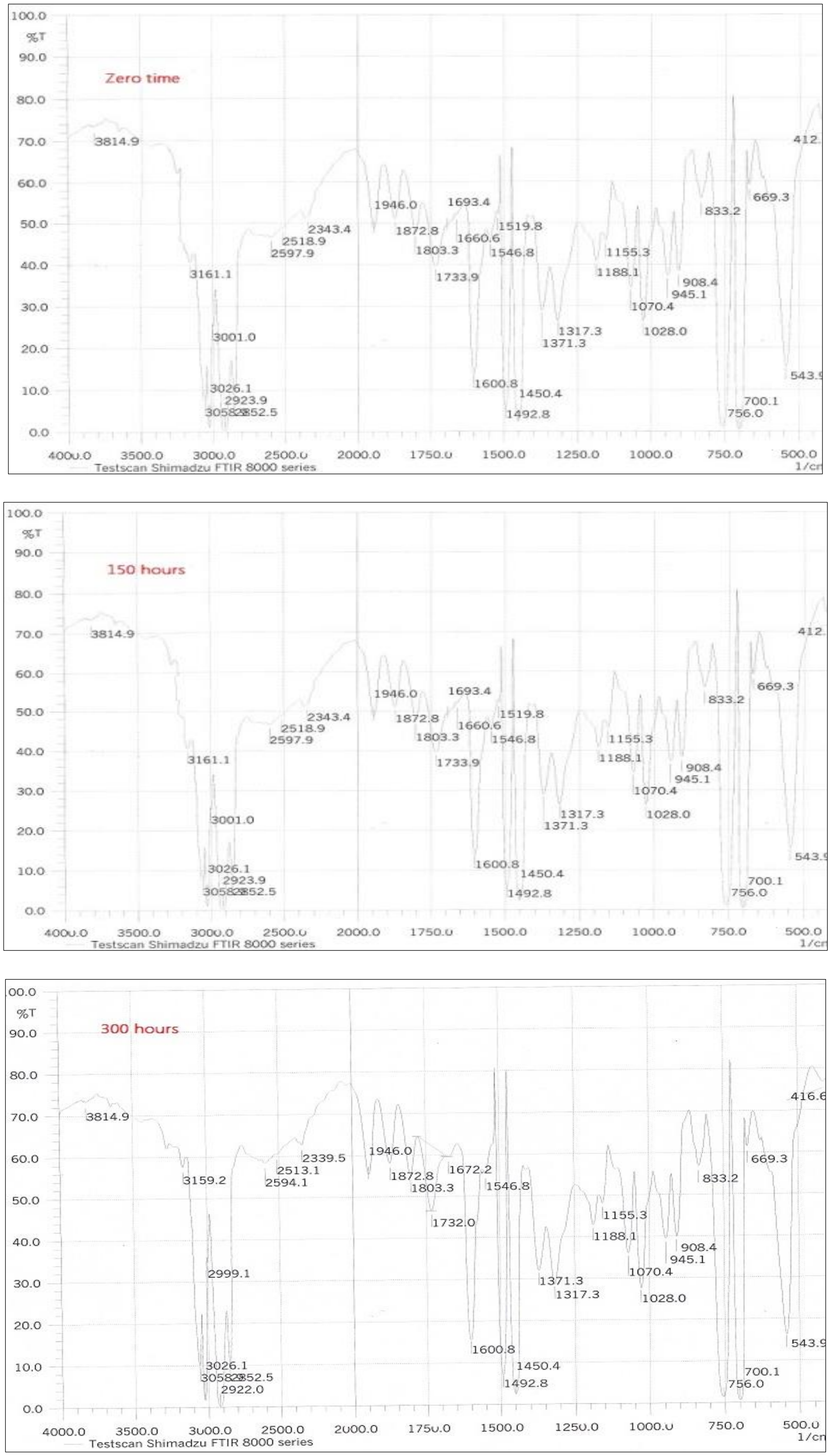

Figure (3.29) FTIR spectrum of (PS +Sn(L)$_2$)films at different irradiation time

3.2.2. Ultra-violet spectral studies of photodegradation rate of in PS films

The photooxidative degradation processes of PS have been discussed in a number of reviews(168-169).

It is generally accepted that carbonyl formed during UV irradiation of polymers, is most probable and are responsible for the yellow coloration of the polymer(170).

The carbonyl groups generated during the photooxidation process of polymer, extend the polymer film absorption to longer wavelengths(171). These groups absorb light when they irradiated with light of wavelength between (200-700 nm) and activated to the singlet and triplet excited states which enhances various successive photooxidation reactions(171).

The physical properties of additives and polymers play a very important role in determining the additives efficiency in photostabilization or photodegradation of polymers. For example, the compatibility that any type of additive (photostabilizer, antioxidant, thermal stabilizer…. etc.) must be evenly distributed which requires that it be compatible with the polymer matrix(172). The additives used in this study were chosen to be completely soluble in polymer solvent (Cloroform).

It has been notice that the additives used in the present work are photodecomposed during the photolysis. Thus the photo decomposition rate constant (K_d) was calculated, See paragraph (2.5.2). The K_d values were computed using the UV. spectra changes of PS films thickness 40μm containing 0.5% w/w from additives.

The plot of irradiation time versus ln (A_t-A_∞), gives straight line which indicate primarily the first order reaction. The slope equal to the decomposition rate constant K_d. Figure (3.30),(3.31),(3.32),(3.33),(3.34) and (3.35) shows the variation of ln (A_t - A_∞) with irradiation time for all additives in PS films at λ=365nm.

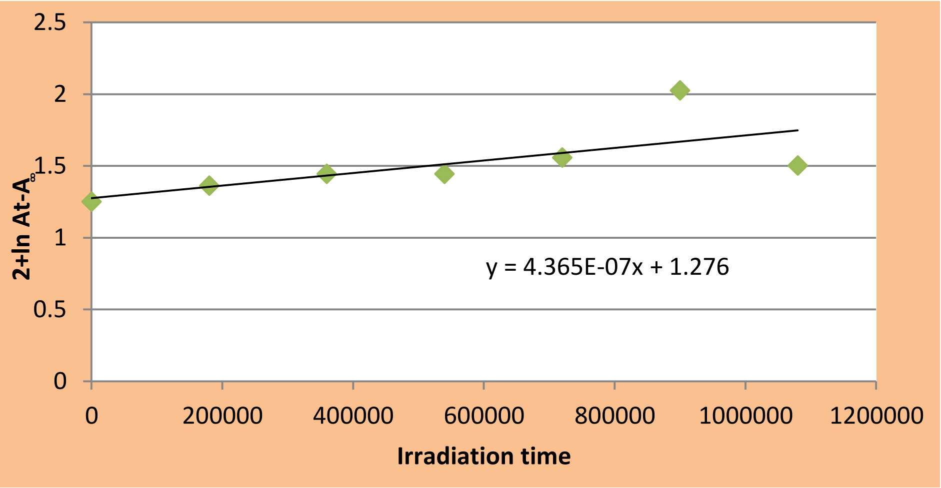

Figure (3.30) Variation of natural logarithm of ln (A_t – A_∞) with irradiation time of PS (blank) film

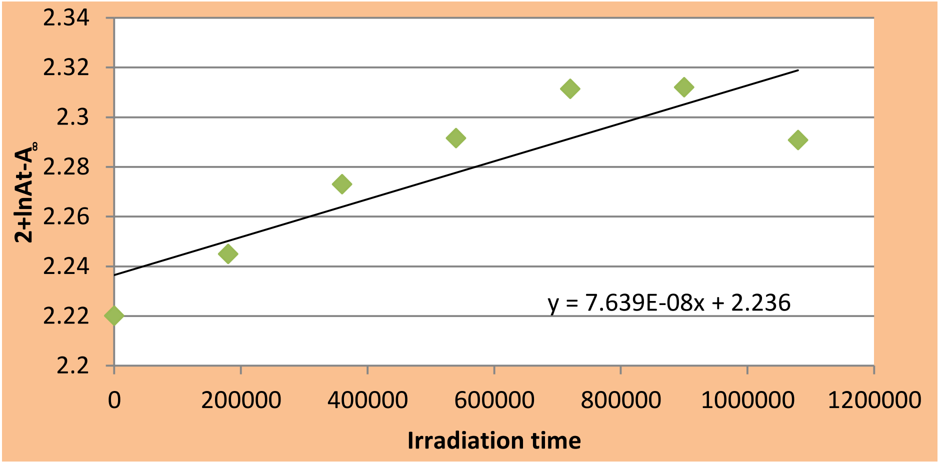

Figure (3.31) Variation of natural logarithm of ln ($A_t - A_\infty$) with irradiation time of Ni(L)$_2$ in PS film

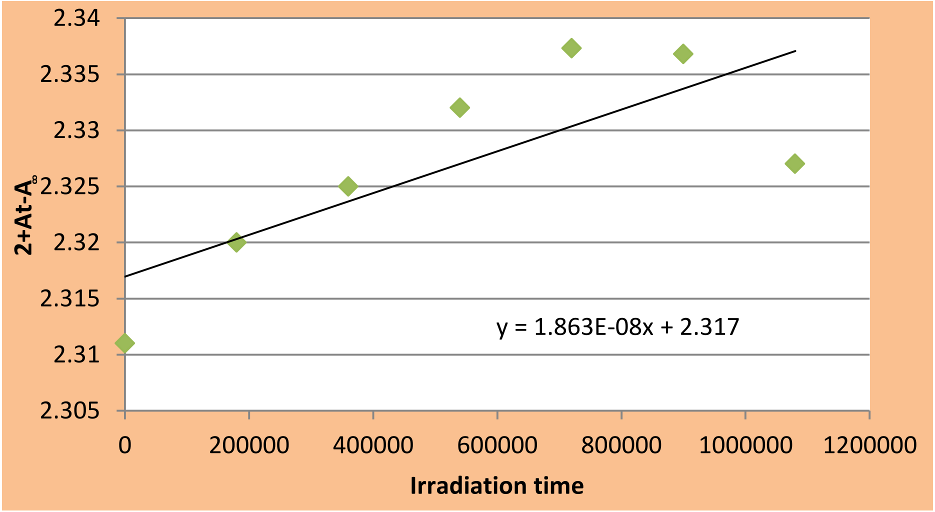

Figure (3.32) Variation of natural logarithm of ln ($A_t - A_\infty$) with irradiation time of Cu(L)$_2$ in PS film

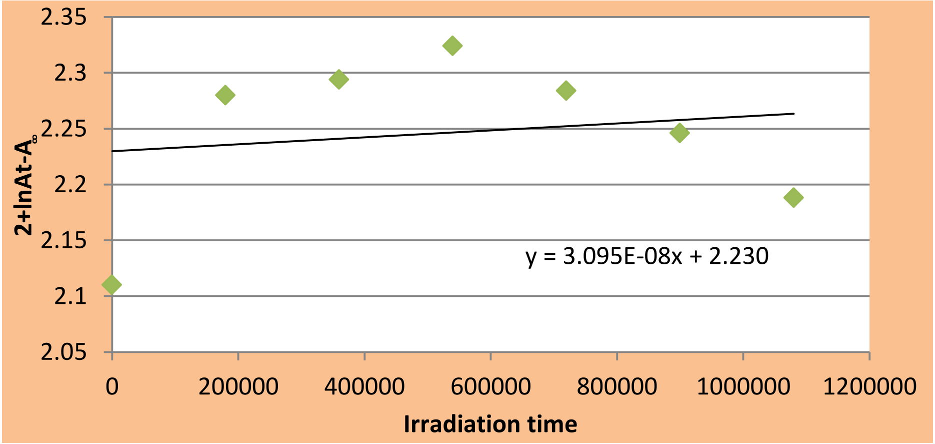

Figure (3.33) Variation of natural logarithm of ln ($A_t - A_\infty$) with irradiation time of Zn(L)$_2$ in PS film

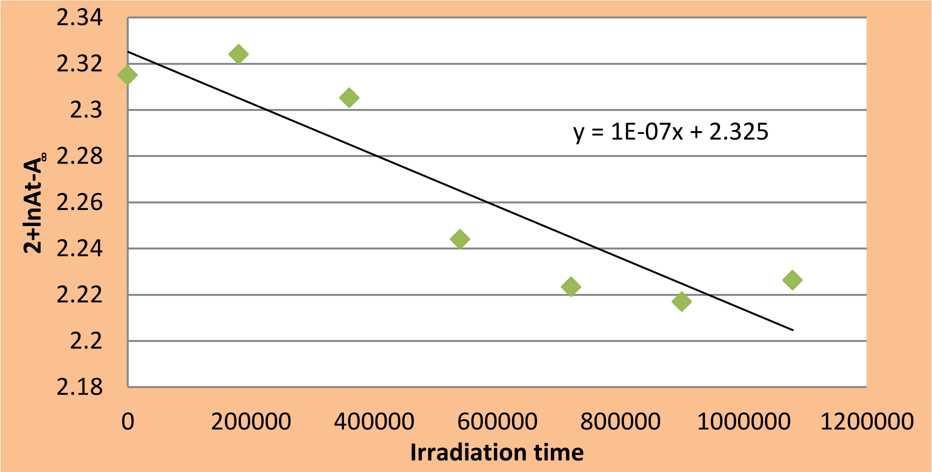

Figure (3.34) Variation of natural logarithm of ln ($A_t - A_\infty$) with irradiation time of Cd$(L)_2$ in PS film

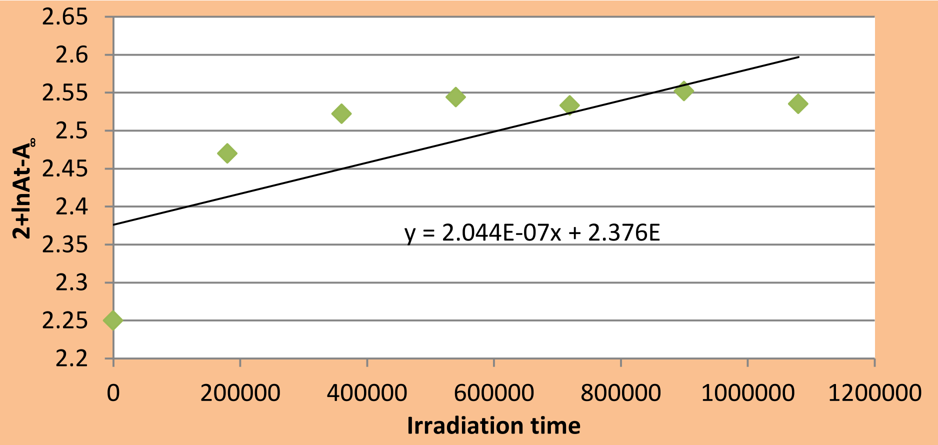

Figure (3.35) Variation of natural logarithm of ln ($A_t - A_\infty$) with irradiation time of Sn $(L)_2$ in PS film

The values of the first order rate constant of all the modified polymers films (k_d) calculated by the same way and shown in Table (3.9).

Table (3.9) Photo-decomposition rate constant (K_d) of PS films thickness (40μm) containing 0.5%w\w of additives

Polymers	K_d (S^{-1})
PS (blank)	4.365×10^{-7}
PS + $Ni(L)_2$	7.639×10^{-8}
PS + $Cu(L)_2$	1.863×10^{-8}
PS + $Zn(L)_2$	3.095×10^{-8}
PS + $Cd(L)_2$	1.000×10^{-7}
PS + $Sn(L)_2$	2.044×10^{-7}

The photostabilizers always posses low K_d values, which mean that these modified polymers are stable towards UV light.

One could notice that K_d values are sensitive to the type of additives in PS films, which decrease in the following order:

PS (blank) > $Sn(L)_2$ > $Cd(L)_2$ > $Ni(L)_2$ > $Zn(L)_2$ > $Cu(L)_2$

and this might point out to increase the photostability of this additives in this term.

3.2.3. Surface Morphology For the Films

Morphology, from the Greek and meaning in general "study of shape", and it may mean:

- Morphology (archaeology), study of the shapes or forms of artefacts.
- Morphology (materials science), the study of shape, size, texture and phase distribution of physical objects.
- Morphology (molecular), study of how the shape and form of molecules affect their chemical properties, dynamic reconfiguration and interactions.
- Morphology (Architecture and Engineering), research which is based on theories of two dimensional and three dimensional symmetries, and then uses these geometries for planning buildings and structures(173).

The morphological study for the surface of polymers gives a clear photo about some of the physical properties of the polymer For example, the crystalline case, irregular surface molecules, smoothing the surface and how to build it. And also shows the nature of the surface defects resulting from Photons of light interaction with the polymer molecule(173).

And can follow photodecomposition or stabilization of polymers that exposed to the UV. light through that appear on the surface of polymers, and see whether that the decomposition process can occur on chain scission or Decomposition for substitutes groups(25).

The morphologic studies also gives a clear indication for the polymers resistance to weathering and how to produce tough polymers as well as to know deformation that occur when polymer exposed to weathering conditions, and to help for production of packaging single-use (disposable), which cause now the problem of pollution and but now required to produce new kinds of packing that can be decomposed.

The PS (blank) film surface was smooth and empty of any white spots, whereas the PS film surface irradiated for 300 h was full of white spots; these spots are the holes or grooves, that is indicating degradation. In the case of modified polymers the surface was almost smooth, and fewer white spots appeared; this indicated the great stabilizing efficiency of the investigated the stabilizer and how much it protected the polymer surface from deterioration(174)see Figures (3.36), (3.37), (3.38) and (3.39).

The morphological study show that the surface of the polymer change in color and presence of cracks on the surface of it, resulting from interaction with high-energy of UV. light (λ = 365nm), and that is proportion With the hours of irradiation(175).

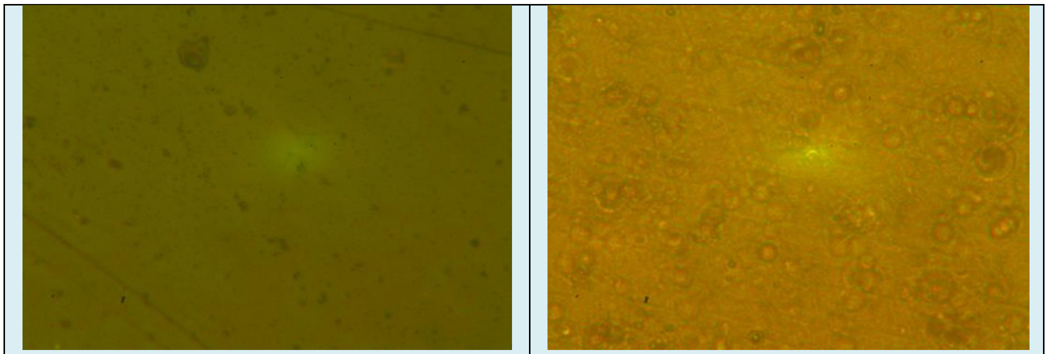

PS nonirradiated **PS irradiated 100h.**

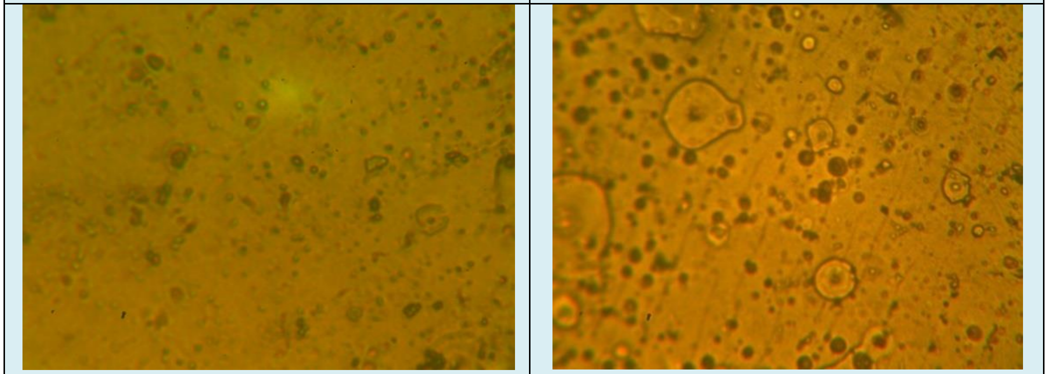

PS irradiated 200h. **PS irradiated 300h.**

Figure (3.36) Microscopic images of PS samples

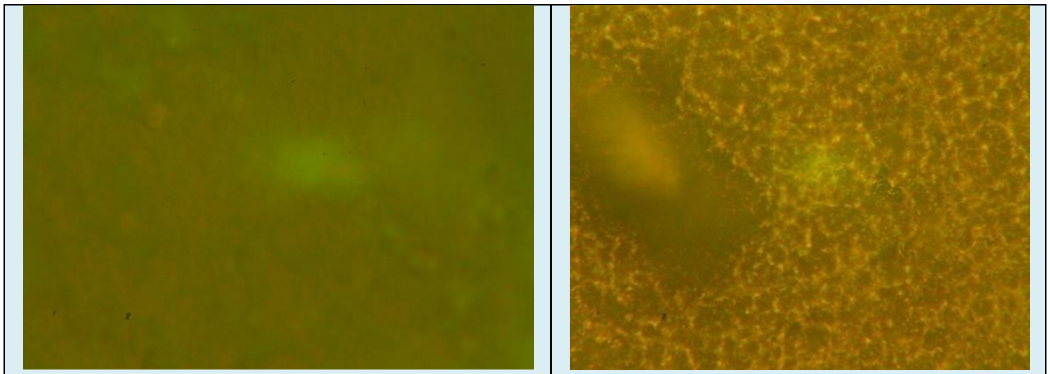

PS + $Zn(L)_2$ nonirradiated **PS+ $Zn(L)_2$ irradiated 100h.**

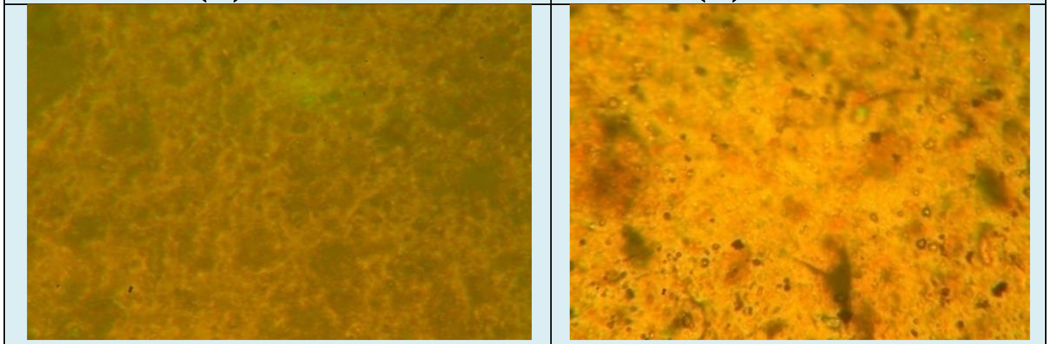

PS+ $Zn(L)_2$ irradiated 200h. **PS+ $Zn(L)_2$ irradiated 300h.**

Figure (3.37) Microscopic images of PS + $Zn(L)_2$ samples

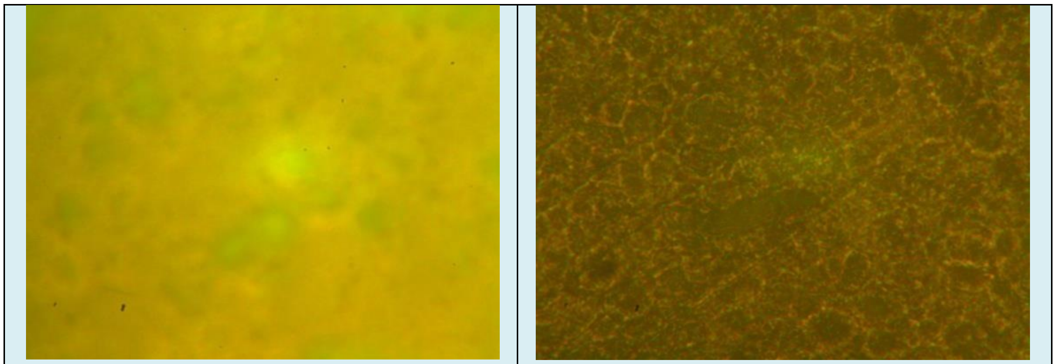

PS + Ni(L)$_2$ nonirradiated **PS+ Ni(L)$_2$ irradiated 100h.**

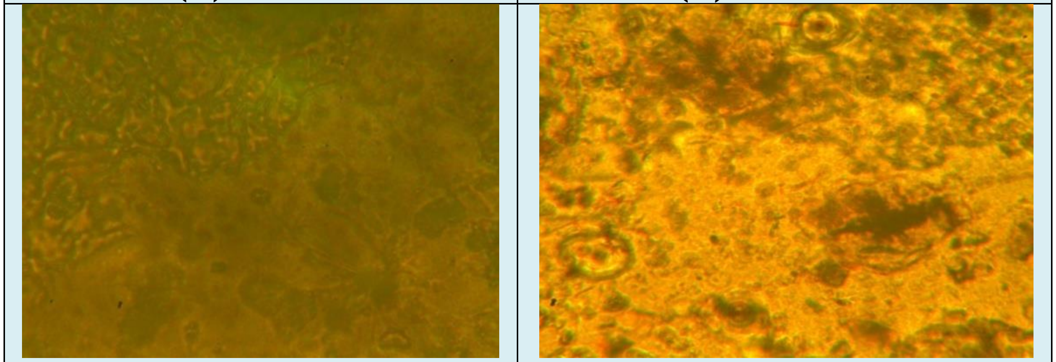

PS+ Ni(L)$_2$ irradiated 200h. **PS+ Ni(L)$_2$ irradiated 300h.**

Figure (3.38) Microscopic images of PS + Ni(L)$_2$ samples

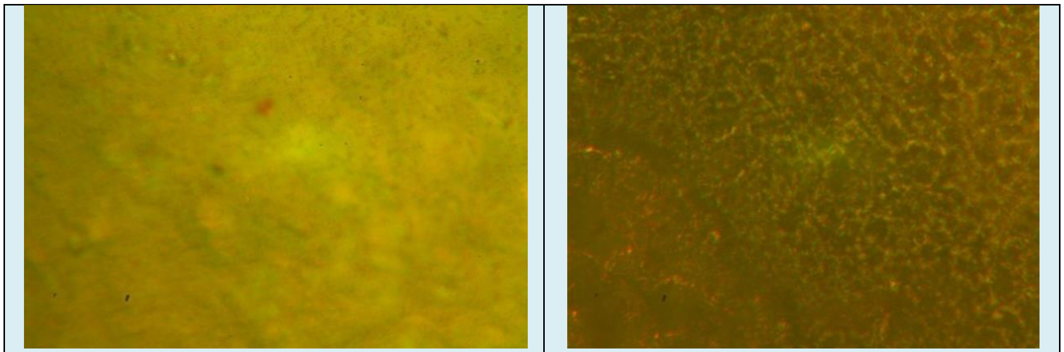

PS + Cd(L)$_2$ nonirradiated **PS+ Cd(L)$_2$ irradiated 100h.**

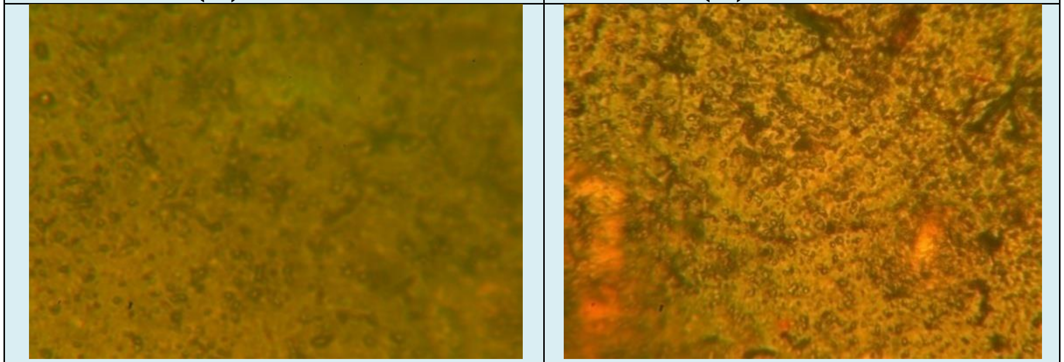

PS+ Cd(L)$_2$ irradiated 200h. **PS+ Cd(L)$_2$ irradiated 300h.**

Figure (3.39) Microscopic images of PS +Cd(L)$_2$ samples

3.2.4. Determination of the Stabilizing Efficiency by Weight Loss Method

The stabilizing efficiency was determined by measuring the % weight loss of photodegraded PS films in absence and in presence of additives by applying the following equation, See Paragraph (2.5.4):

$$\textbf{Weight loss \%} = [\,(W_1 - W_2)\,/\,W_1\,]\,100 \qquad \ldots\ldots\ldots (3.4)$$

Volatile and low molecular weight products(176) formed on photodegradation of PS led to a weight loss phenomenon.

The weight loss of polystyrene films increased gradually with the increasing degradation time(177-178), thus, the weight loss percentage as a function of the irradiation time can be a good measure of the degree of degradation and consequently can measure the stabilizing potency of the stabilizer and how long the stabilizer would protect the polymer.

The results of weight loss % as a function of irradiation time are represented in Figure (3.40) and Table (3.10), the increasing very small with PS film modified by additives.

The results indicate that all of the five additives have stabilizing effect against photodegradation of PS samples and leading to a considerable decrease in % weight loss compared with blank PS. The stabilizing efficiency of the investigated photostabilizers was found to follow this order:

$$\mathbf{Cu(L)_2 > Zn(L)_2 > Ni(L)_2 > Cd(L)_2 > Sn(L)_2 > PS}$$

Table (3.10), Measurement of weight loss for PS films (40µm) thickness containing 0.5% from the additives

Additives	Irradiation time (hours)					
	50	100	150	200	250	300
PS (blank)	1.228	2.763	3.582	4.196	4.401	5.322
PS+Ni(L)$_2$	1.560	2.522	3.250	3.733	4.200	4.439
PS+Cu(L)$_2$	1.639	1.831	2.550	2.900	3.150	3.710
PS+Zn(L)$_2$	1.013	2.094	2.776	3.073	3.381	3.893
PS+Cd(L)$_2$	0.156	2.763	3.582	4.196	4.401	4.910
PS+Sn(L)$_2$	1.870	3.181	4.090	4.431	4.659	5.113

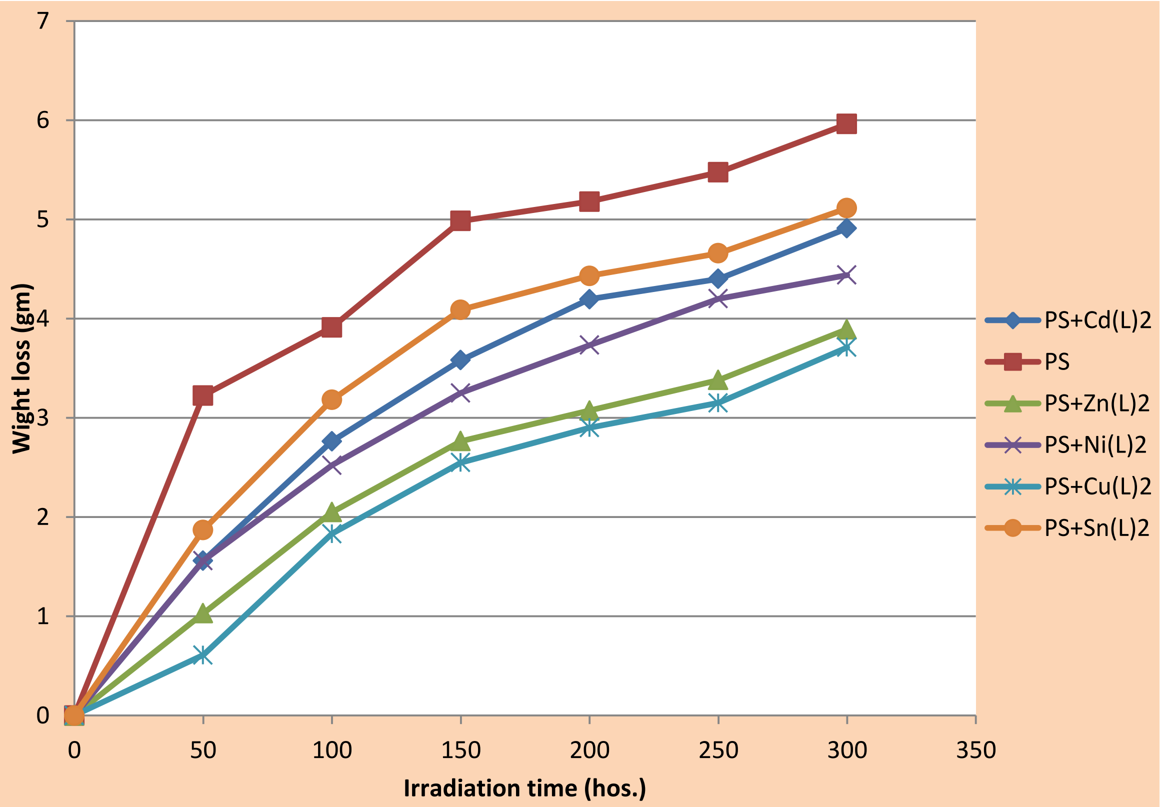

Figure (3.40) loss in weight vs. irradiation time for PS films (40µm) thickness containing 0.5% w\w from the additives

3.3 Variation of PS Molecular Weight during Photolysis

An analysis of the relative change in viscosity average molecular weight (Mv) described by Scott(179) has been shown to provide a test for random chain scission. Figure (3.41) shows the plot of (Mv) versus irradiation time for PS films with and without 0.5% (w/w) of five selected additives with absorbed light intensity of 6.2 X 10^{-9} Ein Dm^{-3} S^{-1}. By measuring the solution viscosity we should be able to get an idea about molecular weight. Viscosity techniques are very popular because they are experimentally simple(180). (Mv) is measured using equation (2.8) in chapter two and Cloroform as a solvent at 25 °C, as shown in Table (3.11).

Table (3.11) Variation of Mv with irradiation time of PS films thickness (40µm) containing 0.5 % of additives

Additives	**Irradiation time (hs.)**					
	0	**50**	**100**	**150**	**200**	**250**
PS (blank)	276500	159000	120000	86500	35500	30000
PS+Ni(L)$_2$	315000	228000	185500	148000	113000	110000
PS+Cu(L)$_2$	313000	290000	234000	206000	176000	170000
PS+Zn(L)$_2$	308000	262000	214000	171000	152000	150000
PS+Cd(L)$_2$	308000	208000	168000	137000	92000	90000
PS+Sn(L)$_2$	290000	187000	145000	111000	69000	55000

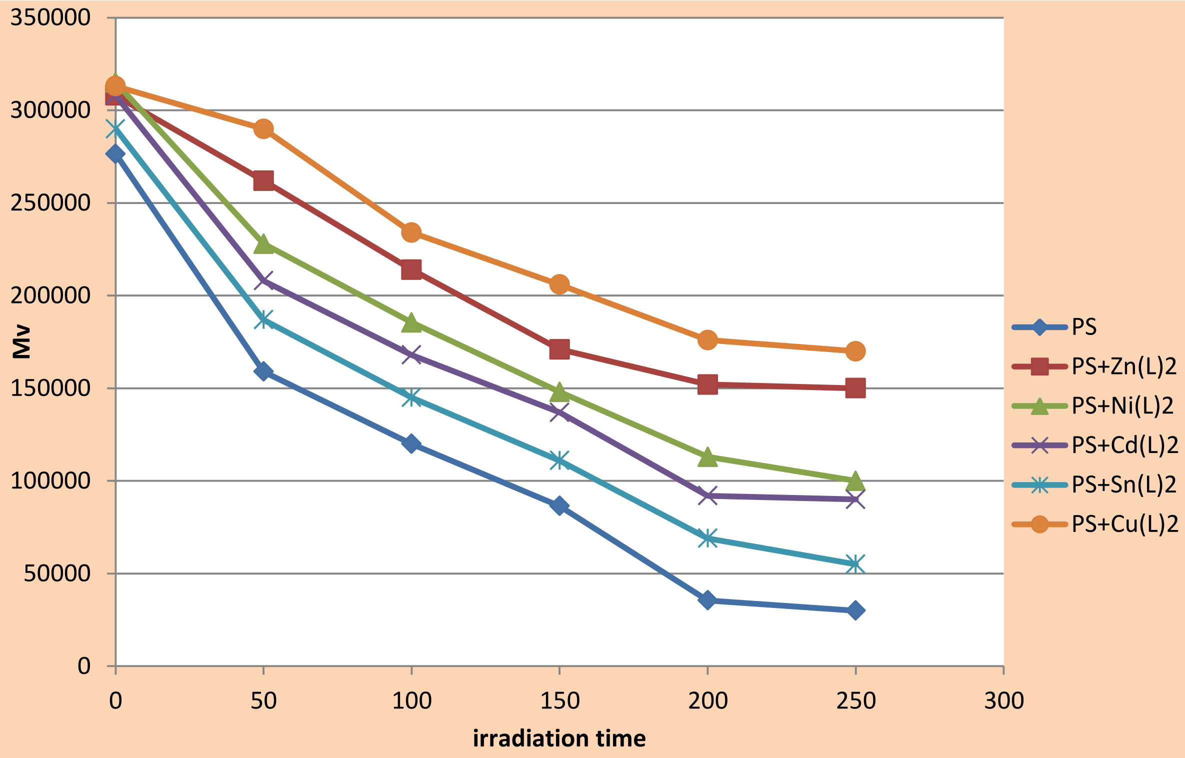

Figure (3.41) Changes in the viscosity average molecular weight during irradiation for PS and modified PS films

The plot indicates a rapid decrease in (Mv) initially then it slows down, suggesting that is due to the main chain scission at various locations along the polymer chain.

The degradation of polystyrene led to decreases in the viscosity because the degraded polystyrene becomes low molecular weight than undegraded polymer because degraded polymer undergoes chain scission that decreases the molecular weight(181).

For better support of this view, the number of average chain scission (S)(182) was calculated using the following relation: $\mathbf{S = M_{v,o} / M_{v,t} - 1}$……. (3.5)

Where ($M_{v,o}$) and ($M_{v,t}$) are viscosity–average molecular weight at initial (o) and at irradiation time (t), respectively.

The plot of S versus time is shown in Figure (3.42). The curve indicates an increase in the degree of branching such as that might arise from crosslinking occurrence. It is observed that insoluble material was formed during irradiation, which provided an additional evidences to the idea that crosslinking does occur.

For randomly distributed weak bond links, which rapidly break in the initial stages of photodegradation, the degree of deterioration (α) is given as follows:

$$\boldsymbol{\alpha = m * S / Mv} \quad \text{……... (3.6)}$$

Where **m** is the initial molecular weight. The plot of α as a function of irradiation time is shown in Figure (3.43).

The values of α of the irradiated samples are higher when additives are absent (PS blank) and lower in the presence of additives when compared with the corresponding values of the additive-free PS. In the initial stages of photodegradation of PS, the value of α increase rapidly with time; these indicators indicate a random breaking of bonds in the polymer chain(119).

Table (3.12) Variation of (S) values with irradiation time of PS films thickness (40µm) containing 0.5 % w\w of additives

Additives	**Irradiation time (hs.)**					
	0	**50**	**100**	**150**	**200**	**250**
PS (blank)	0	0.710	1.304	2.360	6.788	8.216
PS+Ni(L)$_2$	0	0.381	0.698	1.128	1.787	2.150
PS+Cu(L)$_2$	0	0.079	0.337	0.497	0.778	0.841
PS+Zn(L)$_2$	0	0.250	0.439	0.801	1.200	1.480
PS+Cd(L)$_2$	0	0.480	0.833	1.248	2.347	3.000
PS+Sn(L)$_2$	0	0.550	1.000	1.612	3.202	4.272

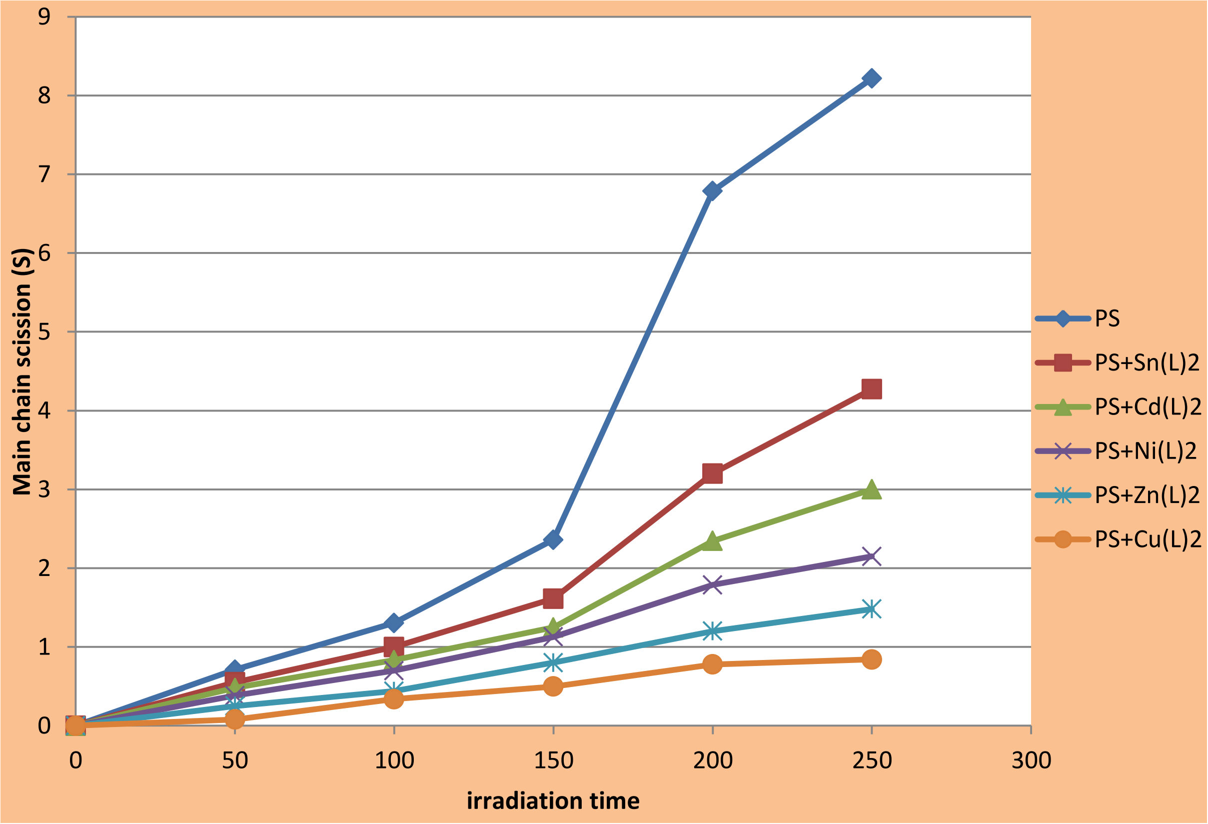

Figure (3.42) Changes in the main chain scission (S) during irradiation for PS and modified PS films

Table (3.13) Variation of the (α) value with irradiation time of PS films thickness (40μm) containing 0.5 % w\w of additives

Additives	**Irradiation time (hs.)**					
	0	**50**	**100**	**150**	**200**	**250**
PS (blank)	0	1.234	3.004	7.587	52.807	75.724
PS+Ni(L)$_2$	0	0.526	1.170	2.400	4.981	6.772
PS+Cu(L)$_2$	0	0.085	0.450	0.744	1.383	1.548
PS+Zn(L)$_2$	0	0.293	0.631	1.442	2.431	3.038
PS+Cd(L)$_2$	0	0.710	1.527	2.805	7.075	10.266
PS+Sn(L)$_2$	0	0.852	2.000	4.211	13.457	22.525

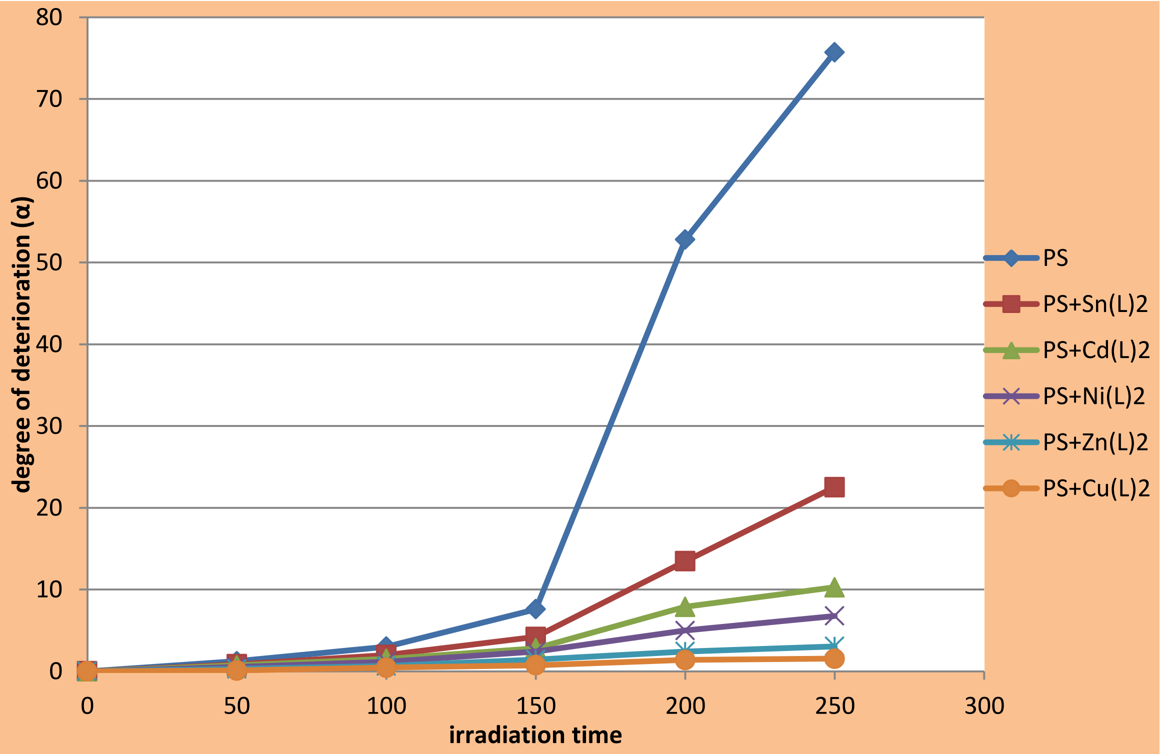

Figure (3.43) Changes in the degree of deterioration (α) during irradiation for PS and modified PS films

The degree of polymerization, or DP, is usually defined as the number of monomeric units in a macromolecule or polymer. For a homopolymer, there is only one type of monomeric unit and the number average degree of polymerization is given by

$$\mathbf{DP_n = X_n = M_n / M_o} \quad \ldots\ldots\ldots (3.7)$$

Where M_n is the number-average molecular weight and M_0 is the molecular weight of the monomer unit(183).

The plot of 1/Pt versus irradiation time is adopted by Yousif et al.(184) to characterize degradation reaction of polymer as shown in Figure (3.44). 1/Pt means the reciprocal of degree of polymerization. The curve indicates that increase in the inverse of number average degree of polymerization with irradiation time.

Table (3.14) The variation of P_t with irradiation time for PS films with 0.5 wt% of additives, film thickness is (40 μm)

Additives	**Irradiation time**					
	0	**50**	**100**	**150**	**200**	**250**
PS (blank)	2078	1195	902	646	267	225.5
PS + $Ni(L)_2$	2368.4	1714.3	1394.7	1112.8	849.6	751.8
PS + $Cu(L)_2$	235.3	2180.4	1827	1571.4	1323.3	1278.1
PS + $Zn(L)_2$	2315.7	1970	1609	1285	1142	1127.8
PS + $Cd(L)_2$	2315.7	1564	1263.1	1030	691.7	676.7
PS + $Sn(L)_2$	2180.4	1406	1090	834.5	518.7	413.5

Table (3.15) The variation of $1/P_t$ with irradiation time for PS films with 0.5% w\w of additives, film thickness is (40 μm)

Additives	Irradiation time					
	0	50	100	150	200	250
PS (blank)	0.0004	0.0008	0.0011	0.0015	0.0037	0.0044
PS + $Ni(L)_2$	0.0004	0.0005	0.00071	0.00089	0.0011	0.0013
PS + $Cu(L)_2$	0.00042	0.00045	0.00054	0.00063	0.00075	0.00078
PS + $Zn(L)_2$	0.00043	0.0005	0.00062	0.00077	0.00087	0.00095
PS + $Cd(L)_2$	0.0004	0.0006	0.00079	0.00095	0.0013	0.0015
PS + $Sn(L)_2$	0.0004	0.0007	0.00091	0.0011	0.0019	0.0024

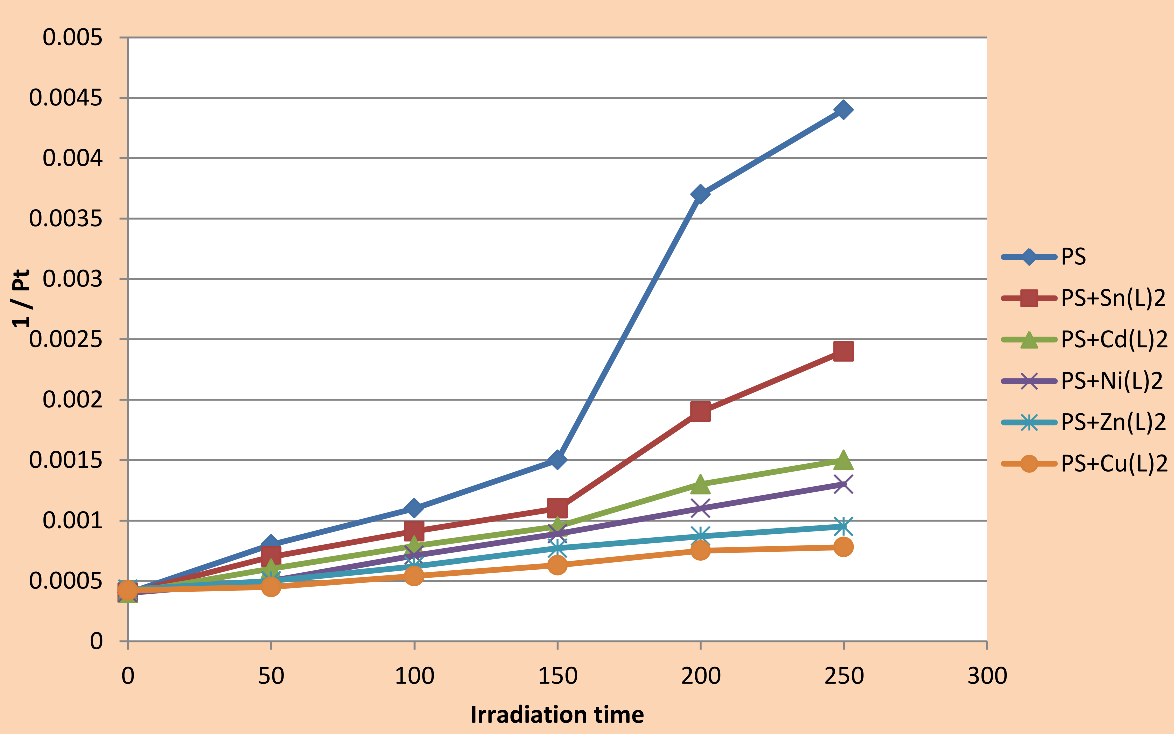

(3.44) Changes in the reciprocal of number average of polymerization (1/Pt) during irradiation for PS films (control) and modified PS films

On the other side, there is another method for characterization degradation reaction it is measurements of the quantum yield of the chain scission (Φ_{cs})(185).

The quantum yield for chain scission was calculated for PS films of modified polymers by using the relation (2-13) in chapter two. The Φ_{cs} values for these polymers are tabulated in Table (3.16).

Table (3.16) Quantum yield (Φ_{cs}) for the chain scission for PS films (40μm) thickness with and without additives after 200 hrs. irradiation time

Additives	Quantum yield
PS (blank)	3.685 * 10^{4}
PS + $Ni(L)_2$	4.990 * 10^{3}
PS + $Cu(L)_2$	3.380 * 10^{3}
PS + $Zn(L)_2$	4.790 * 10^{3}
PS + $Cd(L)_2$	1.147 * 10^{4}
PS + $Sn(L)_2$	1.664 * 10^{4}

The Φ_{cs} values for modified PS films are less than that of unmodified PS (blank).

The explanation of low values of Φ_{cs} is due to that, in large molecule of PS the energy is absorbed at one site, and then the electronic excitation is distributed over many bonds so that the probability of a single bond breaking is small, or the absorbed energy is dissipated by non reactive processes(186) .

Through the overall results obtained, the efficiency of 4-amino-5-(pyridyl)-4H-1,2,4-triazole-3-thiol complexes as stabilizers for PS films can be arranged according to the change in the carbonyl, hydroxyl and weight loss measurement and viscosity average molecular weight as a reference for comparison as shown in Figure (3.24), (3.25), (3.36) and (3.37):

$$Cu(L)_2 > Zn(L)_2 > Ni(L)_2 > Cd(L)_2 > Sn(L)_2 > PS$$

3.4. Suggested Mechanisms of Photostabilization of PS by 4-amino-5-(pyridyl)-4H-1,2,4-triazole-3-thiol Complexes

The photostabilization of PS with triazole complexes proceeds through the UV.absorber, radical scavenger and peroxide decomposer mechanisms. These stabilizers provide very good long term stability and are usually referred to these mechanisms.

Metal chelate complexes generally known as photostabilizers for poly olefins through both peroxide decomposer and excited state quencher(187), therefore these Metal chelate complexes are generally known as photostabilizers for PS through both peroxide decomposer and excited-state quencher. So, it is expected that these complexes act as peroxide decomposer through the proposed mechanism (See Scheme 3.3).

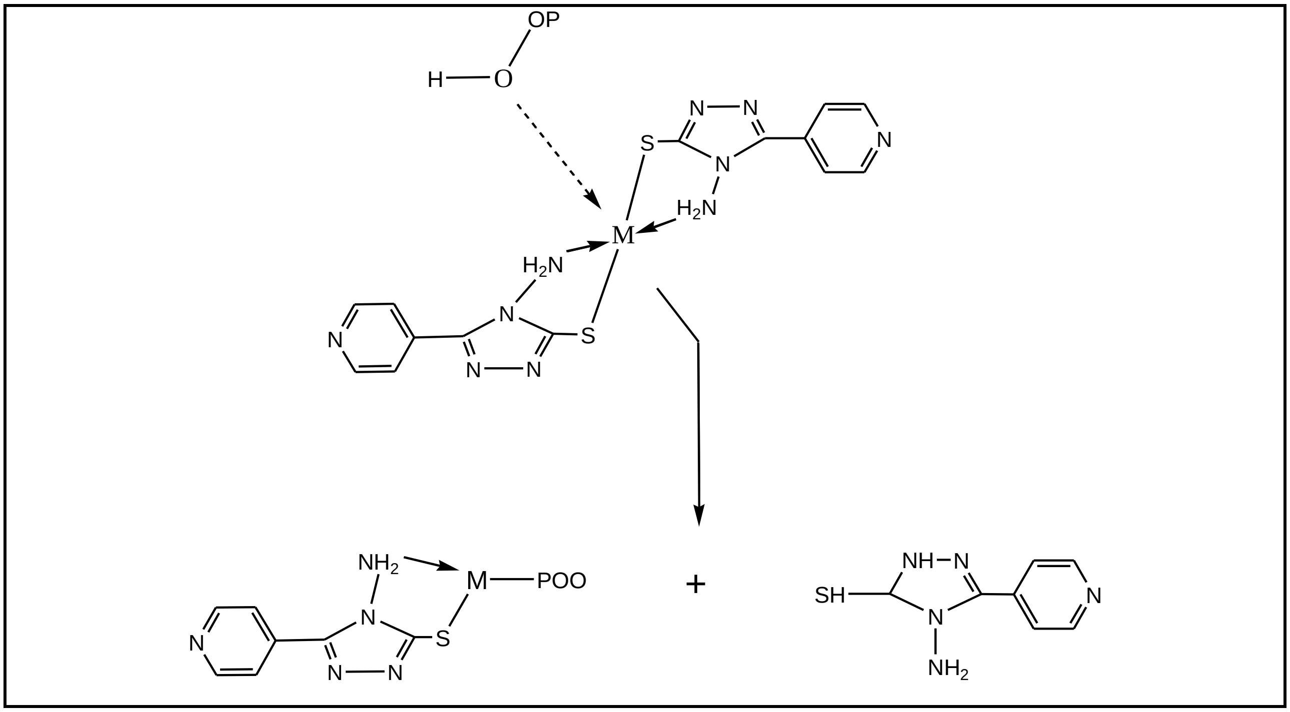

Scheme (3.3) Suggested mechanism of photostabilization of complexes as peroxide decomposer

These metal chelate complexes also function as radical scavengers through energy transfer and by forming unreactive charge transfer complexes between the metal chelate and the excited state of the chromophore (POO$^{.}$) and stabilize through resonating structures$^{(124, 166)}$as shown in Scheme (3.4):

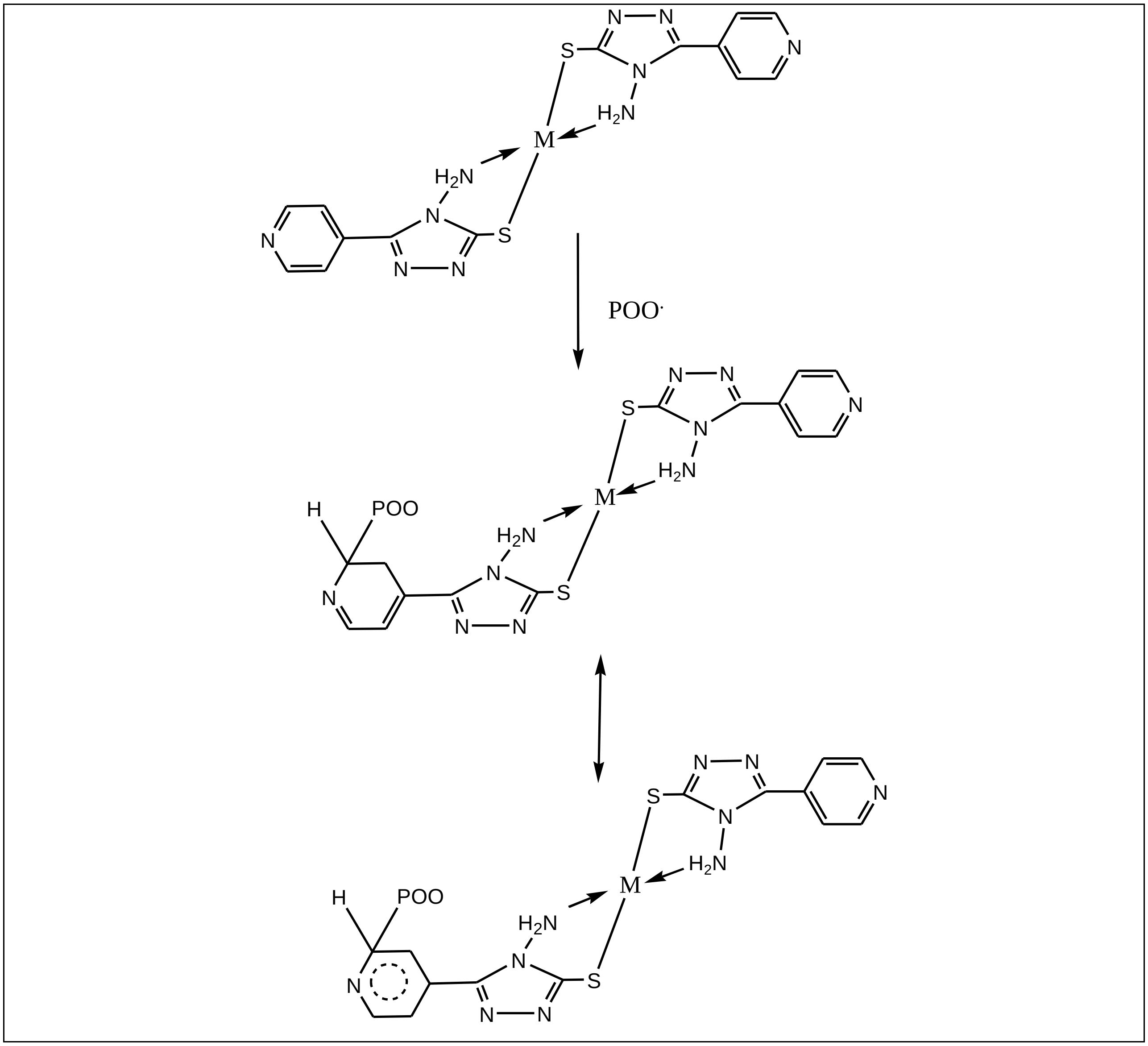

Scheme (3.4) Suggested mechanism of photostabilization of complexes as radical scavengers

The ring of triazole in this compound plays an important role in the mechanism of stabilizing process by acting as UV absorber(184,188, 189). The UV light absorption by these additives containing triazole dissipates the UV energy to harmless heat energy (Scheme 3.5). This mechanism is in agreement with that reported by Adil *et al.*(190).

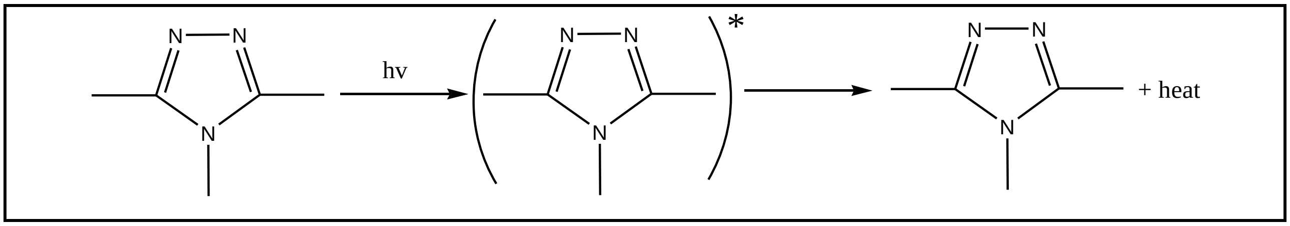

Scheme (3.5) Suggested mechanism of photostabilization of triazole as UV. absorber

A number of Nickel chelates of different structure have found industrial applications for stabilization of polyolefins through peroxide decomposer and excited state quencher(191). Nickel chelates were also tested for photostabilization of PS(192) and PVC(193) .

3.5. Conclusion

In the work described in this thesis, the photostabilization of polystyrene (PS) films by using Bis(4-amino-5-(pyridyl)-4H-1,2,4-triazole-3-thiol) complexes (0.5% w/w) concentration in PS films have been studied.

These additives behave successfully as photostabilizer for PS films. The additives take the following order in photostabilization activity according to their decrease in carbonyl I_{CO}, hydroxyl I_{OH}, and the weight loss for PS films.

$$\mathbf{Cu(L)_2 > Zn(L)_2 > Ni(L)_2 > Cd(L)_2 > Sn(L)_2}$$

These additives stabilize the PS films through UV. absorption or screening, peroxide decomposer, and radical scavenger mechanisms.

The Cupper complex was found to be the more efficient in photostabilization process according to the photostability and mechanism mentioned above. This support to use the Cupper complex as commercial stabilizer for PS.

3.6. Suggestions for future work

1. Studying the photoactivity of the additives in other polymers such as PVC, PVA, LDPE, HDPE and comparing the activity of these additives with PS blank.
2. Comparing the efficiency of the additives with some commercial stabilizer.
3. One can study the effect of additives in the outdoor weathering.
4. Study the effect of additives in polymer solution.
5. One can study the effect of temperature on the efficiency of the additives.
6. Can also study the effect of substitution of the some groups on the aromatic rings in the structure of the complexes and study their effect on polymers.
7. Since fixed thickness was used in this presented study, so one can extend the study by using different films thickness and studying their effect on the photostabilization process.
8. Can extend the study by using different concentration from additives and studying their effect on the photostabilization process.

REFERENCES

References

1. Zamani K., Faghihi K., Tofighi T., Hariatzadeh M.R., (2004), Synthesis and antimicrobial activity of some pyridyl and naphthyl substituted 1,2,4 triazole and 1,3,4 thiadiazole derivatives, Turk. J. Chem., 28(1): 95-100.

2. Carey F., (1980), Organic Chemistry, McGraw-Hill, Inc. America.

3. Acheson R., (1989), An Introduction to the Chemistry of Heterocyclic Compound, 3: 122-136.

4. Clayden J., Greeves N., Warren S. and Wothers P., (2001), Organic Chemistry, Oxford University.

5. Siddiqui N., Ahsan W., Alam M., Ali R., Jain S., Azad B., Akhtar J., (2011), Triazole: as potential bioactivity agents, International J. of Pharmaceutical Sciences Review and Research, 8(1): 161-169.

6. Bele D. and Singhvi I., (2011), A review on1, 2, 4- triazole, Asian J. of Biochemical and Pharmaceutical Research, 1: 88-100.

7. Davari M., Bahrami H., Haghighi Z. and Zahedi M., (2010), Quantum chemical investigation of intramolecular thione-thiol tautomerism of 1,2,4-triazole-3-thione and its disubstituted derivatives, J. Mol. Model., 16(5): 841-855.

8. Jadhav S., Rai M., Durrani A., Bembalkar S., (2010), Synthesis and characterization of substituted 1,2,4-Triazole and its derivatives, Oriental J. of Chemistry, 26(2): 725-728.

9. Hirschfelder J., Henderson D., (1971), Chemical dynamic, paper in Honor of Henry Eyring, Wiley interscience New York, 2: 201.

10. AL-Abidy M., (1997), M Sc Thesis, University of Baghdad, Iraq.

11. Cotton F., Wilkinson G., (1980), Advanced Inorganic Chemistry, John Wiely and Sons, 4th. Ed.

12. Huheey J.,(1988), Inorganic Chemistry, Principles of structure and reactivity , Ed. Harpar and Row, New Yourk, 422-425.

13. Al-Maydama H., Al-Ansi T., Jamil Y. and Ali A., (2008), Biheterocyclic ligands: Synthesis, characterization and coordinating properties of bis(4-amino-5-mercapto-1,2,4-triazol-3-yl) alkanes with transition metal ions and their thermokinetic and biological studies, Ecl. Quim., 33(3): 29-42.

14. Narayana B. and Gajendragad M., (1997), Complexes of Zn(II) , Pd(II), Hg(II), Pb(II), Cu(I), Ag(I), and Ti(I) with 4-amino-5-merccapto-3-(o-tolyloxymethyl)-1,2,4-troazol, Tr. J. of chemistry Tur. J. Chem., 21:71-76.

15. Alias M., (2007), Synthesis and characterization of some new metal complexes with bis [4-phenyl-2-dibutyl aminomethyl-1,2,4-triazole-3-thiol-5yl] methane and theoretical study, J. of Al-Nahrain University, 10(2): 13-24.

16. McCarrick R., Eltzroth M., Squattrito P., (2000), Coordination geometries of bis(4-amino-3-alkyl-1,2,4-triazole-5-thione) complexes of first-row transition metals: crystal structures of complexes with propyl and hydrogen in the 3-position. Relationship to the 3-methyl and 3-ethyl analogs, Inorganica Chimica Acta , 311: 95-105.

17. Hartwig F., (2010), Organotransition Metal Chemistry, from Bonding to Catalysis; University Science Books, New York.

18. Awad I., Abdel-Rahman A., Bakite E., (2008), 4-[(*E*)-(3-Methyl-5-thioxo-4,5-dihydro-1*H*-1,2,4-triazol-4-yl)iminomethyl]benzonitrile, J. Chem. Technol. Biotechnol, 51: 483-486.

19. Majeed A., Alabdeen K., (2012), Synthesis and Characterization of New Thio-Triazole Ligand and Complexes with Selected Metals, Journal of Pharmacy and Biological Sciences (IOSR-JPBS), 4(5): 09-14.

20. Aliwi S., AL-Ani R., Awad J., (2001), photostabilization of polystyrene films by Nickel and Copper tetradentate Shiff base complexes, Iraqi journal polymer, 5(1): 15-30.

21. Zweifel H., (1998), Stabilization of polymeric materials, Berlin Heidelberg, Springer - Verslag.

22. Wypych G., (2008), Handbook of material weathering, 4th edn, Chemtec Publishing, Toronto.

23. Ayako T., Hirose H., (1999), Advance Polymer Science, Polymer Degradation Stabilization, 63: 441.

24. Scott G., (2000), Green polymers, Polymer Degradation and Stabilization, 68: 1-7.

25. Valkoa L., Kleinb E., Kovarikb P., Simonb P., (2001), HPLC stanovenie sacharidov v procese modelovaného zrýchleného starnutia papiera, Eur Polym J., 37: 1123-1133.

26. Guillet J., (1985), Polymer Photophysics and Photochemistry, Cambridge University Press.

27. Hamid H., (2000), Handbook of Polymer Degradation, Marcel Dekker Inc, New York.

28. Rabek F., (1996), Polymer photodegradation of polymers: physical characteristic and applications, Springer- verlag, Beelin.

29. Bottino A., Cinquegrani R., Di Pasquale G., Leonardi L., Pollicino A., (2003), Chemical modification, mechanical properties and surface photooxidation of films of polystyrene, polymer testing, 12: 405-411.

30. Galdi A., Foltis P., Shah A., (2010), UV protecting composition and methods of use, US patent, Application, 2010-118415.

31. Pospisil J., Pilar J., Billingham C., Marek A., Horak Z., Nespurek S., (2006), Factors affecting accelerated testing of polymer photostability, Polymer Degradation Stabilization, 91:417-422.

32. Bojinov B., Grabchev K., (2005), Novel functionalized 2-(2-hydroxyphenyl)-benzotriazole-benzo[de]isoquinoline-1,3-dione fluorescent UV absorbers: Synthesis and photostabilizing efficiency, Polym. Photochem. Photobiol., 172: 308-315.

33. Goldshtein J., Margel S., (2011), Synthesis and characterization of polystyrene/2-(5-chloro-2Hbenzotriazole-2-yl)-6-(1,1-dimethylethyl)-4-methyl-phenol composite microspheres of narrow size distribution for UV irradiation protection, Colloid Polym. Sci., 289: 1863-1874.

34. Andrady AL., (1997), Advance Polymer Science, 128: 49-94.

35. Sampers J., (2002), Polymer Degradation Stabilization, 67: 455-463.

36. Pospisil J., Nespurek S., (2000) Addcon World 2006. Prog Polymer Science, 25: 1261-1335.

37. Grassie N., Scott G., (1985), Polymer Degradation and Stabilization, Cambridge University Press, London.

38. Schnabel W., (1981), Polymer Degradation: Principle and Practical Applications, Chapter 14, Hanser Int, München.

39. Blaga A., (1980), In: Sereda PJ, Litvin GG (eds) Durability of Building Materials and Compounds, ASTM STP 691. ASTM, Philadelphia, 827–837.

40. Feldman D., (2002), Polymer weathering: photooxidation, Journal of polymer and the environmental, 10: 163-173.

41. Weidner S., Kuhn G., Freiedrich J., Schroder H., (1996), Plasmaoxidative and chemical degradation of poly(ethylene terepthalate) studied by matrix-assisted laser desorption/ionisation mass spectrometry, Rapid Communications in Mass Spectrometry, 10(1):40-46.

42. Dindar B., Icli S., (2001), Unusual photo reactivity of zinc oxide irradiated by concentrated sunlight, J. Photochem. Photobio A: Chem., 140:263.

43. Vinhas M., Souto Maiora M., Lapa M., Almeida B., (2003), Degradation studies on plasticized PVC films submitted to gamma radiation, Mat. Res., 6: 497-500.

44. Guaita M., Chiantore O., Costa L., (1985), Changes in degree of polymerization in the thermal degradation of polystyrene, Polymer Degradation stabilization, 12(4):135-332.

45. Potts E., (1991), Plastic environmentally degradation, The Kirk-Othmer Encyclopedia of Chemical Technology, 3rd edn. .

46. Pinto L., Goi B., Schmitt C., Neumann M., (2013), Photodegradation of polystyrene films containing UV-visible sensitizers, Journal of Research Updates in Polymer Science, 2: 39-47.

47. Gijsman P., Diepens M., (2009), Photolysis and photooxidation in engineering plastics, Polymer Degradation and Performance, ACS Symp Ser., 1004: 287-306.

48. Rabek F., (1995), Polymer photodegradation-mechanisms and experimental methods, Chapman Hall, Cambridge.

49. Kuzina, Svetlana, Mikhailov and Alfa, (1998), The photooxidation of polymers, The mainreaction of chain propagation in polystyrene photoxidation, Eur. Polym. J., 34(8): 1157-1162.

50. Kuzina I. and Mikhailov I., (1998), Photooxidation of polymers. 2. Photochain reaction of peroxide radicals in polystyrene, Eur. Polym. J., 34(2): 291-299.

51. Kaczmarek H., Kaminska A., Swiatek M., Sanyal S., (1999), Photoinition degradation of PS in the presence of low molecular organic compounds, European polymer J., 36: 1167-1173.

52. Rabek F., (1993), Polymer photodegradation–mechanism and experimental methods, Chapman and Haal, London.

53. Ranby B., Rabek F., (1981), In: Garnar DP, Stahl GA (eds) The effects of Hostile Environment on Coatings and Plastics, ACS Symp. Ser, ACS Washington, 291-301.

54. Mc Kellar F., Allen S., (1979), Photochemistry of Man-Made Polymers, Ltd. Applied Science Published, London 306: 138-147.

55. Rnby B., Lucki J., (1980), New aspects of photodegradation and photooxidation of PS, Pure & Appl Chem., 52: 295-303.

56. Geuskens G., David C., (1979), Polymer photodegradation: mechanisms and experimental methods, Pure Appl. Chem., 51: 233-240.

57. Trozzolo M., Winslow H., (1968), Macromolecules, American chemical society publishing 98.

58. Kochi K., Wiley J., (1973), Handbook of Free Radical Initiators, J. A Howard in Free Radicals, 2: 3-11.

59. Rabek J., (1974), In: Bamford CH, Tipper CF (eds) Comprehensive Chemical Kinetics, Elsevier, Amsterdam, 14: 425-431.

60. Guillet E., (1972), Thermal characterization of polymeric materials, Polym. Prepr Amer. Chem. Soc., Div Polym. Chem., 13: 628-632.

61. Rabek F., (1994), Polymer Degradation Mechanisms and experimental methods, Springer, Stocholm.

62. Yousif E., (2012), Photostabilization of thermoplastic polymers, Lambert Academic Publishing, Germany.

63. Amin U., Scott G., Tillekeratne K., (1975), Mechanism of the photoinitiation process in polyethylene, Europ. Polym. J., 11: 85-126.

64. Diepens M., (2009), Photodegradation and Stability of Bisphenol, A Polycarbonate in Weathering Conditions, Enschede, The Netherlands.

65. Gijsman P., Diepens M., (2009), Photolysis and photooxidation in engineering plastics, Polymer Degradation and Performance, ACS Symposium Series 1004: 287- 306.

66. Rabek F., (1987), Mechanism of Photophysical Process and Photochemical Reaction in polymers, John Wiley and Sons, New York.

67. Strlic M., Kolar J., (2005), Aging and stabilization of papers, distributed by the National and university Library, Turjaška 1, 1000 Slovenia.

68. Mayo R., (1978), Long-term properties of polyolefins, Macromolecules, 11: 492-496.

69. Mill R., Richarason H., Mayo R., (1978), J. Polym. Sci., 11: 2899-2908.

70. Guillet E., Ng C., (1978), Macromolecules, Studies of the mechanism of polyolefin phorodegradation, Pure & Appi. Chera., 11: 929-935.

71. Yousif E., Salimon J., Salih N., (2011), Photostability of poly (vinyl chloride), VDM, Germany.

72. Ranby B., Rabek F., (1975), Photodegradation, Photooxidation and Photostabilization of Polymers, Wiley periodicals, Inc, New York, 165-184.

73. Ruoko, (2012), Uv light induced degradation of polyethylene and polystyrene-spectroscopic and DSC study, Tampere University of Technology, M Sc thesis.

74. Meenakshi P., Noorjahan E., Rajini R., Venkateswarlu U., Crose S., (2002), Mechanical and microstructure studies on the modification of CA film by blending with Polystyrene, Indian Academy of Sciences, 25(1): 25-29.

75. Atiq N., (2011), Biodegradability of Synthetic Plastics Polystyrene and Styrofoam by Fungal Isolates, Ph D. thesis.

76. Saitoh A., Amutharani D., Yamamoto Y., Tsujita Y., Yoshimizu H., Okamoto S., (2003), Structure and properties of the mesophase of syndiotactic polystyrene IV. Release of guest molecules from δ form of syndiotactic polystyrene by time resolved FT-IR and WAXD measurement, Polym J., 35(11): 868-871.

77. Gupper A., Kazarian SG., (2005), Study of solvent diffusion and solvent induced crystallization syndiotactic polystyrene using FTIR spectroscopy and imaging macromolecules, 38(6): 2327-2332

78. Fried R., (2003), Polymer science and technology, 2nd edn. Publishing as Prentice Hall Professional Technical Reference.p, New Jersey, Pearson Education, Inc, 359.

79. Manzi-Nshuti C., Chen D., Su S., Wilkie A., (2009), Structure–property relationships of new polystyrene nanocomposites prepared from initiator-containing layered double hydroxides of zinc aluminum and magnesium aluminum, Polym. Degrad. Stab., 94: 1290-1297.

80. Safy Eldin M., El-laithy A., (1994), Photooxidative degradation of polystyrene of cover signals lamp of some automobile, Journal of applied polymer science, 55:47-54.

81. Kiatkamjornwong S., Sonsuk M., Wittayapichet S., Prasassarakich P., Vejjanukroh P., (1999), Degradation of styrene-g-cassava starch filled polystyrene plastics, Polym. Degrad. Stab., 66: 323-334.

82. Andrady AL., (1997), Advance Polymer Science, 128: 49-94.

83. Geuskens G., Baeyens-Volant D., Delaunois G., Lu-Vinh Q., Piret W., David C., (1978), Polymer photodegradation: mechanisms and experimental methods, J Europ. Polym., 14: 299-303.

84. Geuskens G., Baeyyens-Volant D., Delaunois G., Lu-Vinh Q., Piret W., David C., (1978), Vacuum-ultraviolet photochemically initiated modification of polystyrene surfaces: morphological changes and mechanistic investigations, J. Eur. Polym., 14: 291-297.

85. Lucki J., Rnby B., (1979), Polymer degradation and stability, Pure Appi. Chem., 1: 1-6.

86. Kuzina I., Mikhailov I., (1993), Plastics and the environment, Eur. Polym. J. , 29(12): 1549-1589.

87. Klopffer W., (1975), Polymer photodegradation: mechanisms and experimental methods, Eur. Polym. J., 11: 203-213.

88. George A., Hodgeman C., (1977), Polymer photodegradation: mechanisms and experimental methods, Eur. Polym. J., 13: 63-71.

89. Ranby G., Rabek F., (1975), Photodegradation, Photooxidation and Photostabilization of Polymers, John Wiley & Sons, London, 101-102.

90. Kuzina S. and Mikhailov A., (2001), photooxidation of polymer 4 the dual mechanism of polystyrene photooxidation: a hydroperoxide and a photochaine one, European polym. Journal, 37: 2319-2325.

91. Baloglu R., Fisch M., (1994), Polymer Degradation Stabilization, 45: 30-35.

92. Kuzina I., Mikhailov A., (1998), Photocatalytic degradation of polystyrene plastic under fluorescent light, Eur. Polym. J., 34: 291-320.

93. Yousif E., Salimon J., Salih N., (2011), New stabilizer for polystyrene based on 2-N-Salicylidene-5-(substituted)-1,3,4-thiadiazole compoundes, J. of Saudia Chemical Society, 16(3): 299-306.

94. Decker C., Biry S., (1996), Light stabilization of polymers by radiation cured acrylic coatings, Prog, Org coat, 29: 81-87.

95. Olson R., Schroeter H., (1978), UV screen progenitor’s thermally labile urethane derivatives of hydroxyphenylbenzotriazoles and hydroxybenzophenones, J. Appli. Poly. Sci., 22: 2165-2176.

96. Senna M., Hamid H., Hussein M., (2002), Nuclear instrument methods, Phys. Res. Section B, 187: 48-55.

97. Pospisil J., Habicher W., Zweifel H., Pilar J., Nespurek S., Piringer O., (2002), Polymer and polymer composites, 10: 37- 42.

98. Patel P., (2007), Additive primer, blown films, cast films and extraction coating, PLACK conference, 16-20.

99. Gugumus F., (1979), In: Scott G (ed) Development in Polymer Stabilization, Applied Science Publishers Ltd, London, 261-273.

100. Yousif E., (2010), Photostabilization of PVC by inorganic complexes, LAP LAMBERT, Germany.

101. Asaad N., Yousif E., Hameed A., (2011), Synthesis and photostability of new polymers derived from PVC, LAP LAMBERT academic publishing.

102. Salem M., (2001), Mechanical Properties of UV-Irradiated Low-Density Polyethylene Films Formulated With Carbon Black and Titanium Dioxide, Egyp. J. Sol., 24(2): 141-150.

103. Williams R., Jordan W., Dannerberg M., (1969), Reinforcement of elastomers by fillers: Review, J. Appl. Polym. Sci., 9: 861-871.

104. David L., Hsuan G., (2003), assessing the photodegradation of geosynthetics by outdoor exposure and laboratory weatherometer, Geotextiles and Geomembranes, 21: 111-122.

105. Chirinos, J., (1989), Mechanistic aspects of polymer photostabilization, j. photochem. Photobio. A:Chem, 49: 1-39.

106. Krevelen D., Nijenhuis K., (2009), Properties of Polymers: Their Correlation with Chemical Structure; their newmerical estimation and prediction from additive group contributions, 4th edition, Elsevier, p. 784.

107. Wiles M., Carlsson J., (1980), Photostabilisation mechanisms in polymers: A review. Polym. Deg. Stabil., 3: 61-72.

108. Beavan W., Phillips D., (1974), Photostabilizing of macromolecule by excited state qyencher, J. Photochem., 3:3149363.

109. Lala D., Rabek J., (1980), Polymer photodegradation: mechanisms and experimental methods, Polymer Degradation Stabilization, 3: 383-391.

110. George A., (1974), Mechanism of photoprotection of polystyrene film by some ultraviolet absorbers, J. Appl. Poly. Sci., 18: 117-124.

111. Chandra R., (1983), Photostabilization of poly(2,6-dimethyl-1,4-phenylene oxide) by nickel(II)thiopicoline anilide, Polym. Photochem., 3: 367-378.

112. Osawa Z., Nagashima K., Ohshima H., Cheu E., (1979), Study of the degradation of polyurethanes the effect of various additives on the photodegradation of polyurethanes, J. Polym. Sci., 17: 409-419.

113. Allen S., Chirinos-Padron A., Appleyard H., (1984), Polymer photodegradation: mechanisms and experimental methods, Polymer Degradation Stabilization, 6: 31-37.

114. Allen S., Chirinos-Padron A., Apployarat H., (1982), Photo stabilization of PVC films by using some novel tetra Schiff's bases derived from1,2,4,5-tetra-[5-amino-1,3,4-thiadiazole-2-yl]-benzene, Polymer Degradation Stabilization, 4: 223-228.

115. Carlsson J., Wiles W., (1974), Physical properties of polymers handbook. J. polym. Sci., polym. ChemEd., 12: 2214-2217.

116. Willis B., (1984), Investigation of test method material properties and processes for solar cell in capsulation, eighth annual report.

117. Kurumoda T., Ohsawa H., Oda O., Fujita T., Toda T., Yoshioka T., (1985), Entropy and enthalpy effects of 4-(phenylthio)-substituted phenols, J. Polym. Sci. Polym. Chem. Ed., 23: 1477-1482.

118. Bottino A., Cinquegrani R., Giovanna D., Leonardi L., Antnino A., (2004), Study on chemical modification, mechanical properties and surface photooxidation of films of polystyrene stabilized by hinderd amines (HAS), Polymer Testing, 23: 779-789.

119. Yousif E., Salimon J., Salih N., (2012), New stabilizer for polystyrene based on 2-Thioacetic Acid Benzothiazol complexes, J. of applied polymer Science, 125: 1922-1927.

120. Sastre R., Claramunt C., Catalina D., Mateo L., Santa-Maria D., Catalan J., (2003), Mechanism of photostabilization of polystyrene film by dihydroxyphenyl-pirazole, J. polym. Sci. A; Polym.Chem., 28: 3661-3663.

121. Bottino A., Di Pasquale G., Pollicino A., Recca A., (1996), Surface photostabilization of polystyrene by Tinuvin 1577, J. of appl. Polym. Sci., 69: 1251-1256.

122. Lefedova O., and Nemtseva M., (2012), 2-(2-Hydroxy-5 methylphenyl) benzotriazole and Its Hydrogenation Products in Polystyrene Stabilization, Russian J. of Appl. Chem., 85(7): 1128-1132.

123. Bottino A., Bottino P., Antonino P., Antonino R., (1999), Surface photostabilization of polystyrene by Tinuvin 1577, J. of Appl. Polym. Sci., 69(6): 1251-1256.

124. Yousif E., Salimon J., Salih N., Abdullah B., (2013), Photochemical study of PS based on Presence Schiff Bases of 2,5-Dimercapto-1,3,4-thiadiazole as photostabilizer, International Engineering Conference, "Energy and Environment" 2nd -4th , Kuching Sarawak.

125. Sun G., Jang H., Kaang S., Chae K., (2002), A new polymeric HALS: preparation of an addition polymer of DGEBA–HALS and its photostabilizing effect, 43: 5855-5863.

126. Yousif E., Hameed A., Salih N., Salimon J., Abdullah BM., (2013), New photostabilizers for polystyrene based on 2,3-dihydro-(5-mercapto-1,3,4-oxadiazol-2-yl)-phenyl-2-(substituted)-1,3,4-oxazepine- 4,7-dione compounds, Springer Plus J., 1-8.

127. Rabie T., Mahran M., Kamel M., Abdel Hamid H., (2008), Photodegradation of polystyrene stabilized with uracil derivative, J. Appl. Sci. Research, 4(12): 2015-2026.

128. Aliwi M., AL-Ani R., Awad J., (2001), Photostabilization of polystyrene films by Nickel and Copper tetradentate Shiff base complexes, Iraqi J. polym., 5(1): 15-30.

129. Abd A., Abdul Zahra I., Shenta A., (2009), Photostabilization of polystyrene films by anthraquinones derivatives and their complexes with copper (II), oxovanadium (IV) and nickel (II) ions, Journal of Basrah Researches 35(3): 81-97.

130. Siddiqui A., Mishra R., Kumar R., Rashid M., Khaidem S., (2010), Synthesis spectral characterization, and pharmacological screening of some 4-[{1-(aryl)methylidene}-amino]-3-(4-pyridyl)-5-mercapto-4H-1,2,4-triazole derivatives, J. Pharm. Bio. Sci., 2(2): 109-112.

131. Majeed A., Hameed A., Yousif E., (2004), Chromium(III), Iron(III), Cobalt(II), Nickel(II) and Copper(II) Complexes of 2-Amino-5- (2-acetyloxyphenyl)-1,3,4 –thiadiazole, national, j. of chemistry, 16: 588-565.

132. Shneshil M., Redayan M., (2010), Photostabilization of PVC films by using some novel tetra Schiff's bases derived from1,2,4,5-tetra-[5-amino-1,3,4-thiadiazole-2-yl]-benzene, Diyala j. for pure science, 7(1): 34-77.

133. Hatchard, C. G.; Parker, C. K. (1956). A New Sensitive Chemical Actinometer .II. Potassium ferrioxalate as a Standard Chemical Actinometer. Proc. Roy. Soc. A 235: 518-536.

134. Ganqlitz G. and Hubiq S., (1986), Chemical Actinometry, Pure and Appl. Chem., 61: 187-195.

135. Yousif E., Hameed A. and Bakir E., (2007), Synthesis and photochemical study of PVC -1,3,4-oxadiazole and 1,3,4-thiadiazole, J. of Al-Nahrain University 10(1): 7-12.

136. J. Rabek and J. Sanetra, (1986), Macromolecules, Springer Berlin Heidelberg, 19:1679.

137. Yousif E., (2004), photostabilization of PVC by 1,3,4 thiadiazole and 1,3,4, oxadiazole chelate complexes and some of their free ligand, Ph D thesis, Al-Nahraine university.

138. Yousif E., Salimon J., Salih N., (2011), Improvement of photostabilization of PVC in the presence of thioacitic acidbenzothiazole complexes, The Malaysian J. of Analytical Sciences, 15(1): 81-92.

139. Braun D., Cherdron H., Rehahn M., Ritter H., (2005), Polymer synthesis: theory and practice, springer scince, USA.

140. Sabaa M., Oraby E., Abdul Naby A., Mohamed R., (2005), N-phenyl-3-substituted 5-Pyrazolone derivatives as organic stabilizer for rigid PVC against photodegradation, j. of applied polymer science, 101: 1543-1555.

141. Shi W., Zhang J., Shi X., Jiang G., (2006), different photodegradation processes of PVC with different average degrees of polymerization, j. of applied polymer science, 107: 528-540.

142. Pavia D., Lampman G., Kris G., (2001), Introduction to spectroscopy, thiredth edn., a guide for students of organic chemistry, Brooks and Cole, Florence, Bellingham Washington.

143. Silvertein R., Bassler G., (1980), Spectrometric identification of organic compounds, 5th edn. John *Wiley* & Sons, New York

144. Majeed A., Yousif E., Farina Y., (2010), Synthesis and characterization of transition metal complexes of -2-thioacetic acid benzothiazole ligand, J. Al-Nahrain Uni., 13: 36-42.

145. Yousif E., Hameed A., Ameer A., (2005), Synthesis and Characterization of Complexes of Some Transition Metals With 2-amino-5- (4-hexyloxyphenyl)-1,3,4-thiadiazole, J. of al-Nahrain University, 8(1): 9-11.

146. Narayana B., Gajendragad M., (1997), Complexes of Zn(II), Pd(II), Hg(II), Pb(II), Cu(I), Ag(I), and Ti(I) with 4-amino-5-merccapto-3-(o-tolyloxymethyl)-1,2,4-troazol, Tr. J. of chemistry Tur. J. Chem., 21:71-76.

147. Sliverstein R., Bassler G., Morrill T., (2005), Spectrometric Identification of Organic Compounds, 7th edn. John Wiley & Sons, New York.

148. Flifel I., Kadhim S., (2012), Synthesis and Chracterization of 1,3,4-oxadiazole derivatives with some new transition metal complexes, J. of kerbala uni., 10(3): 197-209.

149. Cheremisina M., Khlystunova E., Varand V., (1972), IR spectra of complexes of certain metals with thio- and selenourea in the region of the metal-ligand vibrations, Bulletin of the Academy of Sciences of the USSR, Division of Chemical Sci., 21(12): 2604-2606.

150. Qurban S., (2011), Synthesis and Characterization of some transition metal Complexes of Schiff base derived from isonicotinic hydrazide and O-Vanillin. Diyala J. Pure Sci., 7(2): 94-104.

151. Yousif E., Ameer A., Majeed A., (2004), Complexes of 2-Amino −5- (p-propoxyphenyl)-1,3,4-thiadiazole With Some Metal Ions, j. of al-nahrain uni 7(2): 65-69.

152. Yousif E., Adil H., Farina Y., (2010), Synthesis and Characterization of Some Metal Ions with 2-amino Acetate Benzothiazole, J. of Applied Sciences Research, INSInet Publication, 6(7): 879-882.

153. Ibraheem H., Adel H., Ahmed A., Salih N., (2010), synthesis, characterization and antimicrobial activity of some metal ions with 2-thioacitic-5-phenyl-1,3,4-oxadiazole, J. of. Al-Nahrain University, 13(1): 43-47.

154. Cos-kun A., (2006), The Synthesis of 4-Phenoxyphenylglyoxime and 4,4-Oxybis(phenylglyoxime) and Their Complexes with Cu(II), Ni(II) and Co(II), Turk J. Chem, 30: 461-469.

155. Greenwood N., Earnshaw A., (2002), Chemistry of the elements, 2nd edn. Elsevier Science Ltd, New York.

156. Hassan O., Otaiwi A., Abeer A., (2008), Photodegradation Study of PVC By New Metal Complexes of Thiourea Derivatives, National J. Chem., 31: 501-513.

157. Figgis B., (2000), Ligand Field Theory and its Applications, 1st edn. John-Wiley, New York.

158. Schönherr T., (2004), Optical Spectra and Chemical Bonding in Inorganic Compounds, Springer-Verlag Berlin Heidelberg, 256-264.

159. Majeed A., (2008), Synthesis and characterization and study of the biological activity of some new metal complexes of 2-hydroxylbenzeledene-5-(−2-acetyloxyphenyl)-1,3,4-thiodiazole, J. al-Nahrain Uni., 11(1): 44-49.

160. Chohan Z., (2009), Antibacterial dimeric copper (II) complexes with chromone-derived compounds, Trans. Met. Chem., 34: 153-161.

161. D. Nicholis, (1984), Complexes and First-Row Transition elements, 2nd edition, American Elsevier, London: Mac, 141: 545-552.

162. Win Y., Yousif E., Majeed A., Ha S., (2011), Synthesis, characterization and in vitro antimicrobial activity of Co(II), Cu(II), Zn(II), Cd(II) and Sn(II) ions with {[5-(4-bromophenyl)-1,3,4-oxadiazol-2-yl]thio}acetic acid, Asian J. Chem 23(11): 5009-5012.

163. Majeed A., (2010), Synthesis, structure and antibacterial activity of some 2-amino-5-(2-acetyloxyphenyl)-1,3,4- thiadiazole complexes, al Mustansiriya J. Sci 21(5): 195-204.

164. Foo Y., Yousif E., Tiong S., Majeed A., (2013), Synthesis Characterization and Preliminary in vitro Antibacterial Screening Activity of Metal Complexes Derivatives of 2-[5-(4-Nitrophenyl)-1,3,4-thiadiazolylimino]methyl phenol, Asian J. Chem., 25(8): 4203-4206.

165. Trozzolo A., (1971), stabilization against oxidative photodegradation, Wiley interscince publishers, 159-168.

166. Yousif E., Aliwi S., Ameer A., Jaleel R., (2009), Improved photostability of PVC films in the presence of 2-thioacetic acid-5-phenyl-1,3,4-oxadiazole complexes Turk J. Chem., 33: 399-410.

167. Naif O., Salih H., (2011), Synthesis of New Modified PVC and their Photostability Study, Tikrit Journal of Pure Science 16 (4): 1813-1662.

168. Rabek J., Ranby b., (2003), Studies on the photooxidation mechanism of polymers. II. The role of quinones as sensitizers in the photooxidative degradation of polystyrene, j. of polymer sci., 2(2); 295-306.

169. Lawrence J., Weir N., (2003), Photodecomposition of polystyrene on long-wave ultraviolet irradiation: A possible mechanism of initiation of photooxidation, j. polym. Sci., 11(1): 105-118.

170. Mori F., Koyama M. and Oki Y., (1979), Physical Properties of Polymers Handbook, Angew. Makromol. Chem., (75): 113-122.

171. Cooray B. and Scott G., (1980), Polymer Photodegradation: Mechanisms and Experimental Methods, J. Eur. Polym., 169(16): 177-189.

172. Gugumus F., (1979), Development in Polymer Stabilization-1, (G. Scott, ed.), Applied Science Publishers Ltd., London, 261-272.

173. Schultz J., (1998), Deformation morphologies and toughening of polymer system. Capt.8, 349-368.

174. Sabaa M., Oraby E., Abdel Naby, A., Mohamed R., (2006), *N*-Phenyl-3-Substituted 5-Pyrazolone Derivatives as Organic Stabilizers for Rigid Poly(vinyl chloride) Against Photodegradation, J. App. Polym. Sci., 101: 1543-1555.

175. Al. jaleel T., Ali H., Mohammed A., (2007), Morphlogical Study of photodegradation and photstabilization for polystyrene induced by anhydrous ferric chloride, anbar uni. J., 2: 1-12.

176. Kuzina, Svetlana I., Mikhailov and Alfa I., (1998), The photooxidation of polymers, The main reaction of chain propagation in polystyrene photoxidation, Eur. Polym. J., 34(8): 1157-1162.

177. Rabie S. , Ahmed A. , Sabaa M. , Abd El-Ghaffar M., (2013), Maleic diamides as photostabilizers for polystyrene, J. of Industrial and Engineering Chemistry 19: 1869-1878.

178. Zan L., Wang S., Fa W., Hu Y., Tian L. and Deng K., (2006), Solid-Phase Photocatalytic Degradation of Polystyrene with Modified Nano-TiO_2 Catalyst, j. of Polymer, 47(24): 8155-8162.

179. G. Scott, (1973), Polymers and Ecological Problems, (J. E. Guillet, ed.), Plenum press, New York, 3: 27-35.

180. Gooch W., (2007), Encyclopedia dictionary of polymers, springer scince, USA, 772-783.

181. Botelho G., A. Queiro's, A. Machado, P. Frangiosa y J. Ferreira, (2004), Enhancement of the thermooxidative degradability of polystyrene by chemical modification, Polymer degradation and stability, 86: 493-497.

182. Shyichuk, A., White J., (2000), Analysis of chain-scission and crosslinking rates in the photooxidation of polystyrene, J. Appl. Polym. Sci., 77: 3015-3023.

183. Allcock R., Lampe W. and Mark P., (2003), Contemporary Polymer Chemistry, 3d edn Pearson Prentice-Hall, p. 316.

184. Yousif E., Hameed A., Rashed R., Mansoor H., Farina Y., Graisa A., Salih N., Salimon J., (2010), Synthesis and photostability study of some modified poly(vinyl chloride) containing pendant benzothiazole and benzimidozole ring, Int. J. Chem. 2: 65-80.

185. Al-Jibouri M., Al-Ameri S., Al-Jibouri W., Al-Souz M., (2013), Spectroscopic study of the effect of a new metal chelate on the stability of PVC, Journal of the Association of Arab Universities for Basic and Applied Sciences, 14: 67-74.

186. AL-Shimary B., Al-Jibouri N., Ismael A., (2008), The Effect of New Metal Complexes on the Photodegradation of Poly(vinyl chloride) Films, national j. of chem., 31: 428-438.

187. Yousif E., Salimon J., Salih N., (2010), Mechanism of photostabilization of poly(methy methacrylate) films by 2-thioacetic acid benzothiazol complexes, Arabian j. of chemistry.

188. Yousif E., Hameed A., Baker E., (2007), Synthesis and photochemical study of poly (vinyl chloride)-1,3,4-oxadiazole and 1,3,4-thiadiazole, J. Al-Nahrain Univ. 10: 7-12.

189. Mark J., (2007), Physical properties of polymers handbook, Springer, New York.

190. Adil H., Yousif E., Salimon J., (2011), New Stabilizers for PVC Based on Benzothiazole Complexes, LAMBERT Academic Publishing, Germany.

191. Allen S., Chirinos-padron A., Appleyard H.,(1984), Plastics Additives Handbook, Polym. Photo. Chem., 5: 333-349.

192. Allen S., Luc-gardette J., Lemaire J., (1983), J. Polym. Photo. Chem., 3(4): 251-265.

193. Harper J., Mckellar F., (1974), Advances in Photochemistry, j. appl. Polym. Sci., 18: 1233.

الخلاصـــــــــة

في هذا البحث تم تحضير وتشخيص خمسة معقدات مع 4-امين -5- بيريدايل -1,2,4- ترايزول -3- ثايول مع كل من النيكل (II), النحاس (II), الخارصين (II), الكادميوم (II) و القصدير(II) ودراسة تأثيرها في التثبيت الضوئي للبولي ستايرين (PS).

حيث شخصت جميع هذه المركبات من خلال مطيافية الأشعة تحت الحمراء (FTIR) والأشعة فوق البنفسجية والمرئية (UV-Vis.) و طيف الرنين النووي للكاربون والهيدروجين ^{1}H and ^{13}C NMR بالإضافة إلى قياس الحساسية المغناطيسية وقياسات التوصيلية الكهربائية وبعض الخصائص الفيزيائية الأخرى . حيث اتضح على ان هذا الليكند هو ثنائي السن, حيث يرتبط مع ايون الفلز عن طريق S (thione) و مجموعة الامين. و من خلال القياسات وجد جميع اشكال هذه المعقدات هي شكل رباعي السطوح عدا معقد النحاس حيث يأخذ شكل مربع مستوٍ.

استعملت هذه المعقدات كمثبتات للتجزئة الضوئية لمتعدد الستايرين. و تم متابعة سرعة التجزئة والتثبيت الضوئي للرقائق البوليمرية مع زمن التشعيع بقياس قيم معامل الكاربونيل I_{CO} والهيدروكسيل I_{OH}و حسابات نقصان الوزن و حسابات اللزوجة و كذلك تمت الدراسة المورفولوجية لسطح البوليمر , حيث استخدم في تشعيع الرقائق البوليمرية ضوء بطول موجي (365nm) بدرجة حرارة الغرفة وبشدة 6.2×10^{-9}ein. dm^{-3}.S^{-1}.

وجد ان قيم معامل الكاربونيل I_{CO} والهيدروكسيل I_{OH} تزداد مع زيادة زمن التشعيع .من خلال متابعة اصرة الكاربونيل والهيدروكسيل النامية مع زمن التشعيع، حيث وجد أن المضافات المحضرة تسلك كمثبتات للتجزئة الضوئية، والتي أخذت الترتيب التالي :

$$\xrightarrow[\text{زيادة الاستقرارية}]{\mathbf{Cd(L)_2\ ,\ Zn(L)_2\ ,\ Sn(L)_2\ ,\ Ni(L)_2\ ,\ Cu(L)_2}}$$

وتم خلال البحث تم دراسة قطع السلسلة البوليمرية وقيم منتوج الكم وذلك بقياس مقدار التغير في متوسط اللزوجة للوزن الجزيئي مع زمن التشعيع, فوجد ان مقدار التغير في متوسط اللزوجة للوزن الجزيئي يقل بزيادة زمن التشعيع.

ومن خلال النتائج العملية المستحصلة اقترحت بعض الميكانيكيات اعتماداً على الصيغة التركيبية للمادة المضافة، لذلك فهي ممتصات الأشعة الفوق البنفسجية، مجزئات البيروكسيد وقانصات الجذور الحرة .

جمهورية العراق
وزارة التعليم العالي والبحث العلمي
جامعة النهرين
كلية العلوم
قسم الكيمياء

تحضير معقدات لاعضوية مشتقة من4 -امين -5- بيريدايل -4H- 1,2,4 ترايزول-3-ثايول و دراسة الثباتية الضوئية لها لبوليمر البولي ستايرين

رسالة
مقدمة الى كلية العلوم- جامعة النهرين
وهي جزء من متطلبات نيل درجة الماجستير في علوم الكيمياء

من قبل
رغد علي عبد الرسول حداد
بكالوريوس 2011

المشرف
الاستاذ المساعد الدكتور: عماد عبد الحسين يوسف السراج

2014